Confinement and driving effects on model interfaces

11 mai 2020

Table des matières

Introduction

Every statistical model is described by an order parameter, such as the mean magnetization in a magnetic system or the polymer's mean orientation. During a continuous phase transition, the correlation length diverges up to a macroscopical scale. When this length scale becomes as the same order of magnitude as the experimental or numerical cell, finite size effect arise, such as the critical Casimir effect.

We may study the statistical properties of interfaces between two phases through different though complementary methods. Historically, the first method was through lattice models, and more precisely the Ising model. Those models are well-suited for numerical analysis due to their discrete nature, while posing analytical challenges due to the big number of degrees of freedom. The Solid-On-Solid model is an approximation of the Ising model in $d-1$ dimensions allowing us to use the transfer matrix method, which holds analytical results directly comparable with numerical simulations. From the Ising model arose some mean-field approximations, with the Landau-Ginzburg Hamiltonian. This method allows for relatively easy analytical computations of the two-point space correlation function of the system, which gives us some insight about the properties of the interfaces. From the mean field theory we can derive the mean-field equations of a fluctuating interface, which then resembles to a brownian walker. This powerful analogy allows the use of quantum mechanics formalism, as we will see later on.

Systems may exist in many different contexts. Knowing how the thermodynamical ensemble in which we place the system affects its statistical properties is a key to understanding how to transpose the analytical results to actual experiments. A special attention will also be brought to the free energy. From the free energy between a bulk and an interface we can compute the its surface tension. The derivative of the free energy with respect to the length of the system also gives us a confinement force, called the Casimir force. This force is exerced on the boundary conditions because of the confinement of fluctuations.

This outline of this thesis is as following :

— The first chapter derives the interface dynamics from mean field theory. In doing so, we will define all the main interface models that exist, and explain the main results from litterature.

— In the second chapter we explain how do numerical simulations work, some methods to compute the free energy in lattice gas models, and some usefull tips.

— The third chapter is devoted to finite size effects, computed for all the models presented in chapter one, and compoared to numerical results.

— The fourth chapter is about a paper we've published [**?**]. This paper is about the computation of the surface tension of a sheared interface, where we've coupled the field with a virtual one in order to proceed with the computation.

— In the last chapter we introduce a new lattice model which is a better approximation to the Ising model than the Solid-On-Solid model. This new model, the Particles-Over-Particles model, takes into account the entropy, in comparison to SOS.

All our numerical efforts benefited from the numerical resources of the PSMN at the ENS de Lyon [22] and this work was financed by the ERC grant OUTEFLUCOP with principal investigator Sergio Ciliberto (CNRS, ENS de Lyon). This work was performed during three years at the Laboratoire de Physique of the ENS de Lyon, under the direction of Peter Holdsworth.

All our numerical efforts benefited from the numerical resources of the MCIA at

This thesis has been posible thanks to the ANR's grant FISICS, the Laboratoire Onde Matière d'Aquitaine from 'Université de Bordeaux, and the Laboratoire de Physique from ENS Lyon. The numerical simulations benefited from the numerical resources of the Mésocentre de Calcul Intensif Aquitain [**?**], with the help of Nguyen Ky Nguyen. I also wish to thank Josiane Parzych (LOMA) and Laurence Mauduit (ENS LYON) for all the administration procedures.

Chapitre 1

Equilibrium interface dynamics

In this chapter we will analyse the dynamics of statistical systems. The analysis will allow us to understand how phase transitions - in particular those who possess a phase separation - occur dynamically [**?**]. The most famous example is the Ising model without any external field, its order parameter beeing the total magnetization.

In the high temperature phase, the system is homoegeneous and its total magnetization is zero. Below the critical temperature, when the order parameter is conserved (for example with a Kawasaki dynamics or Model B), the system will locally separate into two phases of opposite mean magnetization separated by and interface, this interface minimizing the surface energy between both pahses. When the order parameter is not conserved (for example Glauber dynamics or Model A), a sponteneous symetry breaking will make one of the two phases take over the whole system. In a continuous phase transition where the critical point is reached from the disordered state to the ordered stated, the domain size, which is equal to the system's correlation lengt, diverges close to the critical temperature T_C. In a thermodynamical system, it becomes infinite, implying that the system takes an infinite amount of time to reach equilibrium : it's the critical slowing down. The process of domain growth is known as coarsening and phase ordering kinetics is the theory that has been developed to understand the phenomenon of coarsening[**?**]. In Fig 1.1, we show an example of coarsening in the Ising model with respect to time.

Furthermore, for systems with a conserved order parameter which separate into two phases, the two phases will be separated by an interface. This interface will be characterised by a surface tension, its average position will be fixed but it will exhibit fluctuations. Later we will see how model of phase ordering kinetics and be used to determine the static and

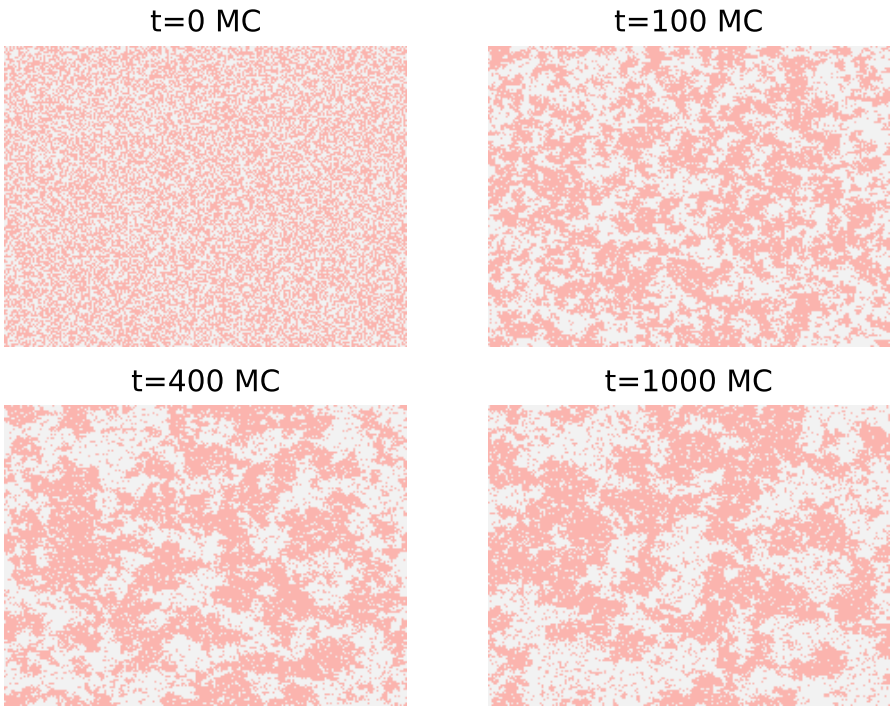

FIGURE 1.1 – Numerical simulations of coarsening from a quench from a disordered state $T = \infty$ to an ordered state $T = T_{2D,C}$ [2] for different times, in Monte Carlo steps, for a 600×600 system with non-conserved Glabuer dynamics.

dynamical properties of interfaces between two coexisiting phases.

While the phase diagram of a system can be determined via its Hamiltonian and equilibrium statistical mechanics, the dynamics of coarsening depends on the details of the systems dynamics that do not show up in single time thermodynamic observables. Therefore one needs to construct dynamical models that capture the underlying evolution of the state of the system. In particular, there is a big difference between systems where the order parameter is conserved and those where it is not conserved.

1.1 Statics of systems with a finite number of degrees of freedom

Thermodynamic systems are naturally described in terms of fields, for example densities.

To explain why systems are naturally described in therms of fields

La mesure des observables nécessite une connaissance parfaite de la dérivée de la fonction de partition Z, et donc d'explorer l'espace des phases des configurations du système. Les appareils de mesure possèdent tous une résolution spatiale et temporelle, c'est-à-dire qu'ils mesurent l'état moyen de toutes les particules dans un volume et dans un laps de temps donné. Plus la résolution des appareils de mesure est bonne, et plus la mesure des observables dérivées de la fonction de partition est précise. Si $\Phi(\mathbf{x}, t)$ est le champ réel de l'observable du système, alors l'appareil, possédant une précision dans le temps et l'espace de $(dt, 2dx, 2dy, 2dz)$ mesure le champ

$$\phi(\mathbf{x}, t) = \frac{1}{V dt} \int_{t-dt}^{t} dt' \int_{x-dx}^{x+xd} dx' \int_{y-dy}^{y+dy} dy' \int_{z-dz}^{z+dz} dz' \Phi(x, y, z, t) \tag{1.1}$$

This means that one is naturally lead to consider statistical field theories where the system is described in terms of a local field $\phi(\mathbf{x})$. Statistical field theories can be applied to both statics, to understand phase diagrams, and dynamics to understand phase ordering. However to start with we will examine the case of systems with a finite number of degrees of freedom.

Consider a system in the canonical ensemble with a Hamiltonian $H(\mathbf{q})$ where q_i for $1 \leq i \leq N$ represent a finite number of continuous spatial degrees of freedom and where in a classical system we have already integrated over the corresponding momenta. The partition function for the system is given by

$$Z = \int d\mathbf{q} \exp\left(-\beta H(\mathbf{q})\right) \tag{1.2}$$

In general the integral which gives the partition function cannot be computed analytically. In equilibrium, the probability density function $P_{eq}(\mathbf{q})$ of the degrees of freedom is given by

$$P_{eq}(\mathbf{q}) = \frac{\exp\left(-\beta H(\mathbf{q})\right)}{Z} \tag{1.3}$$

The simplest approximation to compute Z is the mean field approximation where the integral is approximated by the integrand at its largest value - in mathematics this is the Laplace method for approximating an integral and in this context it is just an expansion about the minimum energy configuration of the system. The mean field approximation is thus

$$Z_{MF} = \exp\left(-\beta H(\mathbf{q}^*)\right) \tag{1.4}$$

where $\mathbf{q}^*$ is the value of $\mathbf{q}$ which minimises H (note that the approximation becomes exact in the zero temperature limit - $\beta \to \infty$ - as the system will minimise its energy). The values q_i^* are determined from

$$\frac{\partial H}{\partial q_i}|_{\mathbf{q}=\mathbf{q}^*} = 0 \tag{1.5}$$

Within this approximation any thermodynamic observable is given by

$$\langle f(\mathbf{q})\rangle = f(\mathbf{q}^*) \tag{1.6}$$

We now consider how one can model dynamics of such systems. We will look for a Langevin equation which is chosen to give the correct equilibrium Gibbs-Boltzmann distribution. We write

$$\frac{dq_i}{dt} = -L_{ij}\frac{\partial H(\mathbf{q})}{\partial q_j} + \eta_i(t) \tag{1.7}$$

where L_{ij} is a matrix which discuss later and $\eta_i(t)$ is zero mean Gaussian white noise with correlation function

$$\langle \eta_i(t)\eta_j(t')\rangle = \Gamma_{ij}\delta(t-t') \tag{1.8}$$

The Gaussian white noise represents the effects of thermal fluctuations on the system we assume that the correlation time of these fluctuations is extremely short with respect to the dynamics of the degrees of freedom q_i (in fact in critical systems the dynamics becomes very slow, critical slowing down, and this approximation becomes better and better as one approaches the critical point). There is no momentum term in this Langevin equation and for this reason it is often called the over damped Langevin equation. Overdamped Langevin equations can also be derived staring from Newton's laws in the presence of friction, due to a solvent, and again white noise (again due to molecular collisions with the solvent) and by taking the limit where the frictional forces are greater than the acceleration term in Newton's equations (equivalent to setting the particle masses to zero).

As Eq. (1.8) is for a correlation function the matrix Γ_{ij} must be symmetric and cannot

have any negative eigenvalues.

In the absence of noise or thermal fluctuations, so at zero temperature, the system will simply minimise its energy. Therefore if

$$\frac{\partial H(\mathbf{q})}{\partial q_j} = 0 \tag{1.9}$$

with no noise we have $\frac{dq_i}{dt} = 0$, that is to say it is the term $\frac{\partial H(\mathbf{q})}{\partial q_j}$ that drives the dynamics if there is no noise. As long as the matrix L_{ij}^{-1} exists the zero temperature dynamics will take the system to the local minimum of H and to the absolute minimum if there are no metastable configurations.

Under these assumptions, the Fokker-Planck equation for the probability density function of the degrees of freedom is

$$\frac{\partial p(\mathbf{q},t)}{\partial t} = \frac{\partial}{\partial q_i}\left[\frac{1}{2}\Gamma_{ij}\frac{\partial p(\mathbf{q},t)}{\partial q_i} + p(\mathbf{q},t)L_{ij}\frac{\partial H(\mathbf{q})}{\partial q_j}\right] \tag{1.10}$$

This can be written as

$$\frac{\partial p(\mathbf{q},t)}{\partial t} + \frac{\partial}{\partial q_i}J_i(\mathbf{q},t) = 0 \tag{1.11}$$

where the $\mathbf{J}(\mathbf{q},t)$ is the probability current. We now insist that the system is in equilibrium with zero current when $p(\mathbf{q},t) = P_{eq}(\mathbf{q})$ as given by Eq. (1.3), this gives

$$\left[-\frac{\beta}{2}\Gamma_{ij} + L_{ij}\right]\frac{\partial H(\mathbf{q})}{\partial q_j} \tag{1.12}$$

and this holds for any choice of H is we chose

$$\Gamma_{ij} = 2TL_{ij} \tag{1.13}$$

where we have taken units where Boltzmann's constant $k_B = 1$.

1.2 Statistical field theory

We now consider a system with Hamiltonian $H[\phi]$ which depends on a continuous field $\phi(\mathbf{x})$. The partition function is given by a functional integral

$$Z = \int d[\phi] \exp(-\beta H[\phi]), \tag{1.14}$$

the functional integral over all possible fields ϕ can be taken as a limit where ϕ is defined at a finite number of points on a lattice and then the lattice spacing is taken to zero. In many cases, the system has been coarse grained and ϕ represents a spatially varying order parameter, for instance the local density averaged over some small volume. In this case the Hamiltonian H is strictly speaking a free energy and contains terms that depend on the temperature.

The mean field approximation to partition function is then given by

$$Z_{MF} = \exp(-\beta H[\phi_{MF}]) \tag{1.15}$$

where ϕ_{MF} is the mean field solution which minimises H. The definition of a functional derivative of a functional is

$$F[\phi + \delta\phi] - F[\phi] = \int d\mathbf{x} \frac{\delta F}{\delta \phi(\mathbf{x})} \delta\phi(\mathbf{x}) \tag{1.16}$$

Therefore if a field ϕ maximises H we must have

$$\frac{\delta H}{\delta \phi(\mathbf{x})} = 0 \tag{1.17}$$

We now consider the standard Landau-Ginzburg Hamiltonian [3] describing Ising like systems where

$$H[\phi] = \int d\mathbf{x} \; \frac{\kappa}{2} [\nabla \phi]^2 + V(\phi) \tag{1.18}$$

The first term represents an energetic cost of varying the field ϕ. The second potential term has two minima at $\phi = \pm\phi_c$, and, in the low temperature or phase separated phase, without loss of generality we can chose $V(\phi_c) = V(-\phi_c)$, while it has a single minimum at $\phi = 0$ in the high temperature phase.

The standard potential for phase separations, called the ϕ^4 model, is given by the

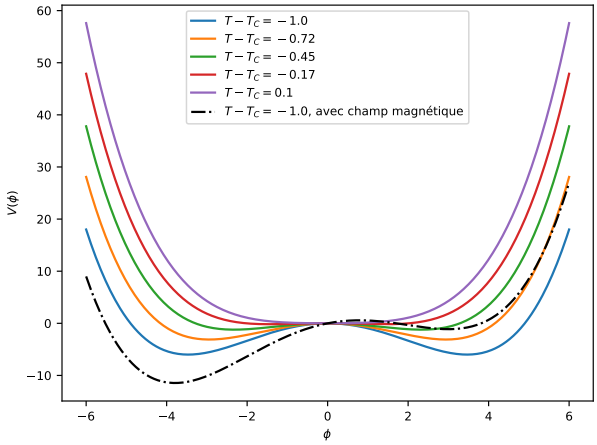

FIGURE 1.2 – Potentiel en double-puits 1.19 pour $\lambda = 1$ en fonction de la différence entre la température et la température critique avec $m^2 = T - T_C$. Dans la phase ordonnée, les mimina stables sont à $\phi_C = \pm\sqrt{-\frac{6m^2}{\lambda}}$, pour la phase désordonnée à $\phi_C = 0$. En noir, l'ajout d'un champ magnétique uniforme $h(\mathbf{x}) = 1$ rend la phase positive métastable.

double-well

$$V(\phi) = \frac{1}{2}m^2\phi^2 + \frac{\lambda}{4!}\phi^4 \tag{1.19}$$

where $m^2 = T - T_C$. For $m^2 < 0$, the minima are at $\phi_C = \pm\sqrt{-\frac{6m^2}{\lambda}}\pm$, while at $m^2 \geq 0$, the single minimum is at $\phi_C = 0$. We can also couple our system with the magnetic field of Hamiltonian

$$H_1 = -\int d^d x h(\mathbf{x})\phi(\mathbf{x}) \tag{1.20}$$

As we in Fig 1.2, the addition of an uniform external field does favour one phase over the other one.

It is easy to see that

$$\frac{\delta H}{\delta\phi(\mathbf{x})} = -\kappa\nabla^2\phi(\mathbf{x}) + V'(\phi) \tag{1.21}$$

Now we return to dynamics. If we compare with systems with a discrete number of

variables we should have a Langevin equation of the form

$$\frac{\partial\phi(\mathbf{x})}{\partial t} = -L\frac{\delta H}{\delta\phi(\mathbf{x})} + \eta(\mathbf{x},t). \tag{1.22}$$

The white noise correlator should have the form

$$\langle\eta(\mathbf{x},t)\eta(\mathbf{x}',t)\rangle = \delta(t-t')\Gamma(\mathbf{x},\mathbf{x}'), \tag{1.23}$$

where here $\Gamma(\mathbf{x},\mathbf{x}')$ is an operator (before it was a matrix) defined by its action on functions f as

$$\Gamma f(\mathbf{x}) = \int d\mathbf{x}'\Gamma(\mathbf{x},\mathbf{x}')f(\mathbf{x}'), \tag{1.24}$$

and L is also an operator with

$$Lf(\mathbf{x}) = \int d\mathbf{x}'L(\mathbf{x},\mathbf{x}')f(\mathbf{x}'), \tag{1.25}$$

Following the same arguments for systems with a finite number of degrees of freedom we thus have the relation (which is sometimes called the fluctuation dissipation theorem as it essentially is equivalent)

$$\Gamma(\mathbf{x},\mathbf{x}') = 2TL(\mathbf{x},\mathbf{x}'). \tag{1.26}$$

The simplest form of dynamics is given by $L(\mathbf{x},\mathbf{x}') = \alpha\delta(\mathbf{x}-\mathbf{x}')$ which gives the model A dynamics

$$\frac{\partial\phi(\mathbf{x})}{\partial t} = -\alpha\frac{\delta H}{\delta\phi(\mathbf{x})} + \eta(\mathbf{x},t), \tag{1.27}$$

with the noise correlator

$$\langle\eta(\mathbf{x},t)\eta(\mathbf{x}',t)\rangle = 2T\alpha\delta(t-t')\delta(\mathbf{x}-\mathbf{x}'). \tag{1.28}$$

The average value of ϕ

$$\overline{\phi}(t) = \frac{1}{V}\int d\mathbf{x}\ \phi(\mathbf{x},t), \tag{1.29}$$

is clearly not generally conserved by this dynamics.

Model B dynamics amounts to choosing

$$L(\mathbf{x}-\mathbf{x}') = -D\nabla^2\delta(\mathbf{x}-\mathbf{x}'), \tag{1.30}$$

here the fact that L is a positive semi-definite operator can be seen by taking its Fourier transform. The evolution equation here is

$$\frac{\partial \phi(\mathbf{x})}{\partial t} = D\nabla^2 \frac{\delta H}{\delta \phi(\mathbf{x})} + \eta(\mathbf{x}, t), \tag{1.31}$$

and where

$$\langle \eta(\mathbf{x}, t)\eta(\mathbf{x}', t)\rangle = -2TD\delta(t - t')\nabla^2\delta(\mathbf{x} - \mathbf{x}'). \tag{1.32}$$

We notice that if we introduce the vectorial white noise with components $\eta_i(\mathbf{x}, t)$ such that

$$\langle \eta_i(\mathbf{x}, t)\eta_i(\mathbf{x}', t')\rangle = \delta_{ij}\delta(\mathbf{x} - \mathbf{x}')\delta(t - t), \tag{1.33}$$

where $\delta_{ij} = 1$ for $i = j$ and is zero otherwise, we can write

$$\eta(\mathbf{x}, t) = \nabla \cdot \boldsymbol{\eta}(\mathbf{x}, t), \tag{1.34}$$

as one can verify the two noises have the same correlation function. In this way Eq. (1.31) becomes

$$\frac{\partial \phi(\mathbf{x})}{\partial t} = \nabla \cdot [D\nabla \frac{\delta H}{\delta \phi(\mathbf{x})} + \boldsymbol{\eta}(\mathbf{x}, t)]. \tag{1.35}$$

From this it is easy to see that the order parameter is conserved - thus model B describes conserved phase ordering dynamics.

1.2.1 Surface tension

If there is non constraint on the system if can simply chose $\phi(\mathbf{x}) = \phi_c$ or $\phi(\mathbf{x}) = -\phi_c$ everywhere which corresponds to a free energy $F = H[\phi_c] = 0$. However in a system with a conserved order parameter

$$\int d\mathbf{x}\ \phi(\mathbf{x}) = 0, \tag{1.36}$$

then the solutions $\phi = \pm\phi_c$ cannot hold. In this case the system will separate into a two phases where $\phi(\mathbf{x}) = \pm\phi_c$. We therefore choose an interface at $z = 0$ where and take $\phi(\mathbf{x}) = \phi_K(z)$ (K standing for kink as it is known as the kink solution in the literature) where $\lim_{z\to\infty} = -\phi_c$ and $\lim_{z\to\infty} = -\phi_c$. We therefore find from Eq. (1.21) that

$$-\kappa \frac{d^2}{dz^2}\phi_K(z) + V'(\phi_K) = 0 \tag{1.37}$$

This equation can be solved for the potential in (**??**) (*you should do it and fill in the details*) but even without knowing the explicit solution we can write

$$H[\phi_K] = A \int dz \; \frac{\kappa}{2} \left(\frac{d\phi_K(z)}{dz} \right)^2 + V(\phi_K(z)), \tag{1.38}$$

where A is the surface area of the system in the plane perpendicular to the direction z. However if we multiply Eq. (1.37) by $d\phi/dz$ and integrate we find

$$-\frac{\kappa}{2}(\frac{d\phi_K}{dz})^2 + V(\phi_K) = C, \tag{1.39}$$

where C is a constant. However as $\phi_K(z) \to \pm\phi_c$ as $z \to \pm\infty$ and $V(\pm\phi_c) = 0$ we find that $C = 0$. Using this we obtain

$$H[\phi_K] = A \int dz \; \kappa \left(\frac{d\phi_K(z)}{dz} \right)^2. \tag{1.40}$$

If the interface has a free energy per unit area of σ then we have the Cahn-Hillard estimate of the surface tension

$$\sigma = \int dz \; \kappa \left(\frac{d\phi_K(z)}{dz} \right)^2. \tag{1.41}$$

Dans le cas du modèle ϕ^4 définie à l'équation 1.19, l'équation **??** devient

$$\kappa\phi_K''(z) = m^2\phi_K(z) \left(1 + \phi_C\phi_K(z)^2\right) \tag{1.42}$$

Dans le modèle, le comportement est seulement déterminé par le ratio entre m^2 et λ. Posons donc sans perte de généralité $\phi_C = 1$. La solution est

$$\phi_K(z) = \phi_C \tanh\left(\frac{z}{\xi}\right) \tag{1.43}$$

où $\xi = \sqrt{\frac{-2\kappa}{m^2}}$. Cette longueur de corrélation diverge lorsque $T \to T_C$. On remarque que pluys la longueur de corrélation augmente, plus la dérivée de l'interface est faible, menant à une diminution de la tension superficielle **??**. Aussi, l'étude expérimentale des systèmes quasi-critiques est une porte d'accès pour l'étude des systèmes à ultra basse tension superficielle [4]. De tels systèmes sont extrêmement sensibles aux instabilités hydrodynamiques causées par l'agitation thermique, présentant de nombreuses applications en microfluiidque

par exemple [5].

1.3 Models for equilibrium interfaces

Here we discuss effective models of interfaces. The simplest model is to assume that the interface is parameterised by a height profile $h(\mathbf{r})$, however one also has to assume that $h(\mathbf{r})$ is a single valued function of $\mathbf{r}$. Given this one can write

$$H[h] = \sigma A[h] \tag{1.44}$$

where A_h is the area of the interface. However the interface area is given by

$$A[h] = \int_A d\mathbf{r}\sqrt{1 + [\nabla h]^2}, \tag{1.45}$$

where the integral is over the plane perpendicular to the z axis which is taken to be of area A. When the fluctuations of the interface are small, we can expand the above to quadratic order in h to obtain

$$H[h] = A\sigma + \frac{\sigma}{2}\int_A d\mathbf{r}\ [\nabla h]^2. \tag{1.46}$$

The first term is independent of the height so we can write the effective Hamiltonian for the surface as

$$H_{eff}[h] = \frac{\sigma}{2}\int_A d\mathbf{r}\ [\nabla h]^2. \tag{1.47}$$

The basic model describing the height of an interface at $z = h(\mathbf{x})$ above a plane with coordinates $\mathbf{x}$ has the Hamiltonian

$$H[h] = \int d\mathbf{x}\frac{\sigma}{2}[\nabla h(\mathbf{x})]^2 + V(h(\mathbf{x})). \tag{1.48}$$

The first term corresponds to the surface energy for a surface of size A_s

$$H_s[h] = \sigma A_s = \sigma\int d\mathbf{x}\sqrt{1 + [\nabla h(\mathbf{x})]^2} \approx \sigma A + \frac{\sigma}{2}\int d\mathbf{x}[\nabla h(\mathbf{x})]^2. \tag{1.49}$$

Here A is the area of the projected plane below the surface which is taken to be constant and thus does not change the statistical mechanics of the system. In principle surfaces can also have bending energies, while surface energies correspond to stretching the surface to increase its size, bending energies correspond to curving the surface. The standard bending

energy for small surface energies is given by

$$H_b[h] = \int d\mathbf{x} \frac{\kappa_b}{2} [\nabla^2 h(\mathbf{x})]^2, \tag{1.50}$$

where κ_b is called the bending rigidity.

The term $V(h)$ is taken to represent the potential energy of the surface. For instance if the surface interacts via an infinite hard core potential with a solid surface at $z = 0$, this can be modelled by the potential $V(z) = 0$ for $z\rangle 0$ and $V(z) = \infty$ for $z \leq 0$. Another example is where the surface describes the surface of a liquid such as water, again with a solid surface at $z = 0$, in the presence of gravity the potential energy of the water column above the area element $d\mathbf{x}$ is given by

$$\delta V = \int_0^{h(\mathbf{x})} dz \ \rho g z = \frac{1}{2} \rho g h^2(\mathbf{x}), \tag{1.51}$$

where ρ is the (mass) density of the liquid. This then gives

$$H[h] = \int d\mathbf{x} \frac{\sigma}{2} [\nabla h(\mathbf{x})]^2 + \frac{1}{2} \rho g h^2(\mathbf{x}). \tag{1.52}$$

We see that the correlation length of the interface is given by

$$\xi = \left(\frac{\sigma}{\rho g} \right)^{\frac{1}{2}}. \tag{1.53}$$

In the more general context if $V(h)$ has a minimum at some point h_m we can write $h = h_f(\mathbf{x}) + h_m$, where $h_f(\mathbf{x})$ represents the height fluctuations about the mechanically stable flat interface $h(\mathbf{x}) = h_m$. Now expand assuming that $h_f(\mathbf{x})$ is small we find the effective Hamiltonian for the fluctuations

$$H_{eff}[h_f] = \int d\mathbf{x} \frac{\sigma}{2} [\nabla h_f(\mathbf{x})]^2 + \frac{1}{2} V''(h_m) h_f^2(\mathbf{x}), \tag{1.54}$$

where we have dropped the constant term $AV(h_m)$. The above field theory is Gaussian and so, when the approximations made to derive it are valid, all of the statistical properties of the height fluctuations can be deduced. However for general potentials $V(h)$ the model cannot be solved exactly in two dimensions but can in principle be solved in one dimension as we will see below.

1.4 Effective dynamics of interface heights

We will now try and derive an approximation for the dynamics of the height of the interface from the original phase ordering kinetics. Here we use the method of Bray and Cavagnha - put in the reference, which was used to study the dynamics of sheared interfaces, in the absence of shear to determine the dynamical properties of interfaces in phase separated systems for both model A and model B dynamics.

We imagine that the system is phase separated in the direction z, on average the interface is taken to be at $z = 0$, and we write

$$\phi(z, \mathbf{r}, t) = f(z - h(\mathbf{r}, t)) \tag{1.55}$$

where $f(z) = \phi_K(z)$ is the kink solution from mean field theory.

1.4.1 Model A dynamics

For model A dynamics, we substitute Eq. (1.55) into Eq. (1.27) and make use of the following results

$$\frac{\partial f(z - h(\mathbf{r}, t))}{\partial t} = -f'(z - h(\mathbf{r}, t))\frac{\partial h(\mathbf{r}, t)}{\partial t} \tag{1.56}$$

$$\nabla f(z - h(\mathbf{r}, t)) = [\mathbf{e}_z - \nabla h(\mathbf{r}, t)] f'(z - h(\mathbf{r}, t)) \tag{1.57}$$

$$\nabla^2 f(z - h(\mathbf{r}, t)) = f''(z - h(\mathbf{r}, t)) - \nabla^2 h(\mathbf{r}, t) f'(z - h(\mathbf{r}, t)) + [\nabla h(\mathbf{r}, t)]^2 f''(z - h(\mathbf{r}, t)) \tag{1.58}$$

and thus find

$$-f'(z - h(\mathbf{r}, t))\frac{\partial h(\mathbf{r}, t)}{\partial t} = \alpha\kappa \times \tag{1.59}$$

$$\Big[f''(z - h(\mathbf{r}, t)) - \nabla^2 h(\mathbf{r}, t) f'(z - h(\mathbf{r}, t)) + [\nabla h(\mathbf{r}, t)]^2 f''(z - h(\mathbf{r}, t))\Big] - \alpha V'(f'(z - h(\mathbf{r}, t))) + \eta(\mathbf{r}, t) \tag{1.60}$$

We now multiply both sides of this equation by $f'(z - h(\mathbf{r}, t))$ and defining $\zeta = z - h(\mathbf{r}, t)$ we integrate ζ over $[-\infty, \infty]$ and use the following identities

$$\int_{-\infty}^{\infty} d\zeta f'(\zeta) f''(\zeta) = [\frac{1}{2} f'^2(\zeta)]_{-\infty}^{\infty} = 0 \tag{1.61}$$

$$\int_{-\infty}^{\infty} d\zeta f'(\zeta) V'(f) = \int_{-\infty}^{\infty} d\zeta \frac{dV(f)}{d\zeta} = [V(f(\zeta))]_{-\infty}^{\infty} = 0, \tag{1.62}$$

note that the first relation above holds as $f(\zeta) = \pm\phi_c$ as $\zeta \to \pm\infty$ and the second as $V(\phi_c) = V(-\phi_c) = 0$. The terms that are left then give

$$-\int_{-\infty}^{\infty} f'^2(\zeta)d\zeta \ \frac{\partial h(\mathbf{r},t)}{\partial t} = -\alpha \int_{-\infty}^{\infty} f'^2(\zeta)d\zeta \ \kappa\nabla^2 h(\mathbf{r},t) + \int_{-\infty}^{\infty} d\zeta \eta(\mathbf{r},\zeta + h(\mathbf{r},t))f'(\zeta) \tag{1.63}$$

Now using the Cahn-Hillard estimate of the surface tension Eq. (1.41) this becomes

$$\frac{\sigma}{\kappa}\frac{\partial h(\mathbf{r},t)}{\partial t} = \alpha\sigma\nabla^2 h(\mathbf{r},t) + \xi(\mathbf{r},t), \tag{1.64}$$

where the noise term is given by

$$\xi(\mathbf{r},t) = \int_{-\infty}^{\infty} d\zeta \eta(\mathbf{r},\zeta + h(\mathbf{r},t))f'(\zeta) \tag{1.65}$$

The noise term has zero mean and correlation function

$$\langle \xi(\mathbf{r},t)\xi(\mathbf{r}',t')\rangle = 2\alpha T\delta(t-t')\delta(\mathbf{r}-\mathbf{r}') \int_{-\infty}^{\infty} d\zeta d\zeta' \delta(\zeta-\zeta')f'(\zeta)f'(\zeta') \tag{1.66}$$

$$= 2\alpha T\delta(t-t')\delta(\mathbf{r}-\mathbf{r}') \int_{-\infty}^{\infty} d\zeta f'^2(\zeta) = \frac{2\alpha T\sigma}{\kappa}\delta(t-t')\delta(\mathbf{r}-\mathbf{r}') \tag{1.67}$$

This now gives

$$\frac{\partial h(\mathbf{r},t)}{\partial t} = \kappa\alpha\nabla^2 h(\mathbf{r},t) + \eta(\mathbf{r},t) \tag{1.68}$$

where

$$\langle \eta(\mathbf{r},t)\eta(\mathbf{r}',t')\rangle = \frac{2\alpha T\kappa}{\sigma}\delta(t-t')\delta(\mathbf{r}-\mathbf{r}'). \tag{1.69}$$

Now defining $\alpha' = \frac{\kappa\alpha}{\sigma}$ we can write

$$\frac{\partial h(\mathbf{r},t)}{\partial t} = \alpha'\sigma\nabla^2 h(\mathbf{r},t) + \eta(\mathbf{r},t). \tag{1.70}$$

This has the form of model A dynamics (as in Eq. (1.27)) for the height profile with Hamiltonian H_{eff} as given in (1.47), that is to say we can write

$$\frac{\partial h(\mathbf{r},t)}{\partial t} = -\alpha'\frac{\delta H_{eff}[h]}{\delta h(\mathbf{r})} + \eta(\mathbf{r},t), \tag{1.71}$$

and where

$$\langle \eta(\mathbf{r},t)\eta(\mathbf{r}',t')\rangle = 2T\alpha'\delta(t-t'). \tag{1.72}$$

This dynamical calculation is thus consistent with the idea of describing the surface in terms of a height variable with an energy given by the surface tension. The equation (1.71) is known as the Edwards-Wilkinson equation. We can use this equation to determine how the domains of a coarsening systems grow at low temperatures. To do this we ignore the noise term and assume that at $t = 0$ the correlations of the height are short range so

$$C(\mathbf{r} - \mathbf{r}', 0) = \langle h(\mathbf{r}, 0)h(\mathbf{r}', 0)\rangle = C_0\delta(\mathbf{r} - \mathbf{r}'). \tag{1.73}$$

In Fourier space the noiseless Edwards-Wilkinson equation becomes

$$\frac{\partial\tilde{h}(\mathbf{k}, t)}{\partial t} = -\alpha'\sigma\tilde{h}(\mathbf{k}, t), \tag{1.74}$$

and so we find

$$\tilde{h}(\mathbf{k}, t) = h(\mathbf{k}, 0)\exp(-\alpha'\sigma\mathbf{k}^2 t). \tag{1.75}$$

We thus find

$$\langle\tilde{h}(\mathbf{k}, t)\tilde{h}(\mathbf{k}', t')\rangle = \langle h(\mathbf{k}, 0)h(\mathbf{k}', 0)\rangle\exp(-\alpha'\sigma[k^2 + k'^2]t). \tag{1.76}$$

Now recall that if

$$\langle h(\mathbf{r}, t)h(\mathbf{r}', t')\rangle = C(\mathbf{r} - \mathbf{r}', t) \tag{1.77}$$

then

$$\langle\tilde{h}(\mathbf{k}, t)\tilde{h}(\mathbf{k}', t')\rangle = (2\pi)^d\delta(\mathbf{k} + \mathbf{k}')\tilde{C}(\mathbf{k}, t), \tag{1.78}$$

where

$$\tilde{C}(\mathbf{k}, t) = \int d\mathbf{r}\exp(-i\mathbf{k}\cdot\mathbf{r})C(\mathbf{r}, t), \tag{1.79}$$

is the Fourier transform of the correlation function which is a function of a single position due to invariance by translation in space, and d is the dimension of space (so here $d = 2$ for a surface in 3d space and $d = 1$ for a surface in a 2d space). Putting all this together gives

$$\tilde{C}(\mathbf{k}, t) = C_0\exp(-2\alpha'\sigma k^2 t). \tag{1.80}$$

Inverting the Fourier transform gives

$$C(\mathbf{r}, t) = \frac{C_0}{(8\pi\alpha'\sigma t)^{\frac{d}{2}}}\exp(-\frac{\mathbf{r}^2}{16\pi\alpha'\sigma t}). \tag{1.81}$$

From this we see that if $C(\mathbf{r},t) \sim g(\frac{\mathbf{r}}{\ell(t)})r(t)$ then the length scale $\ell(t) \sim t^{\frac{1}{2}}$, this agrees with is found in the Ising model under Glauber dynamics, where the growth exponent is also given by $z = \frac{1}{2}$.

1.4.2 Model B dynamics

For model B dynamics, we take the same ansatz as in Eq. (1.55) but we rewrite the model B dynamics as

$$-\nabla^{-2}\frac{\partial\phi(\mathbf{x},t)}{\partial t} = -D\frac{\delta H}{\delta\phi(\mathbf{x})} + \theta(\mathbf{x},t), \tag{1.82}$$

here $-\nabla^{-2}$ represents the Green's function G which obeys

$$\nabla^2 G(\mathbf{x}-\mathbf{x}') = -\delta(\mathbf{x}-\mathbf{x}'), \tag{1.83}$$

and

$$\theta(\mathbf{x},t) = -\nabla^{-2}\eta(\mathbf{x},t) = \int d\mathbf{x}' G(\mathbf{x}-\mathbf{x}')\eta(\mathbf{x},t) \tag{1.84}$$

The correlation function of $\theta(\mathbf{x},t)$ is given by

$$\begin{aligned}
\langle\theta(\mathbf{x},t)\theta(\mathbf{y},t')\rangle &= -2DT\delta(t-t')\int d\mathbf{x}' G(\mathbf{x}-\mathbf{x}')d\mathbf{y}' G(\mathbf{y}-\mathbf{y}')\nabla^2\delta(\mathbf{x}'-\mathbf{y}') && (1.85)\\
&= -2DT\delta(t-t')\int d\mathbf{x}' G(\mathbf{x}-\mathbf{x}')d\mathbf{y}'\nabla^2 G(\mathbf{y}-\mathbf{y}')\delta(\mathbf{x}'-\mathbf{y}') && (1.86)\\
&= 2DT\delta(t-t')G(\mathbf{x}-\mathbf{y}). && (1.87)
\end{aligned}$$

where we have integrated by parts in the second line and used

$$-\nabla^2 G(\mathbf{y}-\mathbf{y}') = \delta(\mathbf{y}-\mathbf{y}'), \tag{1.88}$$

in the third.

Now mutliplying by $f'(z-h(\mathbf{r},t))$ and integrating z over $[-\infty,\infty]$, we find

$$\begin{aligned}
&-\int dz f'(z-h(\mathbf{r},t))\int dz' d\mathbf{r}'\ G(z-z',\mathbf{r}-\mathbf{r}')f'(z'-h(\mathbf{r}',t))\frac{\partial h(\mathbf{r}',t)}{\partial t} = && (1.89)\\
&-D\sigma\nabla^2 h(\mathbf{r},t) + \chi(\mathbf{r},t), && (1.90)
\end{aligned}$$

with the noise

$$\chi(\mathbf{r},t) = \int dz f'(z-h(\mathbf{r},t))\theta(\mathbf{r},z,t). \tag{1.91}$$

As we assume that the height fluctuations are small we keep only the lowest order terms in h in the deterministic terms and the noise, we will see later that this is compatible thermodynamically. We thus have

$$-\int dz\ f'(z)\int dz' d\mathbf{r}'\ G(z-z',\mathbf{r}-\mathbf{r}')f'(z')\frac{\partial h(\mathbf{r}',t)}{\partial t} = \tag{1.92}$$

$$-D\sigma\nabla^2 h(\mathbf{r},t)+\chi(\mathbf{r},t), \tag{1.93}$$

and now the noise is given by

$$\chi(\mathbf{r},t) = \int dz\ f'(z)\theta(\mathbf{r},z',t). \tag{1.94}$$

This equation which is linear in h can now be Fourier transformed in the plane $\mathbf{r}$ and in terms of the Fourier transform of h we find

$$-\int dz\ f'(z)\int dz' d\mathbf{r}'\ \tilde{G}(z-z',\mathbf{k})f'(z')\frac{\partial \tilde{h}(\mathbf{k},t)}{\partial t} = Dk^2\sigma\tilde{h}(\mathbf{k},t)+\tilde{\chi}(\mathbf{k},t). \tag{1.95}$$

The Fourier transform of G in the $\mathbf{r}$ plane obeys

$$\frac{d^2\tilde{G}(z-z',\mathbf{k})}{dz^2} - k^2\tilde{G}(z-z',\mathbf{k}) = -\delta(z-z') \tag{1.96}$$

and the solution to this equation (with the boundary condition that $\tilde{G}(z-z',\mathbf{k})\to 0$ as $|z-z'|\to\infty$) is

$$\tilde{G}(z-z',\mathbf{k}) = \frac{\exp(-k|z-z'|)}{2k}, \tag{1.97}$$

and note that $k=|\mathbf{k}|$. Next we make the sharp interface approximation where we write

$$f(z) = 2\phi_c\delta(z), \tag{1.98}$$

that is to say we have replaced the smooth kink solution with a step like solution $f(z)=\phi_c\,\mathrm{sgn}(z)$. This then gives

$$-4\phi_c^2\tilde{G}(0,k)\frac{\partial h(\mathbf{k},t)}{\partial t} = Dk^2\sigma\tilde{h}(\mathbf{k},t)+\tilde{\chi}(\mathbf{k},t), \tag{1.99}$$

which we rewrite as

$$\frac{\partial \tilde{h}(\mathbf{k},t)}{\partial t} = -\frac{Dk^3\sigma}{2\phi_c^2}\tilde{h}(\mathbf{k},t) + \tilde{\xi}(\mathbf{k},t), \tag{1.100}$$

with

$$\tilde{\xi}(\mathbf{k},t) = -\frac{k}{2\phi_c^2}\tilde{\chi}(\mathbf{k},t), \tag{1.101}$$

where

$$\tilde{\chi}(\mathbf{k},t) = \int dz\ f'(z)\tilde{\theta}(\mathbf{k},z,t), \tag{1.102}$$

The correlation function of $\tilde{\theta}(\mathbf{k},t)$ is

$$\langle\theta(\mathbf{k},t)\theta(\mathbf{k}',t')\rangle = 2DT(2\pi)^d\delta(t-t')\delta(\mathbf{k}+\mathbf{k}')\tilde{G}(z-z',k) \tag{1.103}$$

and from this we find

$$\langle\chi(\mathbf{k},t)\chi(\mathbf{k}',t')\rangle = 2DT(2\pi)^d\delta(t-t')\delta(\mathbf{k}+\mathbf{k}')\int dzdz' f(z)f(z')\tilde{G}(z-z',k), \tag{1.104}$$

now using the sharp interface approximation Eq. (1.98) we obtain

$$\langle\chi(\mathbf{k},t)\chi(\mathbf{k}',t')\rangle = 2DT(2\pi)^d\delta(t-t')\delta(\mathbf{k}+\mathbf{k}')\frac{2\phi_c^2}{k}, \tag{1.105}$$

and consequently

$$\langle\xi(\mathbf{k},t)\xi(\mathbf{k}',t')\rangle = 2DT(2\pi)^d\delta(t-t')\delta(\mathbf{k}+\mathbf{k}')\frac{k}{2\phi_c^2}. \tag{1.106}$$

Finally in we find the interface dynamics for model B in Fourier space is

$$\frac{\partial h(\mathbf{k},t)}{\partial t} = -\frac{Dk^3\sigma}{2\phi_c^2}\tilde{h}(\mathbf{k},t) + \tilde{\xi}(\mathbf{k},t), \tag{1.107}$$

In real space this has the form

$$\frac{\partial h(\mathbf{r})}{\partial t} = -L\frac{\delta H_{eff}}{\delta h(\mathbf{r})} + \xi(\mathbf{r},t). \tag{1.108}$$

where the operator L is defined via its Fourier transform

$$\tilde{L}(\mathbf{k}) = \frac{Dk}{2\phi_c^2}. \tag{1.109}$$

Now if we look at Eq. (1.107) we see that solving the equation without noise will give a function of $k^3 t$, which in real space corresponds to x^3/t. From this we see that the coarsening length scale grows as $\ell(t) \sim t^{\frac{1}{3}}$ and consequently the coarsening exponent is $z = \frac{1}{3}$. Coarsening for conserved model B or diffusive dynamics is slower than that of model A. One of the reasons for this slowing down with respect to nonconserved dynamics is that material must be physically transported by diffusion (by exchanging spins in the language of lattice spin models), where as for model A dynamics the composition can change at any given point by *spin flipping*. As a cautionary note, if we had taken the Hamiltonian in Eq. (1.47) and applied model B conserved dynamics, as in Eq. (1.31), for the height field we would not have obtained this equation.

We can actually do better than the above sharp interface approximation as Eq. (1.95) can be written as

$$Q(k)\frac{\partial \tilde{h}(\mathbf{k},t)}{\partial t} = -Dk^2\sigma\tilde{h}(\mathbf{k},t) - \tilde{\chi}(\mathbf{k},t). \tag{1.110}$$

where

$$Q(k) = \int dz dz' \; f'(z) \; \tilde{G}(z-z',\mathbf{k}) f'(z'). \tag{1.111}$$

Notice that from Eq. (1.110) that

$$\langle \chi(\mathbf{k},t)\chi(\mathbf{k}',t')\rangle = 2DT(2\pi)^d \delta(t-t')\delta(\mathbf{k}+\mathbf{k}')Q(k) \tag{1.112}$$

and so

$$\frac{\partial \tilde{h}(\mathbf{k},t)}{\partial t} = -\tilde{L}(k)\tilde{\mu}(\mathbf{k}) + \eta(\mathbf{k}), \tag{1.113}$$

where $\mu(\mathbf{x}) = \delta H_{eff}/\delta h(\mathbf{x})$ and $\tilde{L}(k) = D/Q(k)$ and

$$\langle \eta(\mathbf{k},t)\eta(\mathbf{k}',t')\rangle = 2T(2\pi)^d \delta(t-t')\delta(\mathbf{k}+\mathbf{k}')\tilde{L}(k). \tag{1.114}$$

1.5 Systems driven by imposed hydrodynamic flows

Here you need to discuss the experiments get some nice photos etc

Here we consider what happens when a system is driven out of equilibrium, by driven we mean that energy is injected into the system by a laser for instance as discussed in the introduction or by inducing a hydrodynamics flow, for instance a shear flow induced in a Couette cell. In principle we should analyse this system with model H dynamics which

couples diffusive model B dynamics to hydrodynamics in the low Reynolds number Stokes flow regime. In this dynamics the order parameter field will itself induce a hydrodynamics flow which will modify the imposed one. However this full situation is very difficult to analyse and to a first approximation we can assume that the back reaction of the order parameter field on the hydrodynamic flow is small with respect to the imposed hydrodynamic flow and so we can simply write

$$\frac{\partial \phi(\mathbf{x},t)}{\partial t} + \nabla \cdot (\mathbf{v}(\mathbf{x})\phi(\mathbf{x},t)) = -L\frac{\delta H}{\delta \phi(\mathbf{x})} + \eta(\mathbf{x},t), \tag{1.115}$$

where L is given by the underlying model A or B dynamical operatorand the noise has the correlation function as given by Eq. (1.26), and $\mathbf{v}(\mathbf{x})$ is the imposed (time independent) hydrodynamic flow or can equally well be an external drive imposed on the colloidal particles, due to the gravitational or electric field for example.

The simplest case one can consider is where the driving field $\mathbf{v}(\mathbf{x}) = \mathbf{v}_0$ is uniform . Unfortunately this simple driving does not lead to a new steady state. Basically all of the colloidal particles acquire an an average velocity $\mathbf{v}$ and so move along at the same speed relative to each other. Mathematically this can be seen by making the Galilean transformation

$$\phi(\mathbf{x},t) = \phi(\mathbf{x} - \mathbf{v}_0 t, t) = \phi(\mathbf{y},t). \tag{1.116}$$

this transform eliminates the driving from the evolution equation (1.115) and so we find an equilibrium system.

The most studies example is where the driving is a shear flow, this corresponds to the experiments of Derks et al and the numerical simulations of Smith et al and the analytical work of Bray and Cavagnah. In Bray and Cavagna, the effective dynamics of the surface term in the presence of a shear flow, parallel to the interface,

$$\mathbf{v}(\mathbf{x}) = \gamma z \mathbf{e}_x \tag{1.117}$$

was studied using the method explained in section (1.4). The addition of a shear flow leads to the appearance of a nonlinear term in h and the interface statistics thus become non-Gaussian.

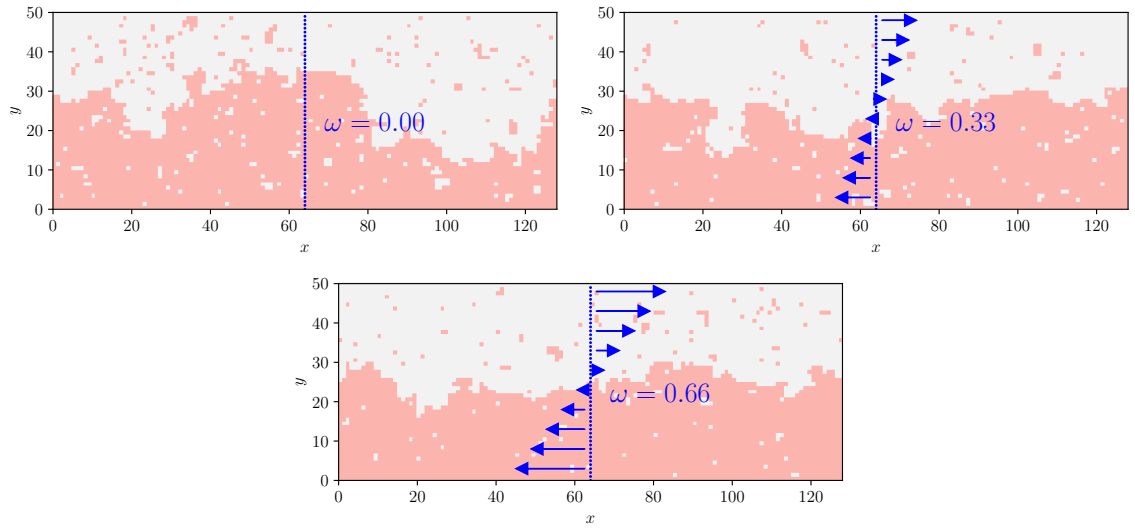

FIGURE 1.3 – Photos d'un système d'Ising en fonction du cisaillement **??** via des simulations de Monte Carlo avec un algorithme de Kawasaki. Ledit algorithme sera expliqué plus en détail au chapitre 2.

1.6 Lattice models

Comme indiqué dans l'équation 1.1, le champ $\phi(\mathbf{x}, t)$ est un champ moyenné sur le temps et l'espace à cause de la précision de nos appareils de mesure. Si par exemple le champ ϕ représente une densité de particules, alors au niveau le plus fondamental, le champ est charactérisé par

$$\phi(\mathbf{x}, t) = \frac{1}{V} \sum_i \delta(\mathbf{x} - \mathbf{x}_i(t) \tag{1.118}$$

où V est le volume d'inégration défini par la précision de notre mesure et $\mathbf{x}_i(t)$ est la position de la particule i à l'instant t. Ainsi à l'échelle des constituants du système, le champ est discontinu. Cette discontnuité inhérente du système microscopique nous mène naturellement sur des modèles de particules sur réseau. Dans les modèles sur réseau, nous fixons un ensemble de positions $\{\mathbf{x}_i\}$ que les particules peuvent occuper, puis nous regardons l'évolution temporelle d'un tel système en fonctoins des interactions désirées entre les sites.

Nous nous intéressons ici aux modèles sur réseaux cubiques, de taille $L' \times L' \times L$, dont le modèle d'Ising est le plus connu. Nous développons les principaux résultats obtenus

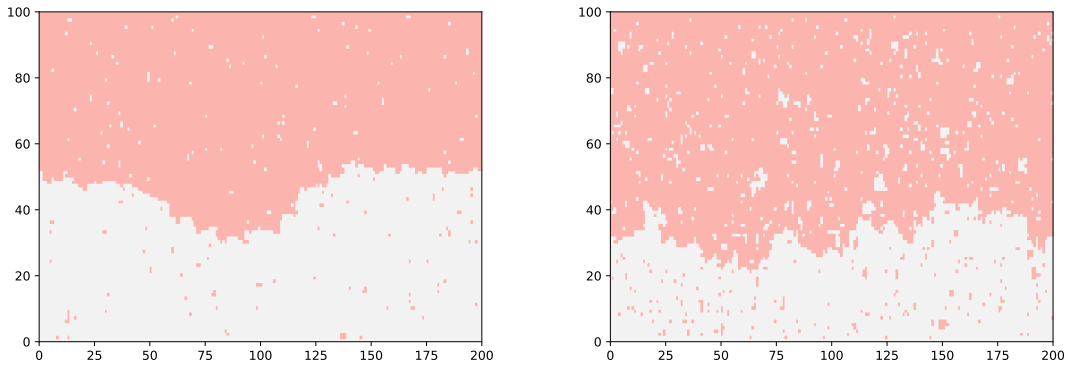

FIGURE 1.4 – Photo d'un modèle d'Ising pour deux températures différentes($T = 0.7T_C$ et $T = 0.95T_C$) avec des conditions périodiques aux bords en X et fixés en Y qui forcent la présence d'une interface entre les phases + (rose) et − (blanc) du système. Plus la température est élevée et plus l'interface fluctue, jusqu'à cesser d'exister pour $T > T_C$.

dans les modèles d'Ising pour la force de Casimir critique et l'importance des forces de cisaillement sur les propriétés des interfaces. Puis nous expliquerons un modèle à $(d-1)$ dimension du modèle d'Ising à basse température, le **modèle Solid-On-Solid** (SOS), avec les techniques propres au système 1D de la matrice de transfert ainsi que les propriétés analytiques de l'interface déjà connues.

La discrétisation du champ $\phi(\mathbf{x}, t)$ afin de faire des simulations numériques mène naturellement vers le modèle sur réseau par excellence, le modèle d'Ising. À partir de deux dimensions, ce modèle de particules à interaction avec les plus proches voisins, possède une transition de second ordre depuis une phase ordonnée vers une phase désordonnée. Si lon suppose l'énergie d'interactiosn entre toutes les particules plus proches voisins égale à J, la température critique est $\beta_{C,2D} = \frac{\ln(1+\sqrt{2})}{2} J \simeq 0.44J$ en deux dimensions [2]. et $\beta_{C,3D} \simeq 0.22J$ en trois dimensions [6] (via des simulations de Monte Carlo).

1.6.1 Le modèle d'Ising

Nous rappelons l'Hamiltonien **??** du champ moyen

$$H[\phi] = \int d\mathbf{x} \frac{\kappa}{2} [\boldsymbol{\nabla}\phi]^2 + V(\phi) \tag{1.119}$$

où $V(\phi)$ est un potentiel de possédant deux minima en $\phi_C = \pm 1$. On considère maintenant que le champ sur les sites de notre réseau est égal à $\pm\phi_C = \pm 1$. On note $\mathbf{i} := (x, y, z)$ le site du réseau correspondant aux coordonnées (x, y, z). Sur un réseau carré discret de pas $a = 1$, la discrétisation du premier terme au premier ordre se traduit par

$$\begin{aligned}[\boldsymbol{\nabla}\phi(\mathbf{i})]^2 &= \left(\frac{\partial\phi(\mathbf{i})}{\partial x}\right)^2 + \left(\frac{\partial\phi(\mathbf{i})}{\partial y}\right)^2 + \left(\frac{\partial\phi(\mathbf{i})}{\partial z}\right)^2 \\ &= (\phi(x,y,z) - \phi(x+1,y,z))^2 + (\phi(x,y,z) - \phi(x,y+1,z))^2 + (\phi(x,y,z) - \phi(x,y,z+1))^2 \\ &= 2(1 - \phi(x,y,z)\phi(x+1,y,z) + 2(1 - \phi(x,y,z)\phi(x,y+1,z) + 2(1 - \phi(x,y,z)\phi(x,y,z+1)\end{aligned} \tag{1.120}$$

Notons $\sigma_i = \phi(\mathbf{i}) = \pm 1$, et $J := \kappa$. On obtient alors l'Hamiltonien du modèle d'Ising

$$H = -\sum_{\langle ij\rangle} J\sigma_i\sigma_j + \frac{V(\sigma_i) + V(\sigma_j)}{2} \tag{1.121}$$

où $\sum_{\langle ij\rangle}$ est une somme sur toutes les paires de premiers voisins. Le champ externe $V(i)$ a ici été symmétrisé et le terme constant de 1.120 a été retiré. Le modèle d'Ising[7, 8] est donc un modèle sur réseau à interactions courtes entre les particules. Puisque les constituants σ_i du système sont tous égaux à $\pm$!, on appelle ce système un système de spin sur réseau. Dans le cas où la variable σ_i est continue, on parle de modèle XY. Pour plus de généralité, il est également possible de varier l'interaction entre les plus proches voisins en posant $J = J_{ij}$. Si $J_{ij} = 0$, on parle d'interaction ferromagnétique favorisant à homogénéiser le système malgré l'agitation thermique. Si $J_{ij}\langle 0$, on parle d'interaction antiferromagnétique favorise les systèmes où chaque spin possède un signe différent de celui de tous ses plus proches voisins. On prendra pour le reste de cette thèse $J = 1$.

Ce modèle décrit précisément les transitions de phases dans les matériaux magnétiques uniaxiaux [9, 10, 11]. Il est par ailleurs le modèle le plus simple à l'intérieur de sa classe d'universalité, qui contient également les transitions liquide/gaz ainsi que l'émulsion de liquides binaires. Ce modèle ne possède pas de transitions de phase en une dimension. La solution en deux dimensions a été trouvée par [2], prouvant l'existant d'une transition de phase à

$$T_{2D,C} = \frac{2J}{k_B \ln(1+\sqrt{2})} \simeq 2.27\frac{J}{k_B} \tag{1.122}$$

Puisque ce modèle découle de la discrétisation du champ moyen, ces approches donnent beaucoup d'informations sur la transition de phase et ses propriétés au point critique en 4 dimensions et au-delà, avec $d = 4$ étant la dimension critique supérieure. Cependant le modèle n'a pas encore été résolu pour $d = 3$, bien que de nombreuses simulations numériques [12] ont permis de trouver que la transition critique était à

$$T_{3D,C} \simeq 4.51 \frac{J}{k_B} \tag{1.123}$$

En faisant la transformation[13]

$$n_i = \frac{\sigma_i + 1}{2} \tag{1.124}$$

afin que $n_i(\sigma_i = 1) = 1$ et $n_i(\sigma_i = -1) = 0$, on obtient l'Hamiltonien

$$H = -\sum_{\langle ij \rangle} J_{ij} \left(4 n_i n_j - 2(n_i + n_j) + 1\right) + \sum_{\langle ij \rangle} J_{ij} \frac{V(\sigma_i) + V(\sigma_j)}{2} \tag{1.125}$$

où le terme constant $\sum_{\langle ij \rangle} J_{ij}$ ne modifie la fonction de partition Z que d'une constante. On définit alors

$$\begin{aligned} H_{LG} &= -4 \sum_{\langle ij \rangle} J_{ij} n_i n_j + 2 \sum_{\langle ij \rangle} J_{ij} (n_i + n_j) + \sum_{\langle ij \rangle} J_{ij} \frac{V(\sigma_i) + V(\sigma_j)}{2} \\ &= -4J \sum_{\langle ij \rangle} J n_i n_j + \mu \sum_i n_i + \sum_{\langle ij \rangle} J \frac{V(\sigma_i) + V(\sigma_j)}{2} \end{aligned} \tag{1.126}$$

où l'on a considéré $J_{ij} = J$ constant et définit le potentiel chimique pour les particules liquide-gaz comme $\mu = 4Jc$, avec c la connectivité du graphe ($z = 2$ en 1D, $z = 4$ en 2D et $z = 6$ en 3D). Une phase magnétique positive dans le modèle d'Ising s'apparente dès lors à un état de haute densité (un liquide), tandis qu'une phase négative est considérée comme une phase de basse densité, c'est-à-dire un gaz. Ce modèle représente également un mélange binaire entre deux types de particules A et B comme par exemple un polymère dans un solvant, les particules identiques s'attirent tandis que les particules d'un type différent se repoussent. Ici, le potentiel chimique μ est la variable conjugée au nombre de particules $\sum_i n_i$, tandis que dans les systèmes de spins, le champ magnétique h est la variable conjugée de l'aimantation $\sum_i \sigma_i$. On peut donc parler d'un champ magnétique

uniforme pour un système de spins dans l'ensemble canonique ou de potentiel chimique pour un système de particules dans l'ensemble grand-canonique, et que la physique reste la même.

needs rewriting L'étude de l'interface entre les phases + et − nécessite la brisure de la symétrie de translation au sein du système. Cela peut se réaliser via des conditions aux bords non-périodiques dans la direction z, soit avec des conditions aux bords fixes avec $\sigma(z=0)=-1$ et $\sigma(z=L)=+1$, soit en favorisant les spins sur les rangées du bords grâce à l'ajout d'un potentiel $V(z)=h(\delta(z)-\delta(z-L))$. Une interface se charactérise par sa position moyenne et sa largeur. La manière la plus simple de mesurer ces charactéristiques est de comparer le profil de magnétisation [14] dans l'axe z perpendiculaire à l'interface

$$m(z)=\frac{1}{L'^2}\langle\sum_{xy}\sigma(x,y,z)\rangle \tag{1.127}$$

aux résultats de champ moyen **??**. Le fit nous donne alors la position moyenne et la largeur de l'interface. La largeur de l'interface est définie comme le déplacement moyen autour de la moyenne, c'est-à-dire

$$w^2=\langle h^2\rangle-\langle h\rangle^2 \tag{1.128}$$

où h est la position de l'interface. On trouve alors que la largeur de l'interface est égale à

$$w^2=2\frac{\int_0^L dzz\frac{dm(z)}{dz}}{\int_0^L dz\frac{dm(z)}{dz}} \tag{1.129}$$

On définit maintenant la tension superficielle de l'interface comme la différence entre l'énergie libre en absence d'interface avec l'énergie libre de l'interface [15, 16, 17], c'est-à-dire

$$\sigma=\lim_{L',L\to\infty}\frac{1}{L'^2}\ln\left(\frac{Z^{+-}}{Z^{++}}\right) \tag{1.130}$$

où Z^{+-} est la fonciton de partition du système avec des conditions aux bords $(+-)$ et Z^{++} la fonction de partition avec des conditions aux bords Z^{++}. Par diagonalisation de la matrice de transfert du système (que nous introduirons plus tard), en absence de champ

externe, nous obtenons la tension superficielle

$$\sigma = 2\beta J + \log(\tanh(\beta J)) \tag{1.131}$$

1.6.2 Modèle Solid-On-Solid

Le modèle d'Ising permet d'étudier de nombreux systèmes différents, que ce soit pour les propriétés de bulk, la dynamique de coarsening ou les propriétés de l'interface. Dans ce dernier cas, il n'est pas nécessaire de posséder toutes les informations sur le bulk afin d'obtenir les propriétés de l'interface. Tout comme on est passés des équations de champ moyen du modèle A et B aux équations d0interface Edwards-Wilkinson, le passage d'un système entier à l'étude spécifique de l'interface peut se faire dans les modèles sur réseau. À très basse température, les interfaces sont bien délimitées et il y a très peu de clusters de la phase + dans la phase −, et vice-versa. En considérant le système très peu mélangé, il est possible de définir la présence d'une phase par rapport à la hauteur h_i de l'interface. Chaque site prend alors la valeur

$$\sigma_{i,j} = \mathrm{sgn}(h_i - j)$$

où la fonction $\mathrm{sgn}(x)$ est égale à $+1$ si $x\rangle 0$ et à -1 sinon. Cela revient à considérer que l'énergie d'interaction J_z dans l'axe perpendiculaire à l'interface est bien supérieure à l'énergie d'interaction perpendiculaire à l'interface.

En utilisant les identités

$$\min(a,b) = \frac{|a+b| - |a-b|}{2} \tag{1.132}$$

$$\max(a,b) = \frac{|a+b| + |a-b|}{2} \tag{1.133}$$

on a

$$\sum_{j=0}^{L} \mathrm{sgn}(h-j)\,\mathrm{sgn}(h'-j) = L - 2|h-h'| \tag{1.134}$$

Pour un système d'Ising en deux dimensions de taille $L' \times L$, l'Hamiltonien du modèle

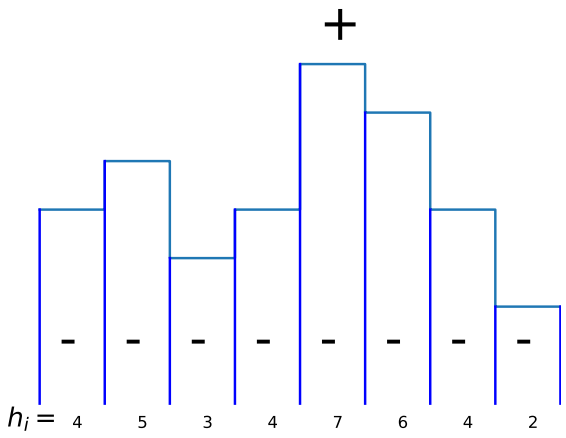

FIGURE 1.5 – Une configuration possible de modèle SOS. Dans la i-ème colonne le bord horizontal de l'interface passe à la hauteur h_i. Toutes les particules au-dessus de l'interface sont des spins positifs, et négatifs en dessous. La représentation classique du modèle SOS diffère de ce schéma par l'hypothèse que les particules sont discernables (voir Chapitre **??**).
David : pourquoi tu veux mettre cette figure dans un autre chapitre ? ?

d'Ising 1.121, se réécrit comme

$$H = 2JL'(1-L) + 2J\sum_{i=0}^{L'}|h_i - h_{i+1}| + \sum_{i=0}^{L'}V(h_i) \tag{1.135}$$

où la somme se fait maintenant sur les sites i de hauteur h_i (voir figure 1.5), et le résultat a été divisé par deux pour ne pas compter deux fois les mêmes liens, et

$$V(h_i) = \sum_{j=0}^{L} V(\mathrm{sgn}(h-j)) \tag{1.136}$$

On pose $h_{L'} = h_0$ comme conditions périodiques aux bords. On peut également calculer directement l'énergie d'un tel système depuis une configuration Solid-On-Solid. Il existe L_Y liens verticaux par colonne, dont tous sauf un ont une énergie de $-J$, et le lien passant à travers l'interface ayant une énergie de $+J$. L'énergie totale des liens verticaux est donc de $E_y = -JL_X(L_Y - 2)$. De même pour les liens horizontaux, il existe $L_X \times L_Y$ liens au total, dont $\sum_i |h_i - h_{i+1}|$ liens d'énergie $+J$, ce qui nous donne une énergie d'interaction horizontale de $E_x = -JL_XL_Y + 2\sum_i |h_i - h_{i+1}|$. La somme des deux énergies redonne 1.135.

Le terme $|h_i - h_{i+1}|$ représente la surface de contact horizontale entre les deux phases qui dépend directement de la hauteur, tandis que le terme constant représente la surface de contact verticale. En simplifiant $2J = J$ et en retirant l'énergie de volume qui est constante, nous obtenons l'hamiltonien du **modèle Solid-On-Solid** (SOS)

$$H = J\sum_{i=0}^{L'}|h_i - h_{i+1}| + \frac{V(h_i) + V(h_{i+1})}{2} \tag{1.137}$$

où l'on a symmétrisé le potentiel $V(h)$. Dans le langage liquide/gaz utilisé précédement dans le modèle d'Ising, on peut interpréter la hauteur h_i comme étant le nombre de particules au site i, avec les sites au-dessus de l'interface étant considérés comme vides. Lorsque le site i augmente d'une unité, on peut considérer qu'une particule s'est ajoutée au système, et qu'elle s'est évaporée si h_i décroit d'une unité.

La croissance des cristaux a été le premier système sur lequel le modèle SOS a été développé en 1972 [18]. Depuis, le modèle a été utilisé pour des systèmes de croissances de cristaux [19], a été trouvé en accord avec les expériences de croissance épitaxiale [20], ou

dans le cas des membranes de polymères [21].

Dans le modèle SOS, les h_i peuvent prendre n'importe quelle valeur en tre 0 et L. Une variante de ce modèle est celui où la hauteur h_{i+1} est restreinte uniquement aux valeurs comprises dans $[h_i - a, h_i + a]$. La version du modèle où $a = 1$ est appelé le modèle Solid-On-Solid Restreint (RSOS)[22]. Ce modèle est une approximation du modèle SOS à très basse température. Dans ces conditions, l'interface est très lisse puisque l'on contraint les modes excités de l'interface [23, 24].

Un modèle qui est plus proche des modèles continus comme l'Hamiltonien 1.47 possède une l'interaction gaussienne

$$H = J\sum_{i=0}^{L'}(h_i - h_{i+1})^2 + \frac{V(h_i) + V(h_{i+1})}{2} \tag{1.138}$$

qui possède également une versione restreinte. Le modèle SOS possède, quelque soit l'exposant de l'interaction, une relation étroite avec le modèle XY [25].

La dimensionalité du système a été réduite en ne prenant en compte que la hauteur h_i au site i à la place de la position de toutes les particules. L'approximation du modèle SOS implique que les configurations sont analogues à celles d'un mouvement brownien partiellement dirigé auto-évitant. Cette analogie a permis de diagonaliser complètement la fonction de partition dans le cas où il existe un champ magnétique et un potentiel confinant l'interface (nous y reviendrons au paragraphe **??**) [26] et d'étudier les statistiques des déviations extrêmes de l'interface [27, 28].

Dans l'ensemble grand-canonique, le nombre de particules dans le système varie, dépendant du potentiel chimique vis-à-vis du réservoir dans lequel il est inséré, ce qui permet à l'interface de bouger librement. Lorsque l'on se place dans l'ensemble canonique, le nombre de particules N sous l'interface est fixe, ce qui introduit une contrainte dans la fonction de partition

$$Z(N) = \sum_{h_0 h_1 \ldots h_{L'}} \exp(-\beta \sum_i H(h_i, h_{i+1}))\delta_{\sum_i h_i, N} \tag{1.139}$$

La position moyenne de l'interface est maintenant imposée, ce qui interdit certains microétats, et change les propriétés thermodynamiques de la matrice de transfert comme la distribution des hauteurs de l'interface [29], même si la moyenne reste la même. Malheureusement, il est impossible de réécrire la contrainte dans le langage des matrices de transfert,

empêchant ainsi de calculer analytiquement les différences entre les deux ensembles pour une taille donnée. Il est possible de construire la fonction de partition *ab initio*, mais le grand nombre de sites et de hauteurs permises dans un système classique empêchent le calcul dans un temps CPU raisonnable.

La fonction de partition 1.139 est en relation vis-à-vis de l'ensemble grand-canonique grâce au potentiel chimique μ par

$$\Xi(\mu) = \sum_N Z(N) \exp((\beta\mu N) \tag{1.140}$$

La grande fonction de partition peut s'écrire comme

$$\Xi = \sum_{h_0 h_1 ... h_{L'}} \exp(-\beta H_{eff}(h_0, h_1, ..., h_{L'}) \tag{1.141}$$

où

$$H_{eff} = J \sum_{i=0}^{L'} |h_i - h_{i+1}| + \sum_{i=0}^{L'} V(h_i) - \mu h_i \tag{1.142}$$

et de matrice de transfert

$$T(h, h') = \exp\left(-\beta(J|h - h'| - \mu\frac{h + h'}{2} + \frac{V(h) + V(h')}{2}\right) \tag{1.143}$$

Dans la figure 1.6, on montre le nombre moyen de particules par site en fonction du potentiel chimique, pour différentes hauteurs maximales L. Ce potentiel chimique simule une pression externe imposée, qui peut soit confiner l'interface vers $h = 0$ si $\mu < 0$ (comme sur la figure), ou le confiner vers $h = L$ si $\mu > 0$. Ainsi, l'équivalence des ensembles canonique et grand-canonique dans la limite thermodynamique à μ fixé n'est valable que lorsque le nombre de particules du système canonique N est égal au nombre de particules dans l'ensemble grand-canonique.

Comme dans le modèle d'Ising, il existe une bijection entre l'usage d'un champ magnétique conjugé à une aimantation par site et l'usage d'un potentiel chimique conjugué à une densité de particules. Nous parlerons donc sans ambigüité de potentiel chimique pour tout potentiel $V(h_i)$ que nous étudierons plus tard, ainsi que de densité de particules M.

Note that the case where $V(h) = P_0 h$ simulates the SOS with and externally imposed pressure. This model is also equivalent mathematically to the SOS model in a grand ca-

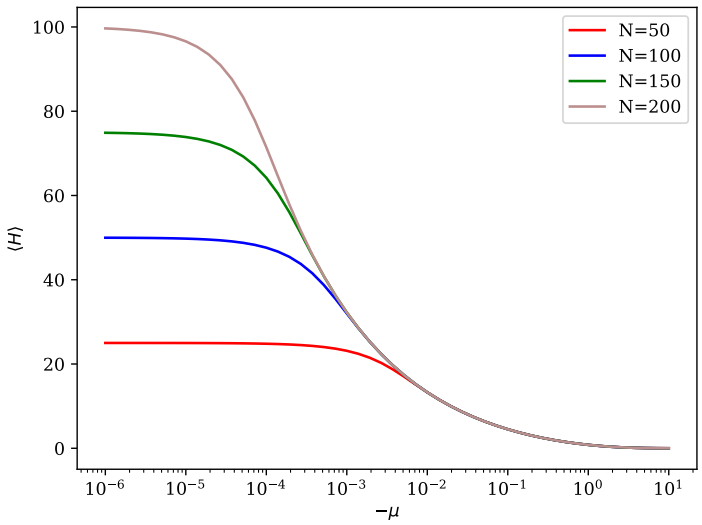

FIGURE 1.6 – Position d'équilibre de l'interface 1.143 en fonction de $-\mu$ via diagonalisation de la matrice de transfert 1.143. Lorsque le potentiel chimique est trop faible, l'interface est délocalisée et se retrouve à la position $\frac{N}{2}$.

nonical ensemble, where we think of the height as representing a number h_i of particles stacked at each site i and $P_0 = -\mu$ where μ is the chemical potential (which can be positive or negative). However this is not strictly true, if we consider the case where $\sigma = 0$ then in the SOS the configuration where all the particles are concentrated at a single site is equally as probable as that where all sites have the same number of particles and physical intuition tells us that the latter configuration should be more probable.

1.6.3 Matrice de Transfert

De manière plus générale, l'Hamiltonien d'un système avec des interactions entre les particules peut se réécrire comme $H = \sum_{\langle ij \rangle} H(h_i, h_j)$ avec

$$H = \sum_{i=0}^{L'} f(h_i, h_{i+1}) + V(h_i, h_{i+1})$$

où $f(h_i, h_j)$ est l'énergie d'interaction entre plus proches voisins et $V(h_i, h_j) = \frac{V(h_i)+V(h_j)}{2}$ le potentiel symmétrisé. Pour un système possédant L' sites pouvant contenir des valeurs

dans $[0, L]$, la fonction de partition de notre système s'écrit

$$Z = \sum_{h_1=0}^{L} \sum_{h_2=0}^{L} ... \sum_{h_{L'}=0}^{L!`} \exp(-\beta \sum_{i=0}^{L'} H(h_i, h_{i+1})) = \sum_{h_1 h_2 ... h_{L'}} \prod_{i=0}^{L'} \exp(-\beta H(h_i, h_{i+1})) \quad (1.144)$$

La matrice

$$T(h_i, h_j) = e^{-\beta H(h_i, h_j)} \quad (1.145)$$

est appelée matrice de transfert. On a représenté dans la figure 1.7 une matrice infinie correspond à la limite thermodynamique dans le cas où les sites peuvent prendre n'importe quelle valeur dans $[-\infty, \infty]$, qui correspond au cas où l'interface est centrée en $h = 0$ et ne possède pas de conditions aux bords. Lorsqu'il s'agit de diagonaliser cette matrice infine numériquement, il suffit de faire la translation $h_i \to h_i - \frac{L}{2}$, où L est la taille de la matrice de transfert, tendant vers l'infini.

Puisque le système est périodique (c'est-à-dire que $h_{L+1} = h_1$), la matrice est périodique également, c'est-à-dire que $T(h_L, h_{L+1}) = T(h_L, h_1)$ [30], et elle est également symétrique, La matrice de transfert peut donc être diagonalisée, nous écrivons ses vecteurs valeurs propres comme

$$T|\lambda\rangle = \lambda|\lambda\rangle \quad (1.146)$$

Ces vecteurs propres sont également orthonormaux

$$\langle\lambda|\lambda'\rangle = \delta_{\lambda\lambda'} \quad (1.147)$$

On note par λ_0 la plus grande valeur propre de T, par λ_1 la deuxième plus grande valeur propre etainsi de suite. Ainsi on peut diagonaliser la fonction de partition par la trace de la matrice de transfert [15]

$$Z = \sum_{h_1 h_2 ... h_{L'}} \prod_{i} T(h_i, h_{i+i}) = Tr(T^{L'}) = \sum_{\lambda} \langle\lambda|T^{L'}|\lambda\rangle = \sum_{\lambda} \lambda^{L'} \quad (1.148)$$

Dans la limite thermodynamique $L' \to \infty$, seul le plus grand vecteur propre est relevant,

$$T = \begin{bmatrix} \ddots & \vdots & \iddots \\ e^{-\beta H(-1,-1)} & e^{-\beta H(-1,0)} & e^{-\beta H(1,-1)} \\ \dots & e^{-\beta H(0,0)} & \dots \\ e^{-\beta H(1,-1)} & e^{-\beta H(1,0)} & e^{-\beta H(1,1)} \\ \iddots & \vdots & \ddots \end{bmatrix} \tag{1.149}$$

FIGURE 1.7 – Matrice de transfert infinie et symmétrique 1.145.

puisque la fonction de partition devient

$$Z(L \to \infty) \simeq \lambda_0^{L'} \tag{1.150}$$

Nous trouvons alors que l'énergie libre par site est égale à

$$F = -\frac{1}{L'\beta} \ln(Z) \simeq -\frac{1}{\beta} \ln(\lambda_0) \tag{1.151}$$

Dans la figure 1.8 on montre l'évolution de l'énergie libre par site $F(L')$ dans le cas d'un potentiel nul.On détermine alors que l'approximation de la limite thermodynamique est vraie pour $L' > 150$. Afin de calculer la densité moyenne par site M, on introduit la matrice des hauteurs $\hat{M}$ définie par son action sur les vecteurs $|h\rangle$ de la base de la matrice de transfert par

$$\langle h|\hat{M}|h'\rangle = \delta_{h,h'} h \tag{1.152}$$

On trouve alors la densité par site

$$M = \langle h \rangle = \frac{1}{L'} \sum_i h_i = \frac{1}{Z} \sum_\lambda \lambda^{L'} \langle \lambda|\hat{M}|\lambda\rangle \simeq \langle \lambda_0|\hat{M}|\lambda_0\rangle \tag{1.153}$$

On en déduit la variance sur la hauteur par site

$$w^2 = \langle (h-M)^2 \rangle = \frac{1}{Z} \sum_\lambda \lambda^{L'} \langle \lambda|\hat{M}^2|\lambda\rangle - \langle \lambda|\hat{M}|\lambda\rangle^2 \simeq \langle \lambda_0|\hat{M}^2|\lambda_0\rangle - M^2 \tag{1.154}$$

On peut retrouver ces deux observables en calculant le premier et le second moment de la

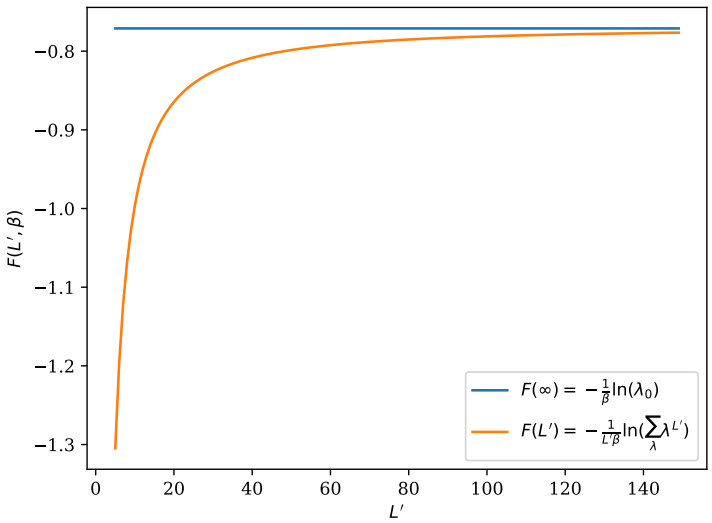

FIGURE 1.8 – Énergie libre par site $F(L')$ en fonction du nombre de sites L' comparé à la limite thermodynamique $F(\infty)$, pour un système de hauteur $L = 100$, $\beta = 1$, $J = 1$ et $V(h_i) = 0$.

densité de probabilité qu'un site se trouve à la hauteur h

$$p(h) = \frac{1}{Z}\sum_{\lambda} \lambda^{L'} \langle\lambda|h\rangle^2 \simeq \langle\lambda_0|h\rangle^2 \tag{1.155}$$

La fonction de corrélation à deux points du système se calcule grâce à la formule

$$C(r) = \langle h_i h_{i+r}\rangle - M^2 = \frac{1}{Z}\sum_{\lambda\neq\lambda_0} \langle\lambda_0|M|\lambda\rangle\langle\lambda|M|\lambda_0\rangle \left(\frac{\lambda}{\lambda_0}\right)^r \tag{1.156}$$

qui devient, dans la limite où r est grand,

$$C(r) \simeq \langle\lambda_0|M|\lambda_1\rangle\langle\lambda_1|M|\lambda_0\rangle \left(\frac{\lambda_1}{\lambda_0}\right)^r \tag{1.157}$$

what did you mean in your corrections by "explain when this is true-what happens to λ_2 etc" ? À grande distance, cette fonciton de corrélation a un charactère exponentiel, ce qui

nous permet de définir la longueur de corrélation à grande distance ξ

$$\xi = -\frac{1}{\ln(\frac{\lambda_1}{\lambda_0})} \tag{1.158}$$

1.7 Conclusion

Chapitre 2

Méthodes numériques

En 1949, Metropolis [31] découvre une méthode pour calculer via des simulations numériques de Monte Carlo, la moyenne d'observables statistiques. Si Q est une quantité observable appartenant à un système statistique, comme l'énergie interne ou la densité moyenne de particules par site, alors la moyenne est calculée en pondérant la valeur de l'observable sur toutes les configurations C du système par rapport au poids statistique de ces configurations. Si l'on considère le système en équilibre thermodynamique alors chaque configuration C suit une distribution de Gibbs-Boltzmann, et la moyenne $\langle Q \rangle$ est vaut

$$\langle Q \rangle = \frac{\sum_C Q(C) \exp(-\beta E(C))}{\sum_C \exp(-\beta E(C))} \tag{2.1}$$

Pour un système SOS de taille 100×100 par exemple, petit par rapport à la limite thermodynamique comme discuté avec la figure 1.8, il existe 100^{100} configurations possibles, bien qu'une simulation numérique ne puisse explorer qu'environ 10^8 configurations différentes en un temps CPU raisonnable. Les modèles sur réseau se prêtent parfaitement aux simulations numériques de Monte Carlo, où le but est de calculer la valeur moyenne des observables telles que l'énergie interne ou la densité moyenne de particule par site. Toutes ces quantités peuvent être calculées directement pour le modèle SOS dans l'ensemble grand-canonique à l'aide des valeurs propres de la matrice de transfert, mais il est impossible d'utiliser une telle méthode dans l'ensemble canonique, comme expliqué dans le chapitre précédent.

Dans ce chapitre, nous commençons par expliquer le principe des simulations de Monte Carlo Metropolis, et comment choisir l'ensemble thermodyique de la simulation numérique. En plus d'étudier l'ensemble canonique, les simulations numériques offrent la possibilité

d'étudier les régimes hors équilibre, dont nous justifierons la validité. Nous finirons le chapitre par expliquer comment accélérer la vitesse de simulation grâce à la parallélisation, ainsi que d'autres astuces de programmation, en insistant sur les écueils techniques à éviter.

Je remercie le Mésocentre de Calcul Intensif Aquitain (MCIA) [1] sur lequel j'ai effectué la très grande majorité de mes simulations numériques. L'intégralité du code produit pour cette thèse est accessible sur Github [2] sous la licence Creative Commons BY 3.0 [3]. Les simulations numériques ont été codées en C++, la parallélisation avec la librairie MPI, l'automatisation du lancement des jobs en Bash, et la visualisation des données ainsi que les diagonalisations des matrices de transfert sous Python.

actuellement, est-ce que j'ai le droit de diffuser librement mon code ? Le CNRS autorise la libre diffusion du code ?

2.1 Estimateur

Les simulations de Monte Carlo explorent l'espace des configurations de manière aléatoire [32] avec une probabilité $p(C$ que nous définirons plus tard. En choisissant M états $C_0, ..., C_M$, l'estimateur Q_M de Q est donnée par

$$Q_M = \frac{\sum_{i=0}^{M} Q(C_i) p(C_i)^{-1} \exp(-\beta E(C_i))}{\sum_{i=0}^{M} p(C_i)^{-1} \exp(-\beta E(C_i))} \tag{2.2}$$

Lorsque M augmente, l'estimateur devient une estimation de plus en plus précise de $\langle Q \rangle$, jusqu'à la limite $Q_{M\to\infty} = \langle Q \rangle$. Si l'on choisit les configurations sur lesquelles on échantillone le système selon la distribution à l'équilibre de Gibbs-Boltzmann $p(\nu) = Z^{-1} e^{-\beta E(C)}$, alors l'éstimateur de $\langle Q \rangle$ devient

$$Q_M = \frac{1}{M} \sum_{i=0}^{M} Q(C_i) \tag{2.3}$$

L'erreur obtenue à la fin sur notre observable au cours d'une simulationest

$$E(Q) = \sqrt{\frac{2\tau}{M} (\langle Q^2 \rangle - \langle Q \rangle^2)} \tag{2.4}$$

1. https://redmine.mcia.fr/projects/mcia
2. https://github.com/Bulbille/Curta
3. https://creativecommons.org/licenses/by/3.0/fr/

Cette variance dépend du temps de corrélation τ puisque si deux configurations sont très rapprochés dans le temps , l'observable n'aura pas suffisement évolué. En pratique, il suffit que $\frac{\tau}{M} < 10^{-4}$ pour obtenir une erreur inférieure à 1%. Ce temps de corrélation τ se calcule via la fonction d'auto-corrélation

$$\mathcal{C}(t) = \langle Q(t')Q(t+t')\rangle - \langle Q\rangle^2 = \frac{1}{t}\int_0^t Q(t')Q(t+t') - \langle Q\rangle^2 dt' \tag{2.5}$$

qui se comporte comme une exponentielle à temps long[33]. Une bonne estimation de τ est alors donnée l'intégrale

$$\tau = \int_0^\infty \mathcal{C}(t)/\mathcal{C}(0)dt \tag{2.6}$$

Le calcul de longueur de corrélation à grande distance ξ du système se fait de manière analogue en intégrant la fonction de corrélation spatiale définie par

$$\mathcal{C}(j) = \frac{1}{L'}\sum_{i=0}^{L'}\langle h_i h_{i+j}\rangle - \langle h\rangle^2 \tag{2.7}$$

2.2 Algorithme de Monte Carlo Metropolis

On se pose maintenant la question de savoir comment choisir les configurations afin que chacune apparaisse avec la bonne probabilité de Boltzmann.

Une dynamique pour les systèmes avec une espace des phases discret peut être construit à partir de chaînes de Markov. On laisse la dynamique évoluer dans un discret noté n, et $p_n(C)$ la probabilité que le système soit dans l'état C au temps n. Au pas de temps suivant, si le système est dans l'état C il peut sauter vers un autre état C' avec la probabilité de transition $\rho(C \to C')$. Le système au tempst $n+1$ dépend alors uniquement de l'état au temps n : c'est un processus markovien. La probabilité $p_{n+1}(X)$ d'être dans l'état C au temps $n+1$ est possible si le système était dans l'état C au temps n et y reste avec une probabilité $\rho(C \to C)$, ou s'il est dans un état C' et bouge vers l'état C avec une probabilité $\rho(C' \to C)$. On a alors l'équation maîtresse

$$p_{n+1}(C) = \rho(C \to C)p_n(C) + \sum_{C' \neq C}\rho(C' \to C)p_n(C') \tag{2.8}$$

Puisque $\rho(C' \to C)$ est une probabilité, on a la condition suivante

$$\sum_{C'} \rho(C' \to C) = 1 \tag{2.9}$$

Maintenant, si la dynamique décrit un système physique en interaction avec un réservoir de chaleur, la distribution à l'équilibre est donnée par

$$p_{eq}(C) = \frac{\exp(-\beta E(C))}{Z} \tag{2.10}$$

avec Z la fonction de partition canonique. Puisque la distribution à l'équilibre n'évolue pas au cours du temps, on a

$$p_{eq}(C) = \rho(C \to C)p_{eq}(C) + \sum_{C' \neq C} \rho(C' \to C)p_{eq}(C') \tag{2.11}$$

Une autre condition que l'on impose à notre chaîne de Markov afin qu'elle génère une probabilité de distribution de Boltzmann après équilibrage, est qu'elle respecte le bilan détaillé. Afin qu'un système respecte le bilan détaillé, il faut que le taux auquel il fait des transitions vers à partir de n'importe quel état C soit égal. Mathématiquement, cela revient à dire que

$$\sum_{C'} p(C)\rho(C \to C') = \sum_{C'} p(C')\rho(C' \to C) \tag{2.12}$$

On peut démontrer que cette relation est équivalente à [32]

$$\frac{\rho(C' \to C)}{\rho(C \to C')} = \frac{p(C)}{p(C')} = \frac{\exp(-\beta E(C))}{\exp(-\beta E(C'))} \tag{2.13}$$

En adoptant le bilan détaillé, on voit facilement que la distribution à l'équilibre calculée via 2.11 redonne bien la distribution de Gibbs-Boltzmann. Durant une étape de Metropolis, la probabilité pour que la transition $C \to C'$ se fasse dépend de la probabilité $g(C \to C')$ que cette transition soit choisie parmis toutes les possibilités de l'espace des configurations, et le taux de transition $A(C \to C')$ que la transition soit acceptée, c'est à dire

$$\rho(C \to C') = g(C \to C')A(C \to C') \tag{2.14}$$

2.2.1 Algorithme de Glauber

Dans un modèle SOS possédant L' sites de hauteur comprise entre 0 et L, l'algorithme de Glauber[34] dit que l'on choisit au hasard un site i avec une probabilité uniforme $\frac{1}{L'}$ et un entier $\alpha = \pm 1$ avec une probabilité $\frac{1}{2}$. Si la configuration C a l'Hamiltonien $H(h_0, h_1..., h_i, ...h_{L'})$, alors la nouvelle configuration générée aura l'Hamiltonien $H(h_0, h_1..., h_i + \alpha, ...h_{L'})$. Si $\alpha = +1$, alors on ajoute une particule au site i, et si $\alpha = -1$, on en retire une. Dans le cas où $h_i + \alpha \notin [0, L]$, la configuration C' ne respecte pas les conditions aux bords et est donc automatiquement refusée. La probabilité de sélection est alors

$$g(C \to C') = \frac{1}{2L'} \tag{2.15}$$

On a alors

$$\frac{\rho(C \to C')}{\rho(C' \to C)} = \frac{A(C \to C')}{A(C' \to C)} = \exp(-\beta(E(C') - E(C')) \tag{2.16}$$

Il est possible de choisir n'importe quel taux de transition $A(C \to C')$ qui satisfait à l'équation précédente. Un algorithme de Metrpoolis est un algorithme qui choisit comme taux de transition

$$A(C \to C') = \begin{cases} \exp(-\beta(E(C') - E(C)) & \text{si } E(C') - E(C) > 0 \\ 1 & \text{sinon} \end{cases} \tag{2.17}$$

Dans la pratique, si $\Delta E > 0$, on tire uniformément au hasard un nombre $r \in [0, 1]$. Si $r < A(C \to C')$ alors la transition est acceptée, et dans le cas contraire la transition est refusée et le système reste dans la configuration C.

Puisque la grandeur $\sum_i h_i$ n'est pas conservée au cours du temps, l'algorithme de Glauber correspond à un système qui échange des particules avec un réservoir dans l'ensemble grand-canonique.

La différence d'énergie entre deux configurations est alors

$$\Delta E = |h_{i-1} - (h_i + \alpha)| + |h_{i+1} - (h_i + \alpha)| - |h_{i-1} - h_i| - |h_{i+1} - h_i| \tag{2.18}$$

Il n'est pas nécessaire de calculer la hauteur totale à chaque étape. La variable $\sum_i h_i$ peut

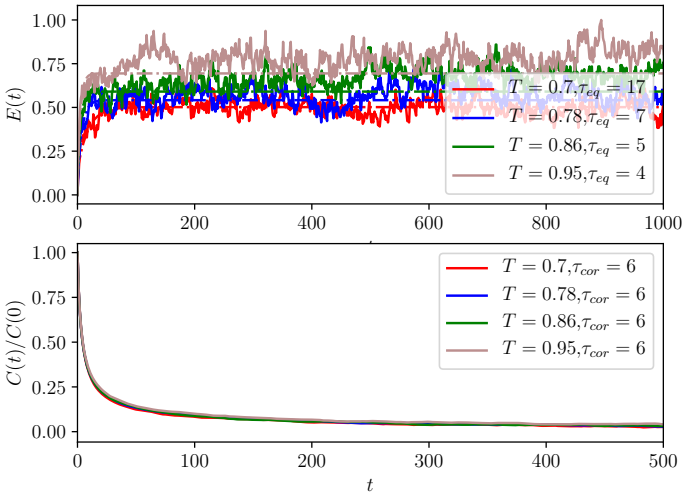

FIGURE 2.1 – Courbe de l'énergie (haut) et fonction d'auto-corrélation (bas) dansavec un algorithme de Glauber à partir d'une condition initiale à $T = \infty$, pour différentes températures.

être mise en mémoire, et mise à jour à chaque fois qu'une transition a été validée par la formule

$$\langle h \rangle_{M+1} = \langle h \rangle_M + \alpha \tag{2.19}$$

On peut faire de même pour la variable $\sum_i h_i^2$, utile pour calculer la largeur de l'interface, ou bien l'énergie totale du système.

Afin d'accélérer le processus d'équilibrage du système, il est recommandé de commencer directement avec la valeur moyenne de magnétisation calculée à partir de la matrice de transfert. On regarde ensuite le temps d'équilibrage par la courbe $E(t)$, en attendant d'atteindre la valeur à l'équilibre. On choisit ici d'étudier l'énergie totale du système contrairement à la hauteur totale, puisqu'en absence de potentiel chimique, l'interface est libre de fluctuer entre 0 et L. Dans la figure 2.1, on montre le temps d'équilibrage et le temps de corrélation du système en absence de potentiel chimique. Les temps assez faibles d'équilibrage te de corrélation assurent qu'une simulation équilibrée sur 10^3 et mesurée sur 10^7 étapes de Monte Carlo donneront des résultats précis.

Dans le modèle SOS, on s'attend à ce que les statistiques générées par la dynamique

de Glauber soient identiques, comme on le voit dans la figure XXX. rajouter figure où on voit $\sum_i h_i$ avec Glauber ET TM en fonciton de μ par exemple, pour prouver que ça marche. Dans ces conditions spéciales qui découlent de notre modèle, les simulations dans l'ensemble grand-canonique n'offrent que peu d'intérêt. Il n'existe cependant pas de matrice de transfert dans l'ensemble canonique, et c'est donc là que l'intérêt des simulations de Monte Carlo apparaît pour le modèle SOS.

2.2.2 Algorithme de Kawasaki

Maintenant, on désire mettre au point un algorithme pour l'ensemble canonique, où la hauteur par site reste constante. Dans l'algorithme de Kawasaki [35], on choisit au hasard un site i avec une probabilité $\frac{1}{L'}$, et un de ses deux voisins $i-1$ ou $i+1$ avec une probabilité $\frac{1}{2}$. Si par exemple on a choisit le site voisin $i-1$ (la discussion est la même pour le site $i+1$), on génère la nouvelle configuration test d'Hamiltonien $H(h_0, ..., h_{i-1}+1, h_i-1, ...h_{L'})$. Ici, on a retiré une particule du site i pour le transférer sur le site adjacent. La probabilité de sélection est à nouveau

$$g(C \to C') = \frac{1}{2L'} \tag{2.20}$$

et on choisit le même taux de transition 2.17.

Ici, on voit bien que la grandeur $\sum_i h_i$ est conservée au cours du temps. Dans le cas où le site i donne une particule au site $i+1$, la différence d'énergie s'écrit

$$\begin{aligned}\Delta E = &|h_{i-1} - (h_i - 1)| + |h_{i+1} + 1 - (h_i - 1)| + |h_{i+1} + 1 - (h_{i+2})| \\ &- (|h_{i-1} - h_i| + |h_{i+1} - h_i| + |h_{i+1} - h_{i+2}|)\end{aligned} \tag{2.21}$$

Dans la figure 2.2, on remarque que le temps d'équilibrage et le temps de corrélation sont plus longs qu'avec la dynamique de Glauber. Bien que la dynamique soit plus lente parce que la longueur de corrélation dans le modèle A croît comme $t^{\frac{1}{2}}$ et comme $t^{\frac{1}{3}}$ dans le modèle B, on s'attend à ce que le temps de simulation reste similaire.

Cette dynamique décrit la diffusion de particules au sein d'une interface. Il est donc possible de rajouter un flux qui brise l'équilibre. La méthode reste pertinente si on suppose que la dynamique du système reste lente comparée aux échanges de chaleur avec le réservoir. Dans ces conditions, on considère que les configurations C respectent encore l'équilibre de Gibbs-Boltzmann.

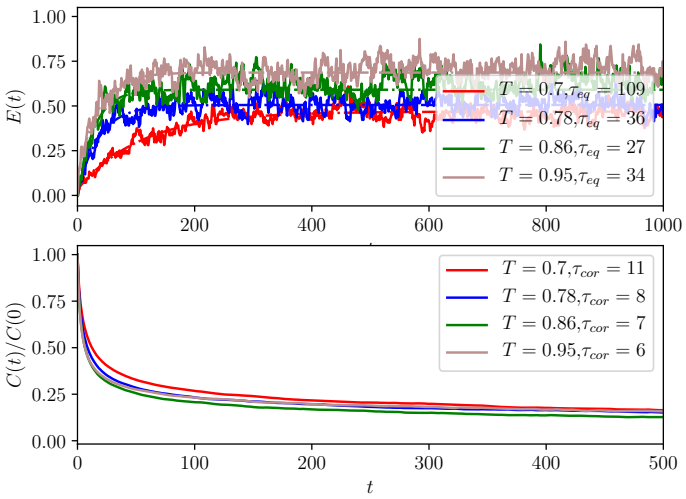

FIGURE 2.2 – Courbe de l'énergie (haut) et fonction d'auto-corrélation (bas) avec un algorithme de Kawasaki à partir d'une condition initiale à $T = \infty$, pour différentes températures.

2.3 Computing size depenedent free energy

2.3.1 The Layer method

Comme vu dans la section **??**, on retrouve dans l'énergie libre du système toute l'information nécessaire sur les effets de taille finie, principalement la force de Casimir critique. L'énergie libre ne peut être exprimée par des moyennes d'observables facilement calculables dans les simulations de Monte Carlo. La force de Casimir étant

$$F(t, h, L) = -\frac{\partial \Omega}{\partial L} \tag{2.22}$$

on remarque que le calcul seul de la dérivée par rapport à la hauteur L du systèème est suffisant. Pour se faire, Vasilyec [36] a développé une méthode pour calculer sa dérivée vis-à-vis d'un paramètre fictif de couplage. Bien que la taille d'un ystème sur réseau soit discrète, il est possible d'obtenir une taille continue du réseau grâce au découplage progressif d'une couche du système. Si H_0 est l'Hamiltonien du système de hauteur L et H_1 l'Hamiltonien

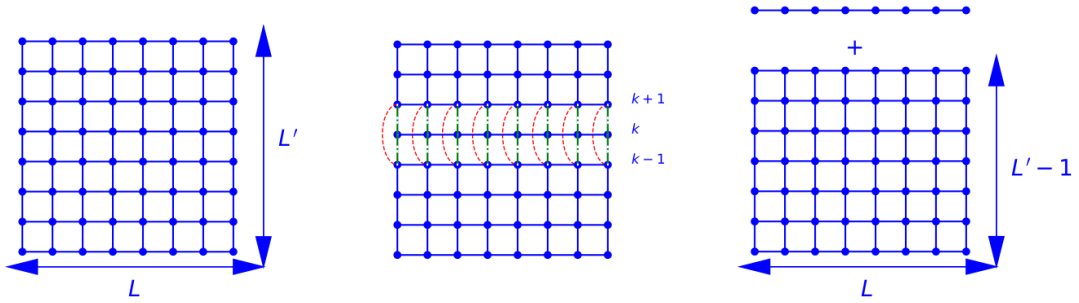

H_0 $H(\lambda)$ H_1

FIGURE 2.3 – Découplage progressif de la k-ième couche du système afin de calculer la variation de l'énergie libre grâce à l'Hamiltonien de transition. Les liens en bleu ont une énergie de βJ, les liens en rouge une énergie de $\lambda\beta J$ et les liens en vert une énergie de $(1-\lambda)\beta J$. Reproduction 2D de [36].

de hauteur $L-1$ (voir figure 2.3), alors on pose l'Hamiltonien de transition

$$H_{tr}(\lambda) = (1-\lambda)H_0 + \lambda H_1 \tag{2.23}$$

avec $\lambda \in [0,1]$, et qui interpole H_0 et H_1 lorsque λ va de 0 à 1. L'Hamiltonien de transition $H_{tr}(\lambda)$ dépend également de la position $k_0 \in 1, 2, ..., L$ (selon la direction z de la couche qui se découple du reste du système en fonction de λ, c'est-à-dire de 2.3(a) à 2.3(c). L'Hamiltonien résultant est charactérisé par les constantes de couplage décrites dans la figure 2.3(b). L'énergie libre associée à cet Hamiltonien est

$$\Omega_{tr}(\lambda) = -k_B T \ln\left(\sum_{h_1 \ldots h_L} \exp(-\beta H_{tr}(\lambda))\right) \tag{2.24}$$

De la dérivée de l'énergie libre découle

$$\frac{\Omega_{tr}(\lambda)}{d\lambda} = \langle H_1 - H_0 \rangle_{H_{tr}(\lambda)} \tag{2.25}$$

où $\langle\cdot\rangle_{H_{tr}(\lambda)}$ représente la moyenne statistique sur le système en transition, facilement calculable dans les simulations numériques. En intégrant sur le couplage, on trouve que

$$\Omega_1 - \Omega_0 = \int_0^1 d\lambda \langle H_1 - H_0 \rangle_{H_{tr}(\lambda)} \tag{2.26}$$

Finalement, dans la limite où l'épaisseur du système est suffisament grande pour que la variation d'une couche soit suffisement petite ($L' \gg 1$), on trouve que

$$-\frac{\partial \Omega(t,h,L)}{\partial L} \simeq \int_0^1 d\lambda \langle H_1 - H_0 \rangle_{H_{tr}(\lambda)} \tag{2.27}$$

Bien que $H_{tr}(\lambda)$ dépende de la rangée k_0 que l'on a décidé de découpler, et par transition $H_1 - H_0$ et $\langle H_1 - H_0 \rangle_{H_{tr}(\lambda)}$, l'intégrale $\int_0^1 d\lambda \langle H_1 - H_0 \rangle_{H_{tr}(\lambda)}$ est indépendante de ce choix tant que les conditions aux borrds ne sont pas affectés par l'extraction de la couche k_0.

Pour le modèle Solid-On-Solid, il est possible de calculer la variation d'énergie créée par le découplage directement. Si le découplage s'est créé à la rangée k, on ajoute un lien d'énergie λJ entre les rangées $k-1$ et $k+1$ et on retire λJ énergie des rangées $k-1$ à k et de k à $k+1$. On obtient

$$H_{tr,SOS}(\lambda) = H_{0,SOS} - \\ \frac{\lambda J}{2} \sum_x \left[\operatorname{sgn}(k-1-h(x)) \operatorname{sgn}(k+1-h(x)) - \operatorname{sgn}(k-h(x)) \left(\operatorname{sgn}(k-1-h(x)) + \operatorname{sgn}(k+1-h(x)) \right) \right] \tag{2.28}$$

où le facteur $\frac{1}{2}$ est obtenu afin de prendre en compte le coefficient 2 dans 1.135. En faisant un tableau de valeurs, on remarque rapidement que la somme est une constante égale à -1 quel que soit k, puisque contraiement au modèle d'Ising, les modèles d'interface ne possèdent pas d'énergie de bulk. Il faut donc utiliser une autre méthode afin de mesurer l'effet Casimir dans les simulations de Monte Ca

2.3.2 The Lopes Cardozo method

Afin d'isoler la force de Casimir du terme de volume dans la force de confinement, il convient de retirer la force de confinement d'un système de taille différente. Ainsi, pour deux systèmes de taille $L_1 < L_2$, on a

$$F(t,h,L_1) - F(t,h,L_2) = f_c(t,h,L_1) - f_c(t,h,L_2) = -\frac{\partial \Omega(t,h,L_1)}{\partial L} + \frac{\partial \Omega(t,h,L_2)}{\partial L} \tag{2.29}$$

Puisque le surplus d'énergie dû au confinement est nul lorsque $L_2 \to \infty$, on obtient une approximation sur la force de Casimir lorsque $\frac{L_1^d}{L_2^d} \ll 1$

$$f_c(t, h, L_1) \simeq \frac{\partial \Omega(t, h, L_2)}{\partial L} - \frac{\partial \Omega(t, h, L_1)}{\partial L} \tag{2.30}$$

Or, nous savons grâce à l'équation **??** que dans le cas d'un champ magnétique uniforme $h(\mathbf{x})$, la moyenne du paramètre d'ordre est reliée à l'énergie libre par

$$\langle \phi(\mathbf{x}) \rangle(t, h, L) = -\frac{\delta \Omega(t, h, L)}{\delta h(\mathbf{x})} \tag{2.31}$$

Si on pose $h(\mathbf{x}) = h$, alors il est possible d'obtenir une différence entre deux énergies libres à champs magnétiques différents [37]

$$\Delta\Omega = \Omega(t, h_1, L) - \Omega(t, h_2, L) = -\int_{h_1}^{h_2} \langle \phi(\mathbf{x}) \rangle(t, h, L) dh \tag{2.32}$$

Dans le cas où l'on connait la configuration lorsque $h_2 \to \infty$ ou $h_1 \to 0$, il est possible de mesurer directement l'énergie libre d'un système pour n'importe quelle température et taille en intégrant selon 2.32. Dans le cas où $h_2 \to \infty$, le potentiel en double-puit 1.19 ne possède qu'un seul minimum, l'énergie libre d'un tel système est alors uniquement lié à l'énergie libre du volume. La différence 2.32 contient donc toute l'information nécessaire afin de mesurer la force de Casimir. On peut alors calculer la dérivée 2.30 avec

$$dL \frac{\partial \Omega(t, h, L)}{\partial L} = \Delta\Omega(t, h, L) - \Delta\Omega(t, h, L - dL) \tag{2.33}$$

2.4 Tips and tricks

en annexe ou je peux le laisser dans le chapitre directement ? La rapidité des simulations des modèles 1D soit rapide comparé aux modèles d'Ising est telle, qu'il est possible de simuler les phénomènes sur une plage plus grande de paramètres. Si une simulation de $10^/$ étapes de Monte Carlo dure en moyenne 20 minutes, le lancement d'une centaine de ces simulations peut vite prendre une journée ou plus. En C++, la première chose à faire pour gagner un facteur 5 dans le temps simulation est d'ajouter le flag d'optimisation -03 dans le compilateur, afin d'optimiser le code au niveau du préprocesseur.

Une fois cela fait, on se tourne vers le générateur de nombre pseudo-aléatoire (pRNG).

En effet, à chaque étape de Monte Carlo on génère trois nombres aléatoires : - le choix du site i - un booléen pour savoir si l'on rajoute ou enlève une particule dans le cas de la dynamique de Glauber,ou un booléen pour savoir à quel plus proche voisin nous alons donner une particule dans le cas de la dynamique de Kawasaki - un double compris entre $[0, 1]$ pour savoir si on accepte ou non la transition, dans le cas où $\Delta E > 0$ La librairie C++ standard propose *default_random_engine* comme générateur standard de nombres aléatoires. Un gain substantiel de temps d'un facteur 5 à 10 peut être fait en optant pour les générateurs *sfc64* ou *xoroshiro*. De plus, la génération d'un booléen ne requiert qu'un bit aléatoire, tandis que les générateurs classiques génères 64 bits à chaque fois, ce qui gâche 63 bits à chaque étape. Il est possible de mettre tous les bits générés en mémoire, afin de n'avoir à générer un nombre aléatoire qu'une fois tous les 64 booléens utilsés[**?**].

Pour finir, l'optimisation la plus évidente est la parallélisation du code. Bien que l'on puisse décomposer les domaines afin d'accélérer la simulation d'un système, les modèles 1D étant rapides, il est plus intéressant de procéder à une parallélisation basique sur les paramètres de la simulation (comme la température ou le potentiel chimique). En C++, il existe deux libraires : OpenMP et MPI. Il m'a fallu plusieurs pour comprendre que bien que la première soit très faicle d'implémentation, la parallélisation avec mémoire partagée rend le pRNG très instable, ce qui fausse complètement l'ensemble des simulations. Il est donc impératif d'utiliser la librairie MPI, qui assure l'étanchéité des pRNG entre chaque thread.

2.5 Conclusion

Dans ce chapitre, nous avons expliqué comment mesurer les moyennes statistiques des observables de nos systèmes grâce aux simulations de Monte Carlo Metropolis. Les hyopthèses sont les suivantes : on demande d'abord que le système soit à l'équilibre thermodynamique avec un réservoir de chaleur ; et on demande également que le système respecte le bilan détaillé. On obtient alors deux deux dynamiques possibles : la dynamique de Glauber permet de simuler les systèmes dans l'ensemble grand-canonique, tandis que la dynamique de Kawasaki permet de simuler les systpèmes dans l'ensemble canonique. La première méthode est en parfait accord avec les reśultats de la matrice de transfert, et nous donne donc peu d'informations nouvelles. C'est donc naturellement dans la dynamique de Kawasaki que les simulations de Monte Carlo pour un modèle SOS prennent tout leur sens. On a également discuté du temps d'équilibrage et de corrélation, qui permettent d'obtenir

des résultats précis en très peu de temps de calcul. Bien que ces simulations soient rapides comparé au modèle d'Ising (une vingtaine de minutes environ lorsque le code est optimisé), il est nécessaire d'optimiser le code via la parallélisation, ou un changement de pRNG.

Chapitre 3

Equilibrium Interface models and their finite size effects

Models for interfaces arise naturally in phase separated systems to describe the region between the two phases. They also arise naturally as descriptions of artificial and biological membranes. Systems undergoing a continuous phase separation exhibit finite size corrections which are manifested by a long range critical Casimir interaction which we describe in the next section. In the sections after we examine finite size effects in interface models in one dimension, and show that while they have similar long range interactions, the forces induced by interface confinement are quite different.

3.1 The Casimir effect

Here we explain the critical Casimir effect. For completeness we start by explaining the quantum Casimir effect as it was in the quantum context that the effect was first observed. We also describe the basis of the Lifshitz theory that generalises Casimir's contribution to general dielectric materials beyond the perfectly conducting plate paradigm.

3.1.1 Quantum Casimir effect

A perfectly conducting plate in the (x, y) plane imposes boundary conditions on the electromagnetic field

$$\mathbf{E} \times \mathbf{n} = \mathbf{0};\ \mathbf{B} \cdot \mathbf{n} = 0, \tag{3.1}$$

as in an ideal conductor the free charges can move arbitrarily quickly to cancel out any electric field within the plane. The quantum Hamiltonian for the electromagnetic field is given by

$$H = \sum_{\mathbf{k},\lambda} \hbar\omega(\mathbf{k},\lambda)\left[a^\dagger(\mathbf{k},\lambda)a(\mathbf{k},\lambda) + \frac{1}{2}\right] \tag{3.2}$$

Here λ denotes the polarisation (there are two polarisation states) and $\mathbf{k}$ the wave vector. The dispersion relation for photons is

$$\omega(\mathbf{k},\lambda) = |\mathbf{k}|c. \tag{3.3}$$

The ground state energy of the electromagnetic field is given by

$$E_0 = \langle 0|H|0\rangle = H = \sum_{\mathbf{k},\lambda} \frac{1}{2}\hbar\omega(\mathbf{k},\lambda) = \sum_{\mathbf{k}} \hbar|\mathbf{k}|c \tag{3.4}$$

The presence of conduction plates at $z = 0$ and $z = L$ means that the wave vectors k_z must be quantised according to $k_z = n\pi/L$ where $n \in \{0,\ 1,\ 2,\ \cdots\}$ while if the (x, y) plane has a large area A we can write

$$\sum_{k_x,k_y} \cdot = \frac{A}{(2\pi)^2}\int d^2\mathbf{k}\cdot \tag{3.5}$$

This then gives

$$E_0(L) = \frac{\hbar cA}{(2\pi)^2}\sum_{n=0}^{\infty}\int d^2\mathbf{k}\left(\mathbf{k}^2 + \frac{n^2\pi^2}{L^2}\right)^{\frac{1}{2}} \tag{3.6}$$

$$= \frac{\hbar cA}{(2\pi)}\sum_{n=0}^{\infty}\int_0^{\infty} kdk\left(\mathbf{k}^2 + \frac{n^2\pi^2}{L^2}\right)^{\frac{1}{2}} \tag{3.7}$$

The problem with the above expression is that it is clearly divergent. However it can be rendered finite by cutting off the high momentum degrees of freedom by writing

$$E_0(L) = \frac{\hbar cA}{(2\pi)}\sum_{n=0}^{\infty}\int_0^{\infty} kdk\left(\mathbf{k}^2 + \frac{n^2\pi^2}{L^2}\right)^{\frac{1}{2}} f\left((\mathbf{k}^2 + \frac{n^2\pi^2}{L^2})^{\frac{1}{2}}\right) \tag{3.8}$$

where f is a smooth function such that $f(p) = 1$ for $p \ll \Lambda$ and $f(p) = 0$ for $p \gg \Lambda$

where Λ is an ultraviolet cut-off and f thus only counts the contribution of photons with a momentum less than $\hbar\Lambda$. For this sort of calculation to make physical sense the physical result we get at the end should be independent of both the choice of f and Λ.

In the list $L \to \infty$ we can replace the sum over discrete modes by an integral, as usual in statistical physics,

$$E_0(L) = \frac{\hbar c A}{(2\pi)} \int_0^\infty \frac{L}{\pi} d\nu \int_0^\infty k dk \left(\mathbf{k}^2 + \nu^2\right)^{\frac{1}{2}} f\left((\mathbf{k}^2 + \nu^2)^{\frac{1}{2}}\right) \tag{3.9}$$

where we have used $d\nu = \pi/L$. We thus see that for large L we have

$$E_0(L) = AL\epsilon_{bulk} \tag{3.10}$$

where ϵ_{bulk} is a bulk energy density per unit of volume. Clearly when two the plates are moved this bulk free energy is not changed as the volume of the system both interior and exterior to the plates does not change. This is basically the idea of a disjoining pressure in colloidal science where to compute the effective interaction the bulk pressure has to be removed. The computation above only calculates the energy of the EM field between the plates, if the physical system has and extent $L' \gg L$ then the total energy is given by

$$E_{total}(L) = E_0(L) + A(L' - L)\epsilon_{bulk} \tag{3.11}$$

so we see that the part of the energy that depends on L is given by

$$U(L) = E_0(L) - AL\epsilon_{bulk} \tag{3.12}$$

Now we simply write

$$AL\epsilon_{bulk} = \frac{\hbar c A}{(2\pi)} \int_0^\infty dn \int_0^\infty k dk \left(\mathbf{k}^2 + \frac{n^2\pi^2}{L^2}\right)^{\frac{1}{2}} f\left((\mathbf{k}^2 + \frac{n^2\pi^2}{L^2})^{\frac{1}{2}}\right), \tag{3.13}$$

putting the L dependence in the integral. This then gives

$$U(L) = \frac{\hbar c A}{(2\pi)} \left[\sum_{n=0}^{\infty} g(n) - \int_0^\infty dn\ g(n)\right], \tag{3.14}$$

where

$$g(n) = \int_0^\infty kdk \left(\mathbf{k}^2 + \frac{n^2\pi^2}{L^2}\right)^{\frac{1}{2}} f\left((\mathbf{k}^2 + \frac{n^2\pi^2}{L^2})^{\frac{1}{2}}\right) = \frac{1}{2}\int_{\frac{n^2\pi^2}{L^2}}^\infty duu^{\frac{1}{2}} f(u^{\frac{1}{2}}). \tag{3.15}$$

We now use the Euler-Mauclarin formula

$$\sum_{n=0}^\infty g(n) - \int_0^\infty dn\ g(n) = -B_1 g(0) - \frac{1}{2}B_2 g'(0) - \frac{1}{24}B_4 g'''(0) - \cdots, \tag{3.16}$$

where B_n are the Bernoulli numbers. The first Bernoulli numbers are explicitly given by

$$B_1 = 1\ , B_2 = \frac{1}{2},\ B_4 = -\frac{1}{30} \tag{3.17}$$

We find that

$$g'(n) = -\frac{\pi^3}{L^3}n^2 f(\frac{n\pi}{L}) \tag{3.18}$$

and noticing than in the region around $n = 0$ we have $f = 1$ is a constant shows that

$$g'(0) = 0 \tag{3.19}$$

$$g''(0) = 0 \tag{3.20}$$

$$g'''(0) = -\frac{2\pi^3}{L^3} \tag{3.21}$$

Higher order derivatives are zero so the full result is given by the first three terms of the Euler-Maclaurin formula. We thus find

$$U(L) = \frac{\hbar cA}{(2\pi)}\left[-g(0) - \frac{\pi^3}{360L^3}\right] \tag{3.22}$$

The first term independent of L can be interpreted as a surface energy. The effective L dependent interaction is given by

$$U_{int}(L) = -\frac{\hbar\pi^2 cA}{720L^3} \tag{3.23}$$

We see that the effective interaction is attractive. Interestingly Casimir thought that his calculation could explain the stability of the electron. The model of the electron is one of a perfectly conducting shell carrying an electric charge e. If the radius of the shell is a then

the electrostatic energy of due to the charge is given by

$$E_{Charge} = \frac{e^2}{8\pi a \epsilon_0} \tag{3.24}$$

There is thus a repulsive force on the shell which should make it expand. Casimir thought that the Casimir force on a spherical geometry, if is an attractive force as is the case for the parallel plate geometry, could stabilise the electron. Clearly by dimensional analysis

$$E_{Cas} = -\frac{Z\hbar c}{a} \tag{3.25}$$

The balance of the Casimir and electric forces would then require

$$Z = \frac{e^2}{8\pi\hbar c}. \tag{3.26}$$

However T. Boyer showed, in 1968, that $Z = -0.040618$, this surprising result was later confirmed by a number of authors. A calculation for a cylindrical geometry however predicts an attractive force.

3.1.2 Lifshitz Theory

The Casimir calculation is based on the boundary conditions imposed on the EM field due to a conductor. However this is an ideal mathematical limit, conductors are conductors because free charges can move to cancel out the electric field in the conducting surface. The Casimir force can also be seen as due to correlations induced in the charge fluctuations in each plate - Schwinger devised an alternative method based on sources which recovers the Casimir force. In a sense therefore the effect can be interpreted without reference to the zero point energy of the vacuum and the Casimir calculation works due to the fact that the mathematical limit in going to a perfect conductor works. Lifshitz and collaborators generalized the Casimir calculation for interactions between arbitrary electrical bodies, characterized by their local electric and magnetic response. They used a stochastic formulation of electrodynamics developed by Rytov. This theory is very general but the microscopic justification is not completely rigorous, source terms (random currents and dipole fluctuations) are introduced to Maxwell's equations to give a Langevin formulation of Maxwell's equations in the presence of dielectric bodies. The correlation functions of the white noise terms depend on the temperature of the system and are determined via the

quantum fluctuation dissipation theorem. The Lifshitz theory is computationally difficult to work with and it was reformulated by Van Kampen and later Ninham and Parsegian in a way more useful for practical calculations and that can be applied to experimental set ups. The Rytov formulation has the advantage that it can be used to treat out of equilibrium situations where different bodies at held at different temperatures interact. This allows both the computation of out of equilibrium forces and radiative heat transfer.

The theory in the presence of electromagnetic media is written in terms of the electric and magnetic fields $\mathbf{E}$ and $\mathbf{B}$ and the displacement and magnetizing fields $\mathbf{D}$ and $\mathbf{H}$ which are assumed to obey local relations in real space and Fourier space

$$\tilde{\mathbf{D}}(\omega) = \epsilon(\omega)\tilde{\mathbf{E}}(\omega);\ \tilde{\mathbf{B}}(\omega) = \mu(\omega)\tilde{\mathbf{H}}(\omega) \tag{3.27}$$

where $\tilde{\epsilon}(\omega)$ and $\tilde{\mu}(\omega)$ are the frequency dependent permittivity and permeability. The boundary conditions at the interface between two materials 1 and 2 are given by

$$B_{1n} = B_{2n} \qquad D_{1n} = D_{2n} \tag{3.28}$$

$$E_{1t} = E_{2t} \qquad H_{1t} = H_{2t} \tag{3.29}$$

where n denotes the normal component and t the tangential component to the interface.

Forces can be computed using the vacuum (assuming that the surface where the force is computed is next to the vacuum) Maxwell stress tensor.

$$T_{ij} = \epsilon\left(E_iE_j - \frac{1}{2}\delta_{ij}E^2\right) + \frac{1}{\mu}\left(B_iB_j - \frac{1}{2}\delta_{ij}B^2\right) \tag{3.30}$$

Notice that the stress tensor is quadratic in the fields $\mathbf{E}$ and $\mathbf{B}$, this means that even if the fields are on average zero, both thermal and quantum fluctuations give rise to forces.

In media Maxwells equations are

$$\nabla \times \mathbf{E} = -\frac{\partial \mathbf{B}}{\partial t} \tag{3.31}$$

$$\nabla \times \mathbf{H} = \mathbf{J} - \frac{\partial \mathbf{D}}{\partial t} \tag{3.32}$$

$$\nabla \cdot \mathbf{D} = \rho \tag{3.33}$$

$$\nabla \cdot \mathbf{B} = 0 \tag{3.34}$$

In a dielectric medium or conductor where there are no applied external fields there

is no free charge or current as such the average values of $\mathbf{E}$ and $\mathbf{B}$ are zero. Rytov's idea was to add a random current to induce both thermal and quantum fluctuations into the problem. If we assume that the only contribution to the current comes from a fluctuating polarization density $\mathbf{P}$ we can write

$$\frac{\partial \rho}{\partial t} + \nabla \cdot \mathbf{J} = 0 \implies \nabla \cdot \left[-\frac{\partial \mathbf{P}}{\partial t} + \mathbf{J} \right] = 0 \tag{3.35}$$

where we have used

$$\rho = -\nabla \cdot \mathbf{P} \tag{3.36}$$

This means that the current is given by

$$\mathbf{J} = \frac{\partial \mathbf{P}}{\partial t}, \tag{3.37}$$

or in Fourier space

$$\tilde{\mathbf{J}}(\omega) = i\omega \tilde{P}(\omega) \tag{3.38}$$

Now if we assume that the fluctuations in the polarization density are uncorrelated in space, the fluctuation dissipation theorem tells us that the correlation function of the polarization density in Fourier space is given by

$$\langle P_\alpha(\omega; \mathbf{x}) P^\dagger_\beta(\omega; \mathbf{x}') \rangle_{sym} = \frac{\hbar \epsilon''(\omega)}{2} \coth\left(\frac{\hbar\omega}{2k_B T} \right) \delta(\omega - \omega') \delta(\mathbf{x} - \mathbf{x}') \delta_{\alpha\beta} \tag{3.39}$$

$$\epsilon(\omega) = \epsilon'(\omega) + i\epsilon''(\omega) \tag{3.40}$$

The Lifshitz calculation for slab geometries gives a force per unit area between two slabs of media separated by a distance L

$$\begin{aligned} \frac{F}{A} &= -\frac{k_B T}{\pi c^3} \sum_{n=0}^{\infty} \omega_n^3 \int_1^\infty dp p^2 \left[1 - \frac{(s_1 + p)(s_2 + p)}{(s_1 - p)(s_2 - p)} \exp(-\frac{2p\omega_n L}{c}) \right] \\ &+ \left[1 - \frac{(s_1 + p\varepsilon_1)(s_2 + p\varepsilon_2)}{(s_1 - p\varepsilon_1)(s_2 - p\varepsilon_2)} \exp(-\frac{2p\omega_n L}{c}) \right] \end{aligned} \tag{3.41}$$

where $\epsilon = \epsilon_0 \varepsilon$, $s_i = \sqrt{\epsilon_i - 1 + p^2}$, $\omega = \frac{2\pi n k_B T}{\hbar}$ are the Mastubara frequencies and $\varepsilon_i = \varepsilon_i(i\omega_n)$. Note that the integral over real frequencies has become a sum over discrete Matsubara frequencies, they come from the poles in the hyperbolic cotangent.

One needs to know the dielectric response at imaginary frequency, this is done using the Kramers-Kronig relation

$$\varepsilon(i\omega) = 1 + \frac{2}{\pi}\int_0^\infty d\zeta \frac{\zeta\varepsilon''(\zeta)}{\omega^2+\zeta^2} \tag{3.42}$$

3.1.3 Critical Casimir effect

Bulk scaling for near critical systems

The free energy for a system consisting of N spins has a singular part at a critical temperature T_c which can be written as

$$F(t,h) = Nf(t,h) \tag{3.43}$$

where $t = (T - T_c)/T_c$ measures the distance from the critical point and h is the external applied magnetic field. We assume that we are in a systems where the only relevant parameters are T and h (equivalently the concentration or chemical potential of a binary mixture). For $d\langle 4$ these are the only relevant fields. Now if we carry out a renormalisation group transformation blocking spins in blocks of linear size b into new effective spins, the RG transformation gives

$$Nf(t,h) = N'f(t',h') \tag{3.44}$$

Clearly the number of spins in the blocked system is given by $b^dN' = N$ and the RG transformation for t and h are given by $t' = b^{y_1}t$ and $h' = b^{y_2}h$ where y_1 and y_2 are positive and are the RG exponents for the fields t and h (from which all critical exponents can be deduced). This then means that

$$f(t,h) = \frac{1}{b^d}f(b^{y_1}t, b^{y_2}h) \tag{3.45}$$

We begin by working with $t\rangle 0$ but the arguments here are trivially generalisable to the case $t\langle 0$. In Eq. (3.45) is we choose b such that $b^{y_1}t = 1$, then, at the critical field $h = 0$, we find

$$f(t,0) = t^{\frac{d}{y_1}}f(1,0) \tag{3.46}$$

The singularity in the specific heat is defined via

$$c \sim \frac{\partial^2}{\partial t^2} f(t,0) \tag{3.47}$$

and so we find

$$c \sim t^{\frac{d}{y_1}-2} \sim t^{-\alpha} \tag{3.48}$$

where α is the exponent associated with the divergence of the specific heat. This means that

$$\alpha = 2 - \frac{d}{y_1} \tag{3.49}$$

The RG transformation for the correlation function has the form

$$C(r,t,h) = \lambda^2(b) C(r/b, b^{y_1}t, b^{y_2}h) \tag{3.50}$$

Clearly length scales transform as $r' = r/b$. Again setting $h = 0$ and choosing $b^{y_1}t = 1$ gives

$$C(r,t,h) = \lambda^2(t^{-\frac{1}{y_1}}) C(r/t^{-\frac{1}{y_1}}, 1, 0). \tag{3.51}$$

The correlation function, by definition is given by

$$C(r,t) \sim f(r/\xi), \tag{3.52}$$

where ξ is the correlation length. This immediately tells us that $\xi = t^{-\frac{1}{y_1}}$ and from the usual definition

$$\xi \sim t^{-\nu} \tag{3.53}$$

we have $\nu = 1/y_1$. These two formula for y_1 then give the hyper scaling relation

$$\alpha = 2 - d\nu. \tag{3.54}$$

The exponents α and ν are the ones that are important in the critical Casimir effect.

Finite size scaling

Consider a system which is finite in one direction with either periodic boundary systems or two surfaces. While the critical system has $h = 0$ there can be local surface fields at each surface a and b. This represents a preference of the surfaces for one phase or the other.

The finite scaling hypothesis for a slab system of large area A but with finite width L can be stated as

$$f(t, h_a, h_b, L^{-1}) = \frac{1}{b^d} f(b^{y_1} t, b^{y_a} h_a, b^{y_b} h_b, bL^{-1}), \tag{3.55}$$

we thus see that the field L^{-1} is a relevant field with RG exponent $y_L = 1$. The surface fields are not necessarily relevant so we han have y_a and y_b positive or negative. The important point about finite size scaling is that when L is finite the singularity due to the thermodynamique phase transition is smoothed out by the system's finite size (note that we assume that the system has no two dimensional phase transition in the region we are looking at). First we see that when L is large there should be a bulk contribution to the free energy plus a surface term (so we are considering the limit $L \to \infty$ before $\xi \to \infty$)

$$\begin{aligned} f(t, h_a, h_b, L^{-1}) &= f(t, h_a, h_b, 0) + L^{-1} \frac{\partial f(t, h_a, h_b, 0)}{\partial x_4} \\ &= \frac{1}{b^d} f(b^{y_1} t, b^{y_a} h_a, b^{y_b} h_b, 0) + \frac{1}{b^{d-1}} L^{-1} \frac{\partial f(b^{y_1} t, b^{y_a} h_a, b^{y_b} h_b, 0)}{\partial x_4} \end{aligned} \tag{3.56}$$

where we have carried out the Taylor expansion for L^{-1} small using both versions of Eq. (3.59) and $\frac{\partial}{\partial x_n}$ indicates the partial derivative with respect to the n^{th} argument. The second term gives a total contribution to the singular part of the free energy of the order $AL \times L^{-1}$ and is thus a surface tension γ and so we have

$$\gamma = \frac{1}{b^{d-1}} \frac{\partial f(b^{y_1} t, b^{y_a} h_a, b^{y_b} h_b, 0)}{\partial x_4}. \tag{3.57}$$

Setting $bt^{y_1} = 1$ then gives close to the critical point

$$\gamma \sim t^{\frac{d-1}{y_1}} \frac{\partial f(1, \lim_{t\to 0} t^{-\frac{y_a}{y_1}} h_a, \lim_{t\to 0} t^{-\frac{y_a}{y_1}} h_b, 0)}{\partial x_4} = t^{(d-1)\nu} C' = \xi^{-(d-1)} C', \tag{3.58}$$

the formula relating the surface tension and the correlation length, in the above C' is a constant depending on the universality class.

Now if we keep L finite and set $b^{y_1} t = 1$ in Eq. (3.59) we find

$$f(t, h_a, h_b, L^{-1}) = t^{\frac{d}{y_1}} f(1, t^{-\frac{y_a}{y_1}} h_a, t^{-\frac{y_b}{y_1}} h_b, t^{-\frac{1}{y_1}} L^{-1}), \tag{3.59}$$

which can be written as

$$f(t, h_a, h_b, L^{-1}) = \frac{1}{\xi^d} f(1, \xi^{y_a} h_a, \xi^{y_b} h_b, \xi/L), \tag{3.60}$$

This can then be written as

$$f(t, h_a, h_b, L^{-1}) = \frac{1}{L^d} \theta(\frac{L}{\xi}, \xi^{y_a} h_a, \xi^{y_b} h_b). \tag{3.61}$$

Now crucially as $\xi \to \infty$ the function θ is analytic so we can take the limit $\xi \to \infty$ without any problems to find

$$f(0, h_a, h_b, L^{-1}) = \frac{1}{L^d} \theta(0, \lim_{\xi\to\infty} \xi^{y_a} h_a, \lim_{\xi\to\infty} \xi^{y_b} h_b) \tag{3.62}$$

Clearly for each surface we have 3 possibilities : $\lim_{\xi\to\infty} \xi^{y_a} h_a = \pm\infty$, if the surface fields are relevant, as well as $\lim_{\xi\to\infty} \xi^{y_a} h_a = 0$ if the surface fields are irrelevant. There is clearly also a similar argument when the system has periodic boundary conditions and there are no surface fields. Near the critical point depending on the boundary conditions there should be scaling functions when the surface fields attract the same phase $\theta_{++}(x)$, where they attract different phases and $\theta_{+-}(x)$, and $\theta_{pbc}(x)$ when the boundary conditions are periodic. There should also be a zero surface field case θ_{00} when the surfaces fields are irrelevant or zero (this is however unlikely). Fisher and de Gennes argued, without proof, that the force for $++$ boundary conditions should be attractive where as the $+-$ case should produce repulsive forces.

The total singular part of the free energy is thus given by

$$F = ALf(t, h_a, h_b, L^{-1}) = \frac{A}{L^{d-1}} \theta(\frac{L}{\xi}, \xi^{y_a} h_a, \xi^{y_b} h_b). \tag{3.63}$$

The scale of the energy is set by the energy of thermal fluctuations $k_B T$ we thus find that

$$F(t = 0) = \frac{k_B T A C}{L^{d-1}} \tag{3.64}$$

where C is a constant depending on the surface universality class.

3.2 Finite size scaling in one dimensional interface models

3.2.1 Continuous models in one dimension

In one dimension the partition function for a surface model of the type discussed above can be written as a functional integral

$$Z(L) = \int d[h] \exp\left(-\frac{\beta\sigma}{2}\int_0^L h'^2(x)dx - \beta\int_0^L V(h(x))dx\right). \tag{3.65}$$

It is convenient to fix both the starting point $h(0) = x$ and the end point $h(L) = x$ and define what is known as the propagator

$$K(h,h',L) = \int_{h(0)=h} d[h]\delta(h'-h(L)) \exp\left(-\frac{\beta}{2}\int_0^L \sigma h'^2(x)dx - \beta\int_0^L V(h(x))dx\right). \tag{3.66}$$

The propagator is an example of a path integral and is the sum over all paths going between h and h' in what can be taken to be the time L. It can be shown that the path integral obeys an imaginary time Schrödinger equation

$$\frac{\partial K(h,h',L)}{\partial L} = -\hat{H}K(h,h',L), \tag{3.67}$$

where $\hat{H}$ is the Hamiltonian operator

$$\hat{H} = -\frac{1}{2\sigma\beta}\frac{\partial^2}{\partial h^2} + \beta V(h), \tag{3.68}$$

and, with a suitable normalisation, the initial condition

$$K(h,h',L) = \delta(h-h'). \tag{3.69}$$

If the Hamiltonian operator $\hat{H}$ has eigenfunctions ψ_n, normalised so that

$$\int dh\ \psi_n^2(h) = 1, \tag{3.70}$$

and with eigenvalues ϵ_n, it is easy to see that the propagator can be written as

$$K(h,h',L) = \sum_n \exp(-L\epsilon_n)\psi_n(h)\psi_n(h'). \tag{3.71}$$

If we take a system with periodic boundary conditions but otherwise leave the initial value $h(0)$ of the height to be free, then using the normalisation of the eigenfunctions, we find

$$Z(L) = \int dh K(h, h', L) = \sum_n \exp(-L\epsilon_n). \tag{3.72}$$

Now in the thermodynamic limit $L \to \infty$ if there is a gap between the ground state energy ϵ_0 and the first excited state, $g = \epsilon_1 - \epsilon_0$ which is non-zero, we can apply ground state dominance

$$Z(L) = \exp(-L\epsilon_0) \tag{3.73}$$

which gives the free energy per unit length as

$$f = \frac{1}{\beta}\epsilon_0. \tag{3.74}$$

As well as the free energy we are interested in the probability distribution of the height at a single point (which is independent of the point choses due to invariance by translation of the system). For instance the probability distribution of $h(0)$ is given by

$$p_1(h) = \frac{\int d[h]\delta(h(0)-h)\exp\left(-\frac{\beta}{2}\int_0^L h'^2(x)dx - \beta\int_0^L V(h(x))dx\right)}{Z(L)} \tag{3.75}$$

$$= \frac{K(h,h,L)}{Z(L)} = \frac{\sum_n \exp(-L\epsilon_n)\psi_n^2(h)}{\sum_n \exp(-L\epsilon_n)} \tag{3.76}$$

and so as $L \to \infty$, ground state dominance gives

$$p_1(h) = \psi_0^2(h). \tag{3.77}$$

We see that the normalisation of the probability density function for h follows from the normalisation of the wave functions.

The joint probability density function for two heights separated by a time or distance x is given by

$$p_2(h,h',x) = \frac{\int d[h]\delta(h(0)-h)\delta(h(x)-h')\exp\left(-\frac{\beta}{2}\int_0^L h'^2(x)dx - \beta\int_0^L V(h(x))dx\right)}{Z(L)} \tag{3.78}$$

$$= \frac{K(h,h',x)K(h',h,L-x)}{Z(L)} = \frac{\sum_{nm}\exp(-x\epsilon_n)\psi_n(h)\psi_n(h')\exp(-[L-x]\epsilon_m)\psi_m(h')\psi_m(h)}{\sum_n \exp(-L\epsilon_n)} \tag{3.79}$$

Due to ground state dominance only the term with $m = 0$ survives in the sum above (as as x is taken such that $x \ll L$) as we find

$$p_2(h, h', x) = \sum_n \psi_0(h')\psi_0(h)\psi_n(h')\psi_n(h) \exp(-x[\epsilon_n - \epsilon_0])) \quad (3.80)$$

$$= p_1(h)p_1(h') + \sum_{n\rangle 0} \psi_0(h')\psi_0(h)\psi_n(h')\psi_n(h) \exp(-x[\epsilon_n - \epsilon_0])). \quad (3.81)$$

From this we see that when $x[\epsilon_n - \epsilon_0] \gg 1$ for all n and so in particular $x[\epsilon_1 - \epsilon_0] \gg 1$ we have

$$p_2(h, h', x) \sim p_1(h)p_2(h'), \quad (3.82)$$

so that the height at large distances are uncorrelated or equivalently are independent random variables. This gives a correlation length

$$\xi = \frac{1}{\epsilon_1 - \epsilon_0}. \quad (3.83)$$

3.2.2 The confined elastic line

Here we consider the case where $V(h) = 0$ for $0\langle h\langle \ell$ and $V(h) = 0$ otherwise. This corresponds to a one dimensional elastic line confined between two impenetrable walls separated by a distance ℓ. The Hamiltonian $\hat{H}$ is that for a quantum well of width ℓ and the eigenfunctions can be found in any elementary textbook on quantum mechanics. The are

$$\psi(h) = \sqrt{\frac{2}{\ell}} \sin(\frac{\pi(n+1)h}{\ell}) \quad (3.84)$$

where $n \geq 0$ are integers. From this we see that

$$\epsilon_0 = \frac{1}{2\sigma\beta} \frac{\pi^2}{\ell^2}, \quad (3.85)$$

and so

$$f = \frac{1}{2\sigma\beta^2} \frac{\pi^2}{\ell^2} = \frac{T^2\pi^2}{2\sigma\ell^2}. \quad (3.86)$$

Here the pressure (in this case pressure in a force per unit length) is given by

$$P = -\frac{\partial f}{\partial \ell} = \frac{\pi^2 T^2}{\sigma\ell^3}, \quad (3.87)$$

and we see that it is repulsive, physically the fluctuations of the surface repel the walls. The pressure has the Casimir like characteristic that it behaves as a long range power law type interaction, however a two dimensional critical Casimir system (see (3.64)) would have a free energy per unit length $f = CT/\ell$. We also see that the free energy scales a T^2 rather than T (as is the case for the Casimir interaction).Having said this, a critical system has zero surface tension and so using a model with a finite surface tension for the interface is clearly not appropriate.

Here, using Eq. (3.83) we find that the correlation length is given by

$$\xi = \frac{2}{3}\frac{\sigma\ell^2}{T\pi^2}, \tag{3.88}$$

thus it increases as the surface tension is increased or the temperature is lower, this makes physical sense as the surface should become *flatter* under these conditions. Also as the system becomes more confined the correlation length increases, again as confinement kills fluctuations. The correlation length tells us that if we wanted to simulate this system then we need to take

$$L \gg \xi, \tag{3.89}$$

in order to be in the thermodynamics limit and so $L \gg \frac{\sigma\ell^2}{T\pi^2}$, thus for ℓ large, in general we would need to simulate rather large systems. The probability distribution function of the height at a single point is given by

$$p_1(h) = \frac{2}{\ell}\sin^2(\frac{\pi h}{\ell}) \tag{3.90}$$

and from this we find

$$\langle h\rangle = \frac{\ell}{2}, \tag{3.91}$$

which is rather obvious. The width of the interface is given by

$$w = \sqrt{\langle h^2\rangle - \langle h\rangle^2}, \tag{3.92}$$

and here it is given by

$$w = \ell\sqrt{\frac{1}{12} - \frac{1}{2\pi^2}} = 0.0326727\ \ell \tag{3.93}$$

3.2.3 The Airy line

In the above well known example we confine the surface and then compute the pressure. This is an example of the constant volume ensemble. Physically we could also consider the case of a system which is confined softly by an externally imposed pressure P_0 the constant pressure ensemble. In this case the potential is given by

$$V(h) = P_0 h \text{ for } h\rangle 0 \; ; = \infty \text{ for } h \leq 0. \tag{3.94}$$

The time independent Schrödinger equation for the eigenfunctions here is

$$-\frac{1}{2\sigma\beta}\frac{d^2\psi_n(h)}{dh^2} + P_0\beta h\psi_n(h) = \epsilon_n\psi_n(h). \tag{3.95}$$

The corresponding eigenfunctions have boundary conditions $\psi_n(0) = 0$ due to the hard wall potential at $h = 0$ and they must also decay to zero as $h \to \infty$ so as to be normalisable.

The key to finding the eigenfunctions is to transform the Schrödinger into the Airy equation which is

$$\frac{d^2y(x)}{dx^2} - xy(x) = 0. \tag{3.96}$$

This equation has solutions $\mathrm{Ai}(x)$ which decay as

$$\mathrm{Ai}(x) \sim \frac{\exp(-\frac{2}{3}x^{\frac{3}{2}})\Gamma(\frac{5}{6})\Gamma(\frac{1}{6})}{4\pi^{\frac{3}{2}}x^{\frac{1}{4}}}, \tag{3.97}$$

as $x \to \infty$ and so are normalizable as eigenfunctions. For $x\langle 0$ the Airy function oscillates and has an infinite number of negative zeros $-\alpha_n$ such that $\mathrm{Ai}(-\alpha_n) = 0$.

We make the change of variable $h = \mu z'$ to find

$$\frac{1}{2\sigma\beta\mu^2}\frac{d^2\psi_n(z')}{dz'^2} - P_0\beta\mu(z' - \varepsilon_n)\psi_n(z') = 0, \tag{3.98}$$

where $\varepsilon_n = \epsilon_n/(P_0\beta\mu)$. Now we chose μ so that

$$2\sigma\beta^2 P_0\mu^3 = 1, \tag{3.99}$$

and we see that

$$\mu = \left(\frac{1}{2\beta^2\sigma P_0}\right)^{\frac{1}{3}}, \tag{3.100}$$

is an intrinsic length scale.

$$\frac{d^2\psi_n(z')}{dz'^2} - (z' - \varepsilon_n)\psi_n(z') = 0. \tag{3.101}$$

Finally if we use $z = z' - \varepsilon_n$ we obtain Airy's equation

$$\frac{d^2\psi_n(z)}{dz^2} - z\psi_n(z) = 0 \tag{3.102}$$

and so

$$\psi_n(z) = c_n \mathrm{Ai}(z), \tag{3.103}$$

where c_n is a normalisation constant. This means that in terms of the original height variable h,

$$\psi_n(h) = c_n \mathrm{Ai}(\frac{h}{\mu} - \varepsilon_n). \tag{3.104}$$

The boundary condition $\psi_n(h)$ then show that we must choose $\varepsilon_n = \alpha_{n+1}$. This means that the ground state energy is

$$\epsilon_0 = \alpha_1 P_0 \beta \mu = \frac{\alpha_1 P_0 \beta}{(2\sigma\beta^2 P_0)^{\frac{1}{3}}} = \frac{\alpha_1 P_0^{\frac{2}{3}} \beta^{\frac{1}{3}}}{2^{\frac{1}{3}} \sigma^{\frac{1}{3}}}, \tag{3.105}$$

and where we note that $\alpha_1 = 2.33811$.

$$f = \frac{\alpha_1 P_0^{\frac{2}{3}}}{2^{\frac{1}{3}} \sigma^{\frac{1}{3}} \beta^{\frac{2}{3}}}. \tag{3.106}$$

From the original partition function we see that h is conjugate to P_0 and so we find the average height is given by

$$\bar{h} = \langle h \rangle = \frac{\partial f}{\partial P_0} = \frac{2}{3} \frac{\alpha_1}{2^{\frac{1}{3}} \sigma^{\frac{1}{3}} \beta^{\frac{2}{3}} P_0^{\frac{1}{3}}} = \frac{2}{3} \alpha_1 \mu, \tag{3.107}$$

and solving for P_0 in terms of $\overline{h}$ gives

$$P_0 = \frac{4}{27} \frac{\alpha_1^3 T^2}{\sigma \overline{h}^3}, \tag{3.108}$$

we see that P_0 behaves exactly in the same way as the pressure of a confined elastic line

in term of the temperature and surface tension. Only the overall numerical prefactor is different.

The correlation length is given by

$$\xi = \frac{2^{\frac{1}{3}}(\sigma T)^{\frac{1}{3}}}{(\alpha_2 - \alpha_1)P_0^{\frac{2}{3}}}. \tag{3.109}$$

When written in terms of $\overline{h}$ the above correlation length behaves in the same way as for the free elastic line, however when P_0 is fixed we see that the behavior as a function of T and σ is quite different. The correlation length still increases with σ but now decreases as the temperature is decreases.

The probability density function for the height of the interface at a single point is given by

$$p_1(h) = \frac{\mathrm{Ai}^2(\frac{h}{\mu} - \alpha_0)}{\int_0^\infty dh' \mathrm{Ai}^2(\frac{h'}{\mu} - \alpha_0)} \tag{3.110}$$

However if we write the height variable in terms of the length scale μ, $h(x) = \mu z(x)$ we find that z has the single point probability density function

$$p(z) = \frac{\mathrm{Ai}^2(z - \alpha_0)}{\int_0^\infty dz' \mathrm{Ai}^2(z' - \alpha_0)}. \tag{3.111}$$

Make a nice plot of p(z) with a properly referenced legend Using this we find the average height is given by

$$\langle h \rangle = \overline{h} = \mu z_0, \tag{3.112}$$

where

$$z_0 = \frac{\int_0^\infty dz z \mathrm{Ai}^2(z - \alpha_0)}{\int_0^\infty dz \mathrm{Ai}^2(z - \alpha_0)}. \tag{3.113}$$

Interestingly comparison with the thermodynamic calculation giving Eq. (3.107) shows that the identity

$$z_0 = \frac{2}{3}\alpha_0, \tag{3.114}$$

must hold- this surprising identity can be verified numerically. Here we find that the width is given by

$$w = 0.697089\ \mu \tag{3.115}$$

3.3 The confined solid on solid model

Here we consider the effect of confining the solid on solid model. The finite size effects in the SOS for both the restricted and unrestricted model were studied by Svravick et al. The formula for the eigenvalues of the even eigenvectors was given without derivation and the eigenvectors and odd eigenvalues were not discussed. In addition the limiting behavior of the free energy at high and low temperatures was not analysed and the correlation length was not discussed either.

Here we give the derivation for a system with sites between 0 and H and with $V = 0$. The SOS transfer matrix is thus given by

$$T_{ij} = \exp(-\beta\sigma|j-i|). \tag{3.116}$$

We no proceed to find the eigenvectors of T. Consider the vector denoted by $[a]$ which has components

$$[a]_i = a^i, \tag{3.117}$$

where i is an index ranging from 0 to H. The action of the SOS transfer matrix on this vector is given by

$$[T\ [a]]_i = \sum_{j=0}^{H} \exp(-\beta\sigma|i-j|)a^j \tag{3.118}$$

and we find

$$\begin{aligned}
[T\ [a]]_i &= \exp(-\beta\sigma i)\sum_{j=0}^{i}\exp(\beta\sigma j)a^j + \exp(\beta\sigma i)\sum_{j=i+1}^{H}\exp(-\beta\sigma j)a^j \\
&= \exp(-\beta\sigma i)\sum_{j=0}^{i}\exp(\beta\sigma j)a^j + \exp(\beta\sigma i)\sum_{k=0}^{H-i-1}\exp(-\beta\sigma[i+1+k])a^{i+1+k} \\
&= \exp(-\beta\sigma i)\frac{1-\exp(\beta\sigma(i+1))a^{i+1}}{1-\exp(\beta\sigma)a} + \exp(-\beta\sigma)a^{i+1}\frac{1-\exp(-\beta\sigma(H-i))a^{H-i}}{1-\exp(-\beta\sigma)a} \\
&= \left[\frac{\exp(-\beta\sigma)a}{1-\exp(-\beta\sigma)a} - \frac{\exp(\beta\sigma)a}{1-\exp(\beta\sigma)a}\right]a^i + \frac{\exp(-\beta\sigma i)}{1-\exp(\beta\sigma)a} - \frac{\exp(-\beta\sigma(H+1))a^{H+1}\exp(\beta\sigma i)}{1-\exp(-\beta\sigma)a} \\
&= \left[\frac{ra}{1-ra} - \frac{\frac{a}{r}}{1-\frac{a}{r}}\right]a^i + \frac{r^i}{1-\frac{a}{r}} - \frac{r^{H+1}a^{H+1}\frac{1}{r^i}}{1-ra}
\end{aligned}$$

where we have introduced

$$r = \exp(-\beta\sigma). \tag{3.119}$$

We now define

$$\lambda(a) = \frac{ra}{1-ra} - \frac{\frac{a}{r}}{1-\frac{a}{r}} = \frac{\frac{1}{r} - r}{\frac{1}{r} + r - a - \frac{1}{a}} \tag{3.120}$$

and notice that

$$\lambda(a) = \lambda(a^{-1}). \tag{3.121}$$

We can thus write

$$[T\ [a]]_i = \lambda(a)a^i + \frac{r^i}{1-\frac{a}{r}} - \frac{r^{H+1}a^{H+1}\frac{1}{r^i}}{1-ra}. \tag{3.122}$$

Now consider the action of the transfer matrix on the vector $[a^{-1}]$, we find

$$\left[T\ [a^{-1}]\right]_i = \lambda(a)a^{-i} + \frac{r^i}{1-\frac{1}{ra}} - \frac{r^{H+1}a^{-(H+1)}\frac{1}{r^i}}{1-\frac{r}{a}}. \tag{3.123}$$

We now look for an eigenvector of the form

$$\mathbf{v} = [a] + c[a^{-1}]. \tag{3.124}$$

The action of T on $\mathbf{v}$ is this

$$\left[T\ ([a] + c[a^{-1}]\right]_i = \lambda(a)[a^i + ca^{-i}] + r^i\left(\frac{1}{1-\frac{a}{r}} + \frac{c}{1-\frac{1}{ra}}\right) - \frac{r^{H+1}}{r^i}\left(\frac{a^{H+1}}{1-ra} + c\frac{a^{-(H+1)}}{1-\frac{r}{a}}\right). \tag{3.125}$$

and we see that $\mathbf{v}$ is an eigenvector, with eigenvalue $\lambda(a)$, if

$$\frac{1}{1-\frac{a}{r}} + \frac{c}{1-\frac{1}{ra}} = 0 \tag{3.126}$$

$$\frac{a^{H+1}}{1-ra} + c\frac{a^{-(H+1)}}{1-\frac{r}{a}} = 0. \tag{3.127}$$

The above equations imply that

$$c = -\frac{ra-1}{a(r-a)} \tag{3.128}$$

and

$$c^2 = a^{2H}. \tag{3.129}$$

Therefore we find

$$v_i = a^i \pm a^{H-i}, \tag{3.130}$$

however we expect the ground state eigenvector (corresponding to the largest eigenvalue) to be symmetric about the middle of the system and so

$$v_i = v_{H-i}, \tag{3.131}$$

which implies that we should have $c = a^H$.

This then gives the equation determining the values of a for the largest eigenvalue, and in general for the eigenvalues which are symmetric $c = 1$,

$$a^{H+1} = \frac{1 - ra}{r - a}. \tag{3.132}$$

As a check on the above derivation we can consider the case $H = 1$ so we have two sites. Here we see that the transfer matrix is given explicitly by

$$T = \begin{pmatrix} 1 & r \\ r & 1 \end{pmatrix} \tag{3.133}$$

and the largest eigenvector is easily seen to be given by

$$\lambda_0 = 1 + r \tag{3.134}$$

Now for $H = 1$ we that Eq. (3.132) gives

$$a^2 = \frac{1 - ra}{r - a} \tag{3.135}$$

has three solutions

$$a_1 = -1 \tag{3.136}$$

$$a_2 = \frac{1}{2}\left(-\sqrt{r^2 + 2r - 3} + r + 1\right) \tag{3.137}$$

$$a_3 = \frac{1}{2}\left(\sqrt{r^2 + 2r - 3} + r + 1\right) \tag{3.138}$$

We see that $a_2 = 1/a_3$, and $|a_2| = |a_3| = 1$, also

$$\lambda(-1) = \frac{1-r}{1+r} \tag{3.139}$$

while

$$\lambda(a_2) = \lambda(a_3) = 1 + r \tag{3.140}$$

corresponds to the maximal eigenvalue. Note that $\lambda(-1)$ is not the other eigenvector of the transfer matrix, this has to be found by considering solutions with $c = -1$, as we will see later.

The equation (3.132) determining a can also be written as

$$a^H = -\frac{r - \frac{1}{a}}{r - a}, \tag{3.141}$$

from this we see that if a is a solution then $1/a$. Also we see that $a = -1$ is always a solution.

If we write $a = \exp(i\theta)$ then

$$\exp(iH\theta) = -\frac{r - \exp(-i\theta)}{r - \exp(i\theta)}, \tag{3.142}$$

while

$$\lambda(\theta) = \frac{\sinh(\beta\sigma)}{\cosh(\beta\sigma) - \cos(\theta)}. \tag{3.143}$$

Notice that in order to construct a real eigenvector corresponding to λ_0 we can use the fact that both $v_i(a) = a^i + a^{H-i}$ and $v_i(a^{-1}) = a^{-i} + a^{-H+i}$ are both eigenvectors with the same eigenvalue. This means that $u_i(a) = v_i(a) + v_i(-a)$ is also and eigenvector and all its components are real.

Clearly the largest eigenvalue corresponds to the value of θ closest to 0. For H large we look for an eigenvalue such that $H\theta \sim 1$ and so we write

$$\theta = \frac{\phi}{H} \tag{3.144}$$

for H large this gives

$$\exp(i\phi) \approx -\frac{r - 1 + i\frac{\phi}{H}}{r - 1 - i\frac{\phi}{H}} \approx -1 + 2i\frac{\phi}{H(1-r)} \tag{3.145}$$

and so we find to leading order in $1/H$,

$$\theta = \frac{(2n+1)\pi}{H}. \tag{3.146}$$

However we notice that this approximation is only valid if $H(1-r) \gg 1$. For large β this approximation is simply equivalent to $H \gg 1$, however when β is small it requires that $H\beta \gg 1$.

The closest to the real axis has $n = 0$ and so we have

$$\lambda_0 \approx \frac{\sinh(\beta\sigma)}{\cosh(\beta\sigma) - \cos(\frac{\pi}{H})} \approx \frac{\sinh(\beta\sigma)}{\cosh(\beta\sigma) - 1 + \frac{\pi^2}{2H^2}} \approx \coth(\frac{\beta\sigma}{2})(1 - \frac{\pi^2}{4\sinh^2(\frac{\beta\sigma}{2})H^2}) \tag{3.147}$$

In order to compute the second eigenvalue λ_1 we look for and odd an antisymmetric solution with $c = -1$. We thus find

$$\exp(iH\theta) = \frac{r - \exp(-i\theta)}{r - \exp(i\theta)}. \tag{3.148}$$

For large H we look for a solution of the form $\theta = \phi/H$ and this gives

$$\exp(i\phi) \approx 1, \tag{3.149}$$

and so we chose solutions $\phi = 2n\pi$ for integer n, however the solution $n = 0$ which corresponds to $a = 1$ has $v(i) = a^i - a^{H-i} = 0$ and so does not correspond to an eigenvector. We thus take the next solution $\phi = 2\pi$ which gives

$$\lambda_1 \approx \frac{\sinh(\beta\sigma)}{\cosh(\beta\sigma) - \cos(\frac{2\pi}{H})} \approx \frac{\sinh(\beta\sigma)}{\cosh(\beta\sigma) - 1 + \frac{2\pi^2}{H^2}} \approx \coth(\frac{\beta\sigma}{2})(1 - \frac{\pi^2}{\sinh^2(\frac{\beta\sigma}{2})H^2}) \tag{3.150}$$

The correlation length is then given by

$$\xi = \frac{1}{\ln(\frac{\lambda_0}{\lambda_1})} = \frac{1}{\ln(\frac{\cosh(\beta\sigma)-\cos(\frac{\pi}{H})}{\cosh(\beta\sigma)-\cos(\frac{2\pi}{H})})} \approx \frac{4}{3}\frac{\sinh^2(\frac{\beta\sigma}{2})H^2}{\pi^2}, \tag{3.151}$$

and we see that this has the same form as that for the free elastic line in Eq. (3.88). Furthermore, the free energy per site is given in the thermodynamic limit and for large H

by

$$f = -\frac{1}{\beta}\ln(\lambda_0) \approx -\frac{1}{\beta}\left[\ln(\coth(\frac{\beta\sigma}{2})) - \frac{\pi^2}{4\sinh^2(\frac{\beta\sigma}{2})H^2}\right] \tag{3.152}$$

and this gives a pressure

$$P = -\frac{\partial f}{\partial H} = \frac{T\pi^2}{2\sigma\sinh^2(\frac{\beta}{2})H^2}. \tag{3.153}$$

This has the same form as the pressure for the elastic line in Eq. (3.87) if we make the identification of the effective surface tension to be used in the elastic line model

$$\sigma_{eff} = \frac{2}{\beta}\sinh^2(\frac{\beta\sigma}{2}). \tag{3.154}$$

We should note that this is also consistent with the equality deduced by comparing the correlation length of the two models.

We see that in the limit of large H and for appropriately low temperatures, the finite size SOS model reproduced the phenomenology of the elastic line (confined Edwards-Wilkinson surface). This is not surprising as a low temperatures jumps of more that two lattice spacings in the height are suppressed by a factor or $\exp(-\beta\sigma)$ with respect to staying at the same height moving up or down by one site. The low temperature SOS model thus becomes effectively equivalent to the RSOS model and thus is equivalent to a local random walk model.

To explore the high temperature limit we can note that if we write

$$z = r - \exp(-i\theta), \tag{3.155}$$

we can write Eq. (3.142) as

$$\exp(iH\theta) = -\frac{z}{\bar{z}} = \exp(2i\psi + i\pi), \tag{3.156}$$

where

$$\tan(\psi) = \frac{\sin(\theta)}{r - \cos(\theta)}. \tag{3.157}$$

This then gives

$$H\theta = 2\psi + \pi, \tag{3.158}$$

and so

$$\tan(\psi) = \frac{\sin(\theta)}{r - \cos(\theta)} = \tan(\frac{H\theta}{2} + \frac{\pi}{2}) = -\cot(\frac{H\theta}{2}) \tag{3.159}$$

which finally gives

$$\tan(\frac{H\theta}{2}) = \frac{\cos(\theta) - r}{\sin(\theta)}. \tag{3.160}$$

In this form we see that our calculations agree with those of Svravick et al. Futhermore when $\beta \to 0$ we know that the elements of the transfer matrix all tend to one and that the largest eigenvalue has all components equal. This means that in the infinite temperature limit $\theta = 0$. Therefore in Eq. (3.160) we look for solutions where θ is small. Taylor expanding gives to leading order

$$\frac{H\theta^2}{2} \approx 1 - r - \frac{\theta^2}{2}, \tag{3.161}$$

which gives

$$\theta \approx \sqrt{\frac{2(1-r)}{H+1}}. \tag{3.162}$$

However the above expansion assumes that $\theta H \ll 1$ and so

$$\sqrt{2H(1-r)} \ll 1. \tag{3.163}$$

Therefore at high temperature this means that $H\beta\sigma \ll 1$. This means that the height can fluctuate by of order H from site to site. The high temperature approximation is thus equivalent to

$$\theta \approx \sqrt{\frac{2\beta\sigma}{H+1}}. \tag{3.164}$$

This gives a maximal eigenvalue

$$\lambda_0 = H + 1, \tag{3.165}$$

and the free energy

$$f = -\frac{1}{\beta}\ln(H+1), \tag{3.166}$$

which is the obvious result coming from the infinite temperature entropy.

This result suggests that the solution for θ at small β can be written as a perturbation series of the form

$$\theta = \sqrt{\beta\sigma}\sum_{n=0}^{\infty} b_n(\beta\sigma)^n. \tag{3.167}$$

The first two terms give

$$\theta = \sqrt{\beta\sigma}\left[\sqrt{\frac{2\beta\sigma}{H+1}} - \beta\sigma\frac{2+2H+H^2}{6\sqrt{2}(1+H)^{\frac{3}{2}}}\right], \tag{3.168}$$

and from this we find

$$f = -\frac{1}{\beta}\ln(H+1-\beta\sigma\frac{H^2+2H}{3}). \tag{3.169}$$

As pointed out above this result gives the high temperature entropy but it also exhibits the correct average energy ϵ per unit length at high temperature. To see this we note that all values of h are equiprobable at infinite temperature and so

$$\epsilon = \frac{1}{(H+1)^2}\sigma\sum_{i,j=0}^{H}|i-j| = \sigma\frac{H^2+2H}{3}. \tag{3.170}$$

3.3.1 Numerical tests of finite size dependence

Chapitre 4

Driven model C interfaces

We consider the effect of uniform driving on the interface between two phases which are described by model C dynamics. The non-driven system has a classical Gaussian interface described by capillary wave theory. The model under driving retains Gaussian statistics but the interface statistics are modified by driving, notably the height fluctuations are suppressed and the correlation length of the fluctuations is increased.

4.1 Introduction

The model we introduce can also be used as a model for the effect of activity on interface dynamics. One of the most natural ways of creating a non-equilibrium steady state is by applying external driving forces. Driving arises naturally in sedimenting systems due to gravity, in systems with free charges under the action of an electric field and also due to the radiation pressure exerted by a laser. Experiments where a phase separated colloidal system is sheared parallel to the interface show that driving due to shear tends to suppress surface fluctuations [**?**], and similar results are found where Ising models are numerically sheared [**?** **?**]. These results are somewhat surprising, for instance they are contrary to the observation that wind generates waves on the ocean. One may think that the precise nature of the driving plays a role, for instance uniformly driving a system may be intrinsically different to applying a shear field which is manifestly nonuniform. In this paper we investigate analytically the effect of uniform driving on a simple interface model. We find that the effect of this type of driving is also to reduce surface fluctuations.

Constructing a continuum model which is analytically tractable and is also affected by

uniform driving is straightforward but contains some subtleties. In a continuum system it is clear that uniform driving can only move a system away from equilibrium when the driving acts differently on different particle types. For instance, consider a system of identical interacting Brownian particles driven by a uniform force. The force will induce the same average velocity on all the particles, consequently, in the frame moving with this average velocity, we will recover the unmodified equilibrium state. However, when multiple particle types are present, the mean velocity induced on different species are different and no Galilean transformation is possible. Perhaps the first such study of this phenomenon was due to Onsager [**?**], who studied the conductivity of electrolytes and in doing so showed how the correlation functions in the steady state were modified by the electric field. Recently there have been many studies of driven multi-particle Brownian systems [**? ? ? ? ? ? ?**], including the electrolyte problem, and rich new physics has been found, even in the case of purely Gaussian theories [**? ?**] based on stochastic density functional theory [**?**].

The dynamics of discrete particle systems is however affected by uniform driving of identical particles. The study of driven lattice gases has revealed a wide range of intriguing physical phenomena and indeed shown how driving can even lead to phase separation [**? ? ? ? ?**]. The discrete nature of the dynamics of these systems, both in space and time, means that no Galilean transformation to an equilibrium state exists. Analytical studies of these systems require a phase ordering kinetics description in terms of a continuum order parameter. In order to break Galilean invariance the local mobility of the particles can be taken to be dependent on the local order parameter, this is then sufficient to induce non-trivial steady states under driving [**? ? ? ?**]. Interfaces between the separated phases in uniformly driven systems have non capillary behaviors which are, even today, not fully understood [**?**]. Taking random driving in a given direction also leads to non-equilibrium steady states, if the noise is Gaussian and white, the fluctuation dissipation theorem is violated and novel interface fluctuations are induced which, again, are not of the capillary type [**?**].

Driving can also be deterministic but space dependent, for instance if one considers applied shear flows, the spatial dependence of the flow means no Galilean transformation to an equilibrium steady state is possible and this therefore leads to non-equilibrium steady states. The effect of shear on interfaces in these type of systems yields interface equations of the stochastic Burgers type and the statistics are no thus longer Gaussian due to the presence of nonlinearities [**? ? ? ? ? ?**].

In this paper we analyse what is known, in the classification of Hohenberg and Halperin [**?**], as model C type dynamics for two fields, one with conserved model B type dynamics, which is in addition convected at a uniform velocity to mimic driving. We refer to this first field as the colloid field. This colloid field is coupled to an additional field which undergoes model A non-conserved dynamics and which is not subjected to the driving. The model A field can be thought of a passive solvent and its coupling to the model B field is chosen in such a way that it has no influence on the non-driven equilibrium steady state. We then derive the effective dynamics between two separated low temperature phases by using a method introduced in [**? ?**] for the study of interfaces under shear flow. This method yields a Gaussian theory for the interface statistics and driving introduces interesting new physics, notably we find that the effective surface tension of the system is increased but also the correlation length of interface fluctuations (due to an effective gravitational term) are increased. These observations are in qualitative agreement with experimental results on sheared low tension interfaces in phase separated colloidal systems [**?**]. In this experimental system the interface fluctuations were also found to be well described by Gaussian statistics and this is our principal motivation for studying theories which remain Gaussian but are modified by driving. While the long wavelength theory we find is of a capillary type, we also find new, higher derivative terms, which are generated in the spectrum of the height fluctuations.

As an aside, we also show how the model introduced here can be used to analyse the effect of activity on the dynamics of the surface between two phases of active colloids. The activity is implemented by taking a different temperature for the colloid and solvent fields, this difference in temperatures leads to significantly modified surface statistics which again develop dependencies on static and dynamical variables of the model which otherwise remain hidden for the equilibrium version of the problem.

4.2 The underling two field model

We consider a coarse grained model for two scalar fields ψ and ϕ with Hamiltonian

$$H[\psi, \phi] = H_1[\psi] + H_2[\psi, \phi] \tag{4.1}$$

The Hamiltonian H_1 is of the classic Landau-Ginzburg form

$$H_1[\psi] = \int d\mathbf{x} \left[\frac{\kappa}{2} [\nabla \psi(\mathbf{x})]^2 + V(\psi(\mathbf{x})) - gz\psi(\mathbf{x}) \right]. \tag{4.2}$$

The last term represents the energy due to a gravitational field and will introduce a finite correlation length in the fluctuations between the two phases. We assume that the above Hamiltonian has two stable phases with average concentrations of the field $\phi(\mathbf{x})$ given by the constant values ψ_1 and ψ_2, the difference between the order parameter in the two different phases is denoted by by $\Delta\psi = \psi_2 - \psi_1 \rangle 0$. This means that we find the phase 1 as $z \to \infty$ and the phase 2 as $z \to -\infty$. The term H_2 is taken to be a simple quadratic coupling between the fields

$$H_2 = \int d\mathbf{x} \frac{\lambda}{2} (1 - \psi(\mathbf{x}) - \phi(\mathbf{x}))^2, \tag{4.3}$$

this is an approximative conservation law of total volume fraction of the phases. The field ϕ can be though of as the local volume fraction of the solvent in a colloidal system. However the presence of this solvent field does not change the effective equilibrium statistical mechanics of the colloid field ψ as the partition function can be written as

$$Z = \int d[\phi] d[\psi] \exp(-\beta H_1[\psi] - \beta H_2[\psi, \phi]) = C Z_{eff}, \tag{4.4}$$

where Z_{eff} is the effective partition function for the field ψ, after we have integrated out the degrees of freedom corresponding to the field ϕ, and C is a constant term resulting from this integration. The effective partition function is thus simply given by

$$Z_{eff} = \int d[\psi] \exp(-\beta H_1[\psi]), \tag{4.5}$$

and, as stated above, we see that the field ϕ thus has no effect on the equilibrium statistical mechanics of the field ψ.

We now consider the dynamics of the fields. We take local diffusive model B dynamics for the field ψ and non-conserved model A dynamics for the field ϕ

$$\frac{\partial \psi(\mathbf{x}, t)}{\partial t} + \mathbf{v} \cdot \nabla \psi(\mathbf{x}, t) = D\nabla^2 \frac{\delta H}{\delta \psi(\mathbf{x})} + \sqrt{2DT} \nabla \cdot \boldsymbol{\eta}_1(\mathbf{x}, t) \tag{4.6}$$

$$\frac{\partial \phi(\mathbf{x}, t)}{\partial t} = -\alpha \frac{\delta H}{\delta \phi(\mathbf{x})} + \sqrt{2\alpha T} \eta_2(\mathbf{x}, t). \tag{4.7}$$

The first equation corresponds to standard model B dynamics but with an advection term by a constant velocity field $\mathbf{v}$. The second equation has no advection term and is simple model A dynamics. In principle we can also treat the case where the dynamics of the field ϕ is also diffusive and thus of model B type, the analysis given here can be extended to this case but the analysis of the resulting equations is considerably more complicated. The use of model A dynamics for the solvent is justified by assuming that its dynamics is faster than that of the colloids and that the volume fraction can vary due to local conformational changes rather than diffusive transport.

The noise terms above are uncorrelated and Gaussian with zero mean, their correlation functions are given by

$$\langle \eta_{1i}(\mathbf{x},t)\eta_{1j}(\mathbf{x}',t)\rangle = \delta_{ij}\delta(t-t')\delta(\mathbf{x}-\mathbf{x}') \tag{4.8}$$

$$\langle \eta_2(\mathbf{x},t)\eta_2(\mathbf{x}',t)\rangle = \delta(t-t')\delta(\mathbf{x}-\mathbf{x}'), \tag{4.9}$$

and T is the temperature in units where $k_B = 1$. These dynamical equations are thus explicitly given by

$$\frac{\partial\psi(\mathbf{x},t)}{\partial t} + \mathbf{v}\cdot\nabla\psi(\mathbf{x},t) = D\nabla^2[\frac{\delta H_1}{\delta\psi(\mathbf{x})} + \lambda(\phi(\mathbf{x},t)+\psi(\mathbf{x},t))] + \sqrt{2DT}\nabla\cdot\boldsymbol{\eta}_1(\mathbf{x},t) \tag{4.10}$$

and

$$\frac{\partial\phi(\mathbf{x},t)}{\partial t} = -\alpha\lambda[\phi(\mathbf{x},t)+\psi(\mathbf{x},t)] + \sqrt{2\alpha T}\eta_2(\mathbf{x},t). \tag{4.11}$$

Taking the temporal Fourier transform, defined with the convention

$$\tilde{F}(\mathbf{x},\omega) = \int_{-\infty}^{\infty} dt\exp(-i\omega t)F(\mathbf{x},t), \tag{4.12}$$

we can eliminate the field $\tilde{\phi}$ which is given by

$$\tilde{\phi}(\mathbf{x},\omega) = \frac{-\alpha\lambda\tilde{\psi}(\mathbf{x},\omega) + \sqrt{2\alpha T}\tilde{\eta}_2(\mathbf{x},\omega)}{i\omega+\alpha\lambda}, \tag{4.13}$$

this then gives the closed equation for $\tilde{\psi}$:

$$\left[1 - \frac{\lambda D\nabla^2}{i\omega+\alpha\lambda}\right] i\omega\tilde{\psi}(\mathbf{x},\omega) + \mathbf{v}\cdot\nabla\tilde{\psi}(\mathbf{x},\omega) = D\nabla^2\tilde{\mu}(\mathbf{x},\omega) + \tilde{\zeta}(\mathbf{x},\omega), \tag{4.14}$$

where

$$\mu(\mathbf{x},t) = \frac{\delta H_1}{\delta \psi(\mathbf{x},t)} \tag{4.15}$$

is the effective chemical potential associated with the field ψ and the noise term is given by

$$\tilde{\zeta}(\mathbf{x},\omega) = \frac{\sqrt{2\alpha T}D\lambda}{i\omega + \alpha\lambda}\nabla^2\tilde{\eta}_2(\mathbf{x},\omega) + \sqrt{2DT}\nabla\cdot\tilde{\boldsymbol{\eta}}_1(\mathbf{x},\omega). \tag{4.16}$$

Inverting the temporal Fourier transform then gives the effective evolution equation

$$\frac{\partial\psi(\mathbf{x},t)}{\partial t} - \lambda D\nabla^2\int_{-\infty}^{t} dt' \exp(-\alpha\lambda(t-t'))\frac{\partial\psi(\mathbf{x},t')}{\partial t} + \mathbf{v}\cdot\nabla\psi(\mathbf{x},t) = D\nabla^2\mu(\mathbf{x},t') + \zeta(\mathbf{x},t). \tag{4.17}$$

4.3 Effective interface dynamics

We now follow the method of [**? ?**] to derive the dynamical equation for the interface between the two phases. It is assumed that the driving is in the $\mathbf{r} = (x, y)$ plane and that the system varies from phase 1 to phase 2 in the z direction. The dynamical evolution for the field ψ in Eq. (4.17) is first written as

$$\nabla^{-2}\left[\frac{\partial\psi(\mathbf{x},t)}{\partial t} + \mathbf{v}\cdot\nabla\psi(\mathbf{x},t)\right] - \lambda D\int_{-\infty}^{t} dt' \exp(-\alpha\lambda(t-t'))\frac{\partial\psi(\mathbf{x},t')}{\partial t'} = D\mu(\mathbf{x},t') + \nabla^{-2}\zeta(\mathbf{x},t). \tag{4.18}$$

We now assume that the field ψ can be written in the form

$$\psi(\mathbf{x},t) = f(z - h(\mathbf{r},t)), \tag{4.19}$$

and $f(z) \to \psi_2$ as $z \to -\infty$ and $f(z) \to \psi_2$ as $z \to \infty$. We now note the following results

$$\frac{\partial f(z-h(\mathbf{r},t))}{\partial t} = -f'(z-h(\mathbf{r},t))\frac{\partial h(\mathbf{r},t)}{\partial t} \tag{4.20}$$

$$\nabla f(z-h(\mathbf{r},t)) = [\mathbf{e}_z - \nabla h(\mathbf{r},t)]f'(z-h(\mathbf{r},t))] \tag{4.21}$$

$$\nabla^2 f(z-h(\mathbf{r},t)) = f''(z-h(\mathbf{r},t))[1+[\nabla h(\mathbf{r},t)]^2] - \nabla^2 h(\mathbf{r},t)f'(z-h(\mathbf{r},t)), \tag{4.22}$$

and thus we find

$$\mu(\mathbf{x},t) = -\kappa\left(f''(z-h(\mathbf{r},t))[1+[\nabla h(\mathbf{r},t)]^2] - \nabla^2 h(\mathbf{r},t) f'(z-h(\mathbf{r},t))\right) + V'(f(z-h(\mathbf{r},t)) - gz. \tag{4.23}$$

Multiplying both sides of the above by $f'(z-h(\mathbf{r},t))$ yields

$$\begin{aligned}
&f'(z-h(\mathbf{r},t))\mu(\mathbf{x},t) = \\
&-\kappa\left(f'(z-h(\mathbf{r},t)f''(z-h(\mathbf{r},t)[1+[\nabla h(\mathbf{r},t)]^2] - \nabla^2 h(\mathbf{r},t) f'(z-h(\mathbf{r},t))^2\right) + V'(f(z-h(\mathbf{r},t))f'(z-h(\mathbf{r},t)) \\
&-gzf'(z-h(\mathbf{r},t))
\end{aligned}$$

and then integrating over z we obtain

$$\begin{aligned}
\int_{-\infty}^{\infty} dz f'(z-h(\mathbf{r},t)\mu(\mathbf{x},t) &= \kappa\nabla^2 h(\mathbf{r},t)\int_{-\infty}^{\infty} dz\ f'(z-h(\mathbf{r},t))^2 - \int_{-\infty}^{\infty} dz g z f'(z-h(\mathbf{r},t)) \\
&= \kappa\nabla^2 h(\mathbf{r},t)\int_{-\infty}^{\infty} dz'\ f'(z')^2 - \int_{-\infty}^{\infty} dz' g(z'+h(\mathbf{r},t))f'(z') \\
&= \kappa\nabla^2 h(\mathbf{r},t)\int_{-\infty}^{\infty} dz'\ f'(z')^2 - \Delta\psi g h(\mathbf{r},t).
\end{aligned} \tag{4.24}$$

In the above we have assumed that $\int_{-\infty}^{\infty} dz' z' f'(z') = 0$ by symmetry (this is also consistent with the approximation made later on in Eq. (4.28)). Furthermore one can show that [**? ?**]

$$\kappa\int_{-\infty}^{\infty} dz'\ f'(z')^2 = \sigma, \tag{4.25}$$

where σ is the mean-field equilibrium Cahn-Hilliard estimate of the surface tension, obtained by assuming that $f(z) = \psi_{MF}(z)$ is the equilibrium mean field profile of the field ψ. We thus find

$$\int_{-\infty}^{\infty} dz f'(z-h(\mathbf{r},t)\mu(\mathbf{x},t) = \sigma[\nabla^2 h(\mathbf{r},t) - m^2 h(\mathbf{r},t)] \tag{4.26}$$

where $m^2 = \Delta\psi g/\sigma$. We now carry out the same operation on the left hand side of Eq. (4.18). First we have

$$\begin{aligned}\nabla^{-2}\frac{\partial\psi(\mathbf{x},t)}{\partial t} &+ \mathbf{v}\cdot\nabla\psi(\mathbf{x},t) + \lambda D\int_{-\infty}^{t} dt' \exp(-\alpha\lambda(t-t'))\frac{\partial\psi(\mathbf{x},t')}{\partial t'} = \\ &- \nabla^{-2}f'(z-h(\mathbf{r},t))[\frac{\partial h(\mathbf{r},t)}{\partial t} + \mathbf{v}\cdot\nabla h(\mathbf{r},t)] + \lambda D\int_{-\infty}^{t} dt' \exp(-\alpha\lambda(t-t'))f'(z-h(\mathbf{r},t')) \\ &\approx -\nabla^{-2}f'(z)[\frac{\partial h(\mathbf{r},t)}{\partial t} + \mathbf{v}\cdot\nabla h(\mathbf{r},t)] + \lambda D\int_{-\infty}^{t} dt' \exp(-\alpha\lambda(t-t'))f'(z)\frac{\partial h(\mathbf{r},t')}{\partial t'},\end{aligned}$$

where in the last line above we have neglected terms quadratic in h. Note that the neglecting of these additional terms is not strictly justified, they could potentially induce non-perturbative effects which render the surface fluctuations non-Gaussian. However we see here that the first order computation we carry out tends to reduce fluctuations with respect to equilibrium or non-driven interfaces and so if the equilibrium theory can be described by an equation which is linear in height fluctuations, it seems physically reasonable to assume that the the approximation also holds for the driven interface. Again, we multiply the above by $f'(z)$ and integrate over z. In the first term we make use of the approximation

$$f'(z) = \Delta\psi\delta(z) \tag{4.28}$$

and in the second we use the relation in Eq. (4.25). Putting this all together we obtain

$$\Delta\psi^2\int d\mathbf{r}G(0,\mathbf{r}-\mathbf{r}')[\frac{\partial h(\mathbf{r},t)}{\partial t}+\mathbf{v}\cdot\nabla h(\mathbf{r},t)]+\frac{\sigma\lambda D}{\kappa}\int_{-\infty}^{t} dt' \exp(-\alpha\lambda(t-t'))\frac{\partial h(\mathbf{r},t')}{\partial t'} = \sigma[\nabla^2 h(\mathbf{r},t)-m^2 h(\mathbf{r},t)] \tag{4.29}$$

where $G = -\nabla^{-2}$, or more explicitly

$$\nabla^2 G(z-z',\mathbf{r}-\mathbf{r}') = -\delta(z-z')\delta(\mathbf{r}-\mathbf{r}'). \tag{4.30}$$

The noise term ξ is given by

$$\xi(\mathbf{r},t) = \int_{-\infty}^{\infty} dz f'(z-h(\mathbf{r},t))\nabla^{-2}\zeta(\mathbf{x},t). \tag{4.31}$$

Now, as the equations of motion have been derived to first order in h and we wish to recover the correct equilibrium statistics for the non-driven system, we ignore the h dependence in

the noise and make the approximation

$$\xi(\mathbf{r},t) \approx \int_{-\infty}^{\infty} dz f'(z) \nabla^{-2} \zeta(\mathbf{x},t). \tag{4.32}$$

The correlation function of this noise is most easily evaluated in terms of its Fourier transform with respect to space and time defined by

$$\hat{F}(\mathbf{q},\omega) = \int dt d\mathbf{r} \exp(-i\omega t - i\mathbf{q}\cdot\mathbf{r}) F(\mathbf{r},t). \tag{4.33}$$

Using the relations Eqs. (4.25) and (4.28) one can show that

$$\langle \hat{\xi}(\mathbf{q},\omega)\hat{\xi}(\mathbf{q}',\omega')\rangle = 2T(2\pi)^d \delta(\omega+\omega')\delta(\mathbf{q}+\mathbf{q}') \left[\frac{\sigma}{\kappa}\frac{\alpha D^2\lambda^2}{\omega^2+\alpha^2\lambda^2} + \frac{D\Delta\psi^2}{2q}\right]. \tag{4.34}$$

In full Fourier space the equation of motion for the field ψ then reads

$$\left[i(\omega+\mathbf{q}\cdot\mathbf{v})\frac{\Delta\psi^2}{2q} + \frac{D\sigma\lambda}{\kappa}\frac{i\omega}{\alpha\lambda+i\omega}\right]\hat{h}(\mathbf{q},\omega) = -D\sigma(q^2+m^2)\hat{h}(\mathbf{q},\omega) + \hat{\xi}(\mathbf{q},\omega) \tag{4.35}$$

From this, the full Fourier transform of the correlation function of the interface height is given by

$$\hat{C}(\mathbf{q},\omega) = 2TD \frac{\left[\frac{\Delta\psi^2}{2q}(\omega^2+\alpha^2\lambda^2) + \frac{\sigma\alpha D\lambda^2}{\kappa}\right]}{\left|i[\frac{\alpha\lambda\Delta\psi^2}{2q}(\omega+\mathbf{q}\cdot\mathbf{v}) + \frac{\lambda\sigma D}{\kappa}\omega + D\sigma(q^2+m^2)\omega] + [\alpha\lambda D\sigma(q^2+m^2) - \frac{\Delta\psi^2}{2q}\omega(\omega+\mathbf{q}\cdot\mathbf{v})]\right|^2}. \tag{4.36}$$

Using the above we can extract the equal time height-height correlation function in the steady states. Its spatial Fourier transform can shown to be given by

$$\begin{aligned}\tilde{C}_s(\mathbf{q}) &= \frac{1}{2\pi}\int d\omega \hat{C}(\mathbf{q},\omega) \\ &= T\frac{\left(2D\sigma q(\kappa[q^2+m^2]+\lambda) + \alpha\kappa\lambda\Delta\psi^2\right)^2 + \kappa^2\Delta\psi^4(\mathbf{q}\cdot\mathbf{v})^2}{\sigma[q^2+m^2]\left(2Dq\sigma(\kappa[q^2+m^2]+\lambda) + \alpha\kappa\lambda\Delta\psi^2\right)^2 + \kappa\left(\kappa\sigma[q^2+m^2]+\lambda\sigma\right)\Delta\psi^4(\mathbf{q}\cdot\mathbf{v})^2}\end{aligned} \tag{4.37}$$

An outline of the derivation of this result is given in the Appendix to the paper. In the absence of driving, *i.e.* when $\mathbf{v}=\mathbf{0}$ we recover the equilibrium correlation function

$$\tilde{C}_s(\mathbf{q}) = \tilde{C}_{eq}(\mathbf{q}) = \frac{T}{\sigma[q^2+m^2]}, \tag{4.38}$$

here we see that $1/m = \xi_{eq}$ is the so called capillary length, which is the equilibrium correlation length of the height fluctuations. We also notice that the correlation function for wave vectors perpendicular to the driving direction is simply the equilibrium one.

If we write $C_s(\mathbf{q}) = T/H_s(\mathbf{q})$ we can interpret $H_s(\mathbf{q})$ as an effective quadratic Hamiltonian for the height fluctuations, it is thus given by

$$H_s(\mathbf{q}) = \sigma[q^2 + m^2] + \frac{\kappa\lambda\sigma\Delta\psi^4(\mathbf{q}\cdot\mathbf{v})^2}{(2D\sigma q(\kappa[q^2+m^2]+\lambda) + \alpha\kappa\lambda\Delta\psi^2)^2 + \kappa^2\Delta\psi^4(\mathbf{q}\cdot\mathbf{v})^2} \tag{4.39}$$

For small q we find

$$H_s(\mathbf{q}) = \sigma m^2 + \sigma q^2(1 + \frac{v^2\cos^2(\theta)}{\alpha^2\lambda\kappa}), \tag{4.40}$$

where θ is the angle between the wave vector $\mathbf{q}$ and the direction of the driving. This thus gives a direction dependent surface tension

$$\sigma_s(\theta) = \sigma(1 + \frac{v^2\cos^2(\theta)}{v_0^2}), \tag{4.41}$$

where we have introduced the intrinsic velocity $v_0 = \sqrt{\alpha^2\lambda\kappa}$ which depends on the microscopic *dynamical* quantity α associated with the model A dynamics of the field ϕ, as well as the microscopic static quantities κ (which generates the surface tension) and λ the coupling between the field ψ and ϕ. This appearance of dynamical and static quantities that are otherwise hidden in equal time correlation functions in equilibrium is already implicit in the works of Onsager [**?**] where it is used to compute the conductivity of Brownian electrolytes and the explicit expressions were derived using stochastic density functional theory in [**?**]. We also note that the universal thermal Casimir effect between model Brownian electrolyte systems driven by an electric field exhibits similar features, developing a dependency on both additional static and dynamical variables with respect to the equilibrium case [**?**]

However for this small q expansion we see that the microscopic quantities D, the diffusion constant of the field ϕ, and the order parameter jump $\Delta\psi$ do not appear.

From the above, we see that in the direction of the driving the surface tension increases and the fluctuations of the surface are thus suppressed. We may also write

$$H_s(\mathbf{q}) = \sigma_s(\theta)[q^2 + m_e^2(\theta)], \tag{4.42}$$

with

$$m_s^2(\theta) = \frac{m^2}{1 + \frac{v^2 \cos^2(\theta)}{v_0^2}}, \tag{4.43}$$

this corresponds to a correlation length

$$\xi_s = \xi_{eq} \sqrt{1 + \frac{v^2 \cos^2(\theta)}{v_0^2}}, \tag{4.44}$$

and we see that it is increased in the direction of the driving.

As we have just remarked that the above results appear to be independent of the order parameter jump $\Delta\psi$ and the diffusion constant D, however the next order correction to H_s for small q is given by

$$H_s(\mathbf{q}) = \sigma_s(\theta)[q^2 + m_e^2(\theta)] - \frac{4Dq\sigma^2(\lambda + \kappa m^2)(\mathbf{q} \cdot \mathbf{v})^2}{\alpha^3 \kappa^2 \lambda^2 \Delta\psi^2}, \tag{4.45}$$

and so the small $\mathbf{q}$ expansion breaks down at $\Delta\psi = 0$, indeed one can see that the system has exactly the equilibrium correlation function when $\Delta\psi = 0$.

In the limit of large q we see that the effective Hamiltonian is given, to leading order, by the original equilibrium Hamiltonian and so the out of equilibrium driving has no effect on the most energetic modes of the system.

The results here predict that for unconfined surfaces the long range height fluctuations are described by an isotropic form of capillary wave theory with an anisotropic surface tension which is largest in the direction of driving. Numerical simulations of driven lattice gases in two dimensions [**?**] show a more drastic change upon driving and find $C_s(q) \sim 1/q^{.66}$ and thus a strong deviation from capillary wave theory.

4.4 A model of active interfaces

We can apply the results derived in the previous section to analyse a simple model for surfaces formed between two phases of active colloids. Activity is modelled by assuming that the colloidal field ψ has a temperature different to that of the solvent field ϕ. This models the effect that activity leads to enhanced colloidal diffusivity over and above the Brownian motion of particles due to thermal fluctuations [**?**].

In the absence of any driving the dynamical equations for the field ψ and ϕ become

$$\frac{\partial\psi(\mathbf{x},t)}{\partial t} = D\nabla^2\frac{\delta H}{\delta\psi(\mathbf{x})} + \sqrt{2DT_1}\nabla\cdot\boldsymbol{\eta}_1(\mathbf{x},t) \tag{4.46}$$

$$\frac{\partial\phi(\mathbf{x},t)}{\partial t} = -\alpha\frac{\delta H}{\delta\phi(\mathbf{x})} + \sqrt{2\alpha T_2}\eta_2(\mathbf{x},t). \tag{4.47}$$

Following the same arguments as above we find that

$$\hat{C}(\mathbf{q},\omega) = 2D\frac{\left[T_1\frac{\Delta\psi^2}{2q}(\omega^2+\alpha^2\lambda^2) + T_2\frac{\sigma\alpha D\lambda^2}{\kappa}\right]}{\left|i\omega[\frac{\alpha\lambda\Delta\psi^2}{2q} + \frac{\lambda\sigma D}{\kappa} + D\sigma(q^2+m^2)] + [\alpha\lambda D\sigma(q^2+m^2) - \frac{\Delta\psi^2}{2q}\omega^2]\right|^2}. \tag{4.48}$$

The equal time steady state height fluctuations thus have correlation function

$$\tilde{C}_s(q) = \frac{T_1}{\sigma(q^2+m^2)}\left[1-(1-\frac{T_2}{T_1})\frac{\lambda\sigma}{\kappa}\frac{1}{\frac{\alpha\lambda\Delta\psi^2}{2Dq} + \frac{\lambda\sigma}{\kappa} + \sigma(q^2+m^2)}\right]. \tag{4.49}$$

We see, again, that the inclusion of a non-equilibrium driving changes the statistics of height fluctuations and leads to a steady state that depends on both dynamical variables D and α as well as static ones $\Delta\psi,\ \lambda$ and κ that remain hidden in the equilibrium case. This phenomenon is again seen in the behavior of the universal thermal Casimir force between Brownian conductors held at different temperatures [**?**].

If we assume strong activity we can take the limit $T_1 \gg T_2$, in this case we find

$$\tilde{C}_s(q) = \frac{T_1}{\sigma(q^2+m^2)}\frac{\frac{\alpha\lambda\Delta\psi^2}{2Dq} + \sigma(q^2+m^2)}{\frac{\alpha\lambda\Delta\psi^2}{2Dq} + \frac{\lambda\sigma}{\kappa} + \sigma(q^2+m^2)}. \tag{4.50}$$

Interpreted in terms of an effective Hamiltonian for an equilibrium system at the temperature T_1 the above gives

$$H_s(q) = \sigma(q^2+m^2)\left[1+\frac{\lambda\sigma}{\kappa}\frac{q}{\frac{\alpha\lambda\Delta\psi^2}{2D} + q\sigma(q^2+m^2)}\right]. \tag{4.51}$$

psi In the case of an unconfined interface (where there is no gravitational effect on the

surface fluctuations) *i.e.* $m = 0$ we see that for small q

$$H_s(q) \approx \sigma q^2 + \frac{2D\sigma^2}{\kappa\alpha\Delta\psi^2} q^3. \tag{4.52}$$

We see that the effective surface tension is not modified but a reduction of fluctuations due to the presence of the term in q^3 arises. As in the case of a driven system, we see that the large q behavior of the effective Hamiltonian is given by the equilibrium case where $T = T_1 = T_2$.

In the case where the interface is confined, we see that for small q one obtains

$$H_s(q) \approx \sigma m^2 \left[1 + \frac{2D\sigma}{\kappa\alpha\Delta\psi^2} q\right], \tag{4.53}$$

and thus at the largest length scales of the problem there is a qualitative departure from capillary wave behavior induced by activity, and the correlation length of height fluctuations at the largest length scales is given by

$$\xi_a = \frac{2D\sigma}{\kappa\alpha\Delta\psi^2}. \tag{4.54}$$

The above result should be compared with that obtained in [**?**] for systems with anisotropic thermal white noise, which breaks detailed balance and mimics random driving of the system parallel to the interface; for free interfaces it was found that $C_s(q) \sim 1/q$.

4.5 Conclusions

We have presented a model to analyse the effect of uniform driving on the dynamics of the interface in a two phase system. In order to generate a non-equilibrium state a second *hidden* order parameter was introduced. This models the behaviour of a local or solvent degree of freedom which is not influenced by the driving field. In this way, we obtain out of equilibrium interface fluctuations which are described by Gaussian statistics as found in the experimental study of [**?**]. The agreement with this experimental study also extends to qualitative agreement with the increase of the effective surface tension in the direction of driving and also an increase in the correlation length of the height fluctuations with respect to a non-driven equilibrium interface. However, we note that numerical simulations of a sheared Ising interface [**? ?**] also reveal a reduction of interface fluctuations but the

lateral correlation length is found to be reduced.

The basic idea underlying this study would be interesting to apply to a number of possible variants of this model, for instance both the dynamics of the main field ϕ and the solvent field ϕ could be varied. To make a direct link with driven colloidal interfaces one should study model H type dynamics for the main field ϕ and other variants for the dynamics of the solvent field ϕ could also be considered.

As mentioned above, in lattice based models driving induces non-equilibrium states even in the simple Ising lattice gas. A model analogous to that studied here can be formulated in a lattice based systems using the Hamiltonian

$$H = -J \sum_{(ij)} S_i S_j (1 + \sigma_{(ij)}), \tag{4.55}$$

where $S_i = \pm 1$ are Ising spins at the lattice sites i, and $\sigma_{(ij)} = \pm 1$ are Ising like dynamical solvent variables associated with the lattice links (ij). The static partition function is given by

$$Z = \mathrm{Tr}_{\sigma_{ij}, S_i} \exp \left[\beta J \sum_{(ij)} S_i S_j (1 + \sigma_{(ij)}) \right], \tag{4.56}$$

and the trace over the solvent variables can be trivially carried out to give

$$Z = \mathrm{Tr}_{S_i} \left(\exp \left[\beta J \sum_{(ij)} S_i S_j \right] \prod_{(ij)} 2 \cosh(\beta J S_i S_j) \right) = [2 \cosh(\beta J)]^L \mathrm{Tr}_{S_i} \exp(\beta J \sum_{(ij)} S_i S_j), \tag{4.57}$$

where L is the number of links on the lattice of the model. We thus see that the underlying effective static model is precisely the zero field Ising model.

This model can then be driven in a number of ways, for instance using conserved Kawasaki dynamics for the Ising spins to model diffusive dynamics in the presence of a uniform driving field parallel to the surface between the two phases at a temperature below the ferromagnetic ordering temperature T_c. The dynamics of the Ising spins on the lattice links can be given by non-conservative single spin flip, for instance Glauber, dynamics to keep the analogy with the continuum model discussed in the paper but diffusive dynamics or indeed a mixture of diffusive and non-conserved dynamics could be implemented. It would be interesting to see to what extent this modification of the driven lattice gas model affects the non-equilibrium driven states that arise.

It is also clear that this lattice model can be used to simulate the effect of activity where the Ising spins S_1 corresponding to the colloid field undergo Kawasaki dynamics at the temperature T_1 where as the link variables $\sigma_{(ij)}$ undergo single spin flip non-conserved dynamics at the temperature T_2.

Chapitre 5

Beyond Solid-On-Solid : the Particles-Over-Particles model

In fact, if the height profiles represent particle numbers, if we fix the total number of particles to be N and take them to be identical the partition function is given by

$$Z_N = \frac{1}{N!} \sum_{h_1,h_2\cdots h_L} \delta_{\sum_{i=1}^{L} h_i,N} \frac{N!}{\prod_{i=1}^{L} h_i!} \exp\left(-\beta\sigma \sum_{i=1}^{L} |h_{i+1} - h_i| - \beta \sum_{i=1}^{L} V(h_i)\right). \quad (5.1)$$

Here the combinatorial term $\frac{N!}{\prod_{i=1}^{L} h_i!}$ represents the number of ways that the h_i particles on each site can be chosen from the N particles available. The constraint on the particle number makes the computation of the partition function at fixed N complicated both analytically and numerically. However if we change to the grand canonical ensemble using the formula

$$\Theta = \sum_N \exp(\beta\mu N) Z_N, \quad (5.2)$$

where Θ is the grand partition function and μ the chemical potential, we find

$$\Theta = \sum_{h_1,h_2\cdots h_L} \frac{1}{\prod_{i=1}^{L} h_i!} \exp\left(-\beta\sigma \sum_{i=1}^{L} |h_{i+1} - h_i| - \beta \sum_{i=1}^{L} [V(h_i) - \mu h_i]\right). \quad (5.3)$$

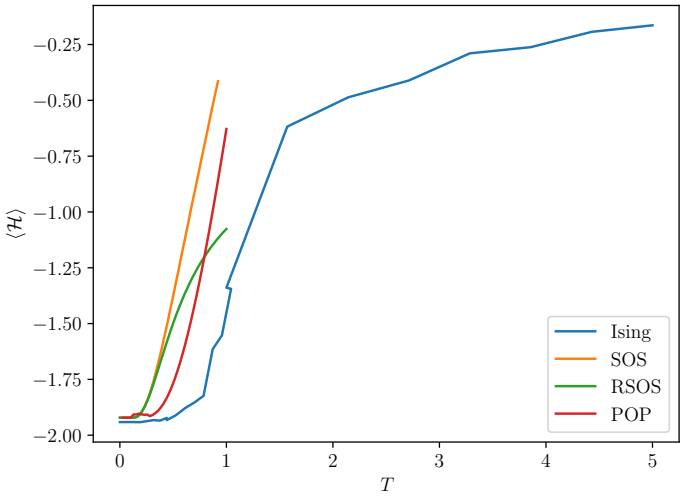

The grand partition function can then be written as

$$\Theta = \sum_{h_1, h_2 \cdots h_L} \exp\left(-\beta H_{eff}(h_1, h_2 \cdots h_L)\right) \tag{5.4}$$

where

$$H_{eff} = \sigma \sum_{i=1}^{L} |h_{i+1} - h_i| + \sum_{i=1}^{L} [V(h_i) - \mu h_i + \frac{1}{\beta} \ln(h_i!)]. \tag{5.5}$$

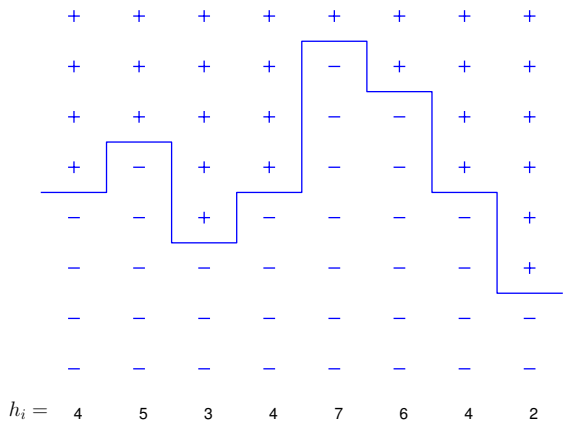
+ + + + + + + +
+ + + + − + + +
+ + + + − − + +
+ − + + − − + +
− − + − − − − +
− − − − − − − +
− − − − − − − −
− − − − − − − −
$h_i =$ 4 5 3 4 7 6 4 2

Annexe A

Evaluating Fourier integrals

Here we outline how the Fourier integration leading to Eq. (4.37) is carried out. Defining

$$I(f(\omega)) = \int \frac{d\omega}{2\pi} \frac{f(\omega)}{|i(A\omega + B) + (C - D\omega - E\omega^2)|} \tag{A.1}$$

we see that the integral we need to evaluate can be written in the form

$$I = aI(\omega^2) + bI(1). \tag{A.2}$$

The calculation leading to Eq. (4.35) can be carried out in the presence of a forcing term on the height profile in order to compute the response function for the surface which has a denominator of the form

$$\text{Den} = i(A\omega + B) + (C - D\omega - E\omega^2), \tag{A.3}$$

and due to causality the above only has poles in the upper complex plane (due to the convention of Fourier transforms used here). Consequently we find that

$$\int \frac{d\omega}{2\pi} \frac{1}{i(A\omega + B) + (C - D\omega - E\omega^2)} = 0, \tag{A.4}$$

as one may close the integration contour in the lower half of the complex plane. Taking the real and imaginary part of Eq. (A.4) leads to

$$CI(1) - DI(\omega) - EI(\omega^2) = 0 \tag{A.5}$$

$$AI(\omega) + BI(1) = 0. \tag{A.6}$$

Using this we can express $I(\omega^2)$ as a function of $I(1)$, and explicitly we have

$$I(\omega^2) = \frac{I(1)}{E}[C + \frac{DB}{A}]. \tag{A.7}$$

To evaluate $I(1)$ we now use

$$I(1) = -\mathrm{Im} \int \frac{d\omega}{2\pi} \frac{1}{A\omega + B} \frac{1}{i(A\omega + B) + (C - D\omega - E\omega^2)}. \tag{A.8}$$

The integrand above has no poles in the lower half of the complex plane but has a *half pole* at $\omega = -B/A$ on the real axis, thus using standard complex analysis we find

$$I(1) = \frac{1}{2(CA + BD - \frac{EB^2}{A})}. \tag{A.9}$$

Then after some laborious, but straightforward algebra, the results Eq. (4.37) is obtained.

Bibliographie

[1] Dirk G. A. L. Aarts, Henk N. W. Lekkerkerker, Hua Guo, Gerard H. Wegdam, and Daniel Bonn. Hydrodynamics of Droplet Coalescence. *Physical Review Letters*, 95(16) :164503, October 2005.

[2] Lars Onsager. Crystal Statistics. I. A Two-Dimensional Model with an Order-Disorder Transition. *Physical Review*, 65(3-4) :117–149, February 1944.

[3] L. Landau and E. Lifchitz. *Physique théorique - T9 Physique Statistique.* Éditions Mir Moscou. 1990.

[4] Y. Hennequin, D. G. A. L. Aarts, J. H. van der Wiel, G. Wegdam, J. Eggers, H. N. W. Lekkerkerker, and Daniel Bonn. Drop Formation by Thermal Fluctuations at an Ultralow Surface Tension. *Physical Review Letters*, 97(24), December 2006.

[5] Javier Atencia and David J. Beebe. Controlled microfluidic interfaces. *Nature*, 437(7059) :648–655, September 2005.

[6] A L Talapov and H W J Blöte. The magnetization of the 3D Ising model. *Journal of Physics A : Mathematical and General*, 29(17) :5727–5733, September 1996.

[7] Martin Niss. History of the Lenz-Ising Model 1920–1950 : From Ferromagnetic to Cooperative Phenomena. *Archive for History of Exact Sciences*, 59(3) :267–318, March 2005.

[8] Martin Niss. History of the Lenz–Ising Model 1950–1965 : from irrelevance to relevance. *Archive for History of Exact Sciences*, 63(3) :243, May 2009.

[9] L.J. de Jongh and A.R. Miedema. Experiments on simple magnetic model systems. *Advances in Physics*, 23(1) :1–260, January 1974.

[10] W.P. Wold. The Ising Model and Real Magnetic Materials. *Brazilian Journal of Physics*, 30(4) :794–810, December 2000.

[11] Hironobu Ikeda and Kinshiro Hirakawa. NEUTRON SCATI'ERING STUDY OF TWO-DIMENSIONAL ISING NATURE OF K2CoF4. 14 :4.

[12] Tobias Preis, Peter Virnau, Wolfgang Paul, and Johannes J. Schneider. GPU accelerated Monte Carlo simulation of the 2D and 3D Ising model. *Journal of Computational Physics*, 228(12) :4468–4477, July 2009.

[13] Nigel Goldenfeld. *Lectures on Phase Transitions and the Renormalization Group*. CRC Press, 1 edition, March 2018.

[14] J. Stecki, A. Maciol/ek, and K. Olaussen. Magnetization profiles of the planar fluctuating interface in a d=2 Ising strip. *Physical Review B*, 49(2) :1092–1103, January 1994.

[15] D. B. Abraham and A. Martin-Löf. The transfer matrix for a pure phase in the two-dimensional Ising model. *Communications in Mathematical Physics*, 32(3) :245–268, September 1973.

[16] D. B. Abraham and P. Reed. Interface profile of the Ising ferromagnet in two dimensions. *Communications in Mathematical Physics*, 49(1) :35–46, February 1976.

[17] Howard L. Richards, M. A. Novotny, and Per Arne Rikvold. Numerical transfer-matrix study of surface-tension anisotropy in Ising models on square and cubic lattices. *Physical Review B*, 48(19) :14584–14598, November 1993.

[18] G. H. Gilmer and P. Bennema. Simulation of Crystal Growth with Surface Diffusion. *Journal of Applied Physics*, 43(4) :1347–1360, April 1972.

[19] M. Elwenspoek and J. P. van der Eerden. Kinetic roughening and step free energy in the solid-on-solid model and on naphthalene crystals. *Journal of Physics A : Mathematical and General*, 20(3) :669, 1987.

[20] M. R. Wilby, D. D. Vvedensky, and A. Zangwill. Scaling in a solid-on-solid model of epitaxial growth. *Physical Review B*, 46(19) :12896–12898, November 1992.

[21] G Gompper and D. M Kroll. Steric Interactions in Multimembrane Systems : A Monte Carlo Study. *Europhysics Letters (EPL)*, 9(1) :59–64, May 1989.

[22] V. Privman and N. M. Švrakić. Transfer-Matrix Spectrum for Systems with Interfaces. *Physical Review Letters*, 62(6) :633–636, February 1989.

[23] Yup Kim, D. K. Park, and Jin Min Kim. Conserved growth in a restricted solid-on-solid model. *Journal of Physics A : Mathematical and General*, 27(15) :L533, 1994.

[24] I. Vaysburd. Critical RSOS models in external fields. *Nuclear Physics B*, 446(3) :387–404, July 1995.

[25] H. J. F. Knops. Exact Relation between the Solid-on-Solid Model and the XY Model. *Physical Review Letters*, 39(12) :766–769, September 1977.

[26] Aleksander L. Owczarek and Thomas Prellberg. Exact solution of the discrete (1+1)-dimensional SOS model with field and surface interactions. *Journal of Statistical Physics*, 70(5-6) :1175–1194, March 1993.

[27] Satya N. Majumdar and Alain Comtet. Airy Distribution Function : From the Area Under a Brownian Excursion to the Maximal Height of Fluctuating Interfaces. *Journal of Statistical Physics*, 119(3-4) :777–826, May 2005.

[28] Grégory Schehr and Satya N. Majumdar. Universal asymptotic statistics of maximal relative height in one-dimensional solid-on-solid models. *Physical Review E*, 73(5) :056103, May 2006.

[29] Martin Siegert and Michael Plischke. Scaling behavior of driven solid-on-solid models with diffusion. *Journal de Physique I*, 3(6) :1371–1376, June 1993.

[30] Paul A Pearce and Katherine A Seaton. Exact solution of cyclic solid-on-solid lattice models. *Annals of Physics*, 193(2) :326–366, August 1989.

[31] Nicholas Metropolis and S. Ulam. The Monte Carlo Method. *Journal of the American Statistical Association*, 44(247) :335–341, September 1949.

[32] M. E. J. Newman and G. T. Barkema. *Monte Carlo Methods in Statistical Physics*. Oxford University Press, Oxford, New York, February 1999.

[33] S. Wansleben and D. P. Landau. Monte Carlo investigation of critical dynamics in the three-dimensional Ising model. *Physical Review B*, 43(7) :6006–6014, March 1991.

[34] Roy J. Glauber. Time-Dependent Statistics of the Ising Model. *Journal of Mathematical Physics*, 4(2) :294–307, February 1963.

[35] Kyozi Kawasaki. Diffusion Constants near the Critical Point for Time-Dependent Ising Models. I. *Physical Review*, 145(1) :224–230, May 1966.

[36] O. Vasilyev, A. Gambassi, A. Maciołek, and S. Dietrich. Monte Carlo simulation results for critical Casimir forces. *EPL (Europhysics Letters)*, 80(6) :60009, 2007.

[37] David Lopes Cardozo, Hugo Jacquin, and Peter C. W. Holdsworth. Critical Casimir forces in a magnetic system : An experimental protocol. *Physical Review B*, 90(18), November 2014.